UNIVERSITY OF TWENTE.

Critical Current versus Transverse Stress and Thermal Stability of a RRP Nb_3Sn Rutherford Cable.

Master assignment report within the MSc. Program Applied Physics carried out within the research chair Energy, Materials and Systems at the University of Twente.

Author: W. van de Camp
Supervisor: Dr. M. Dhallé

Date: November 16, 2012

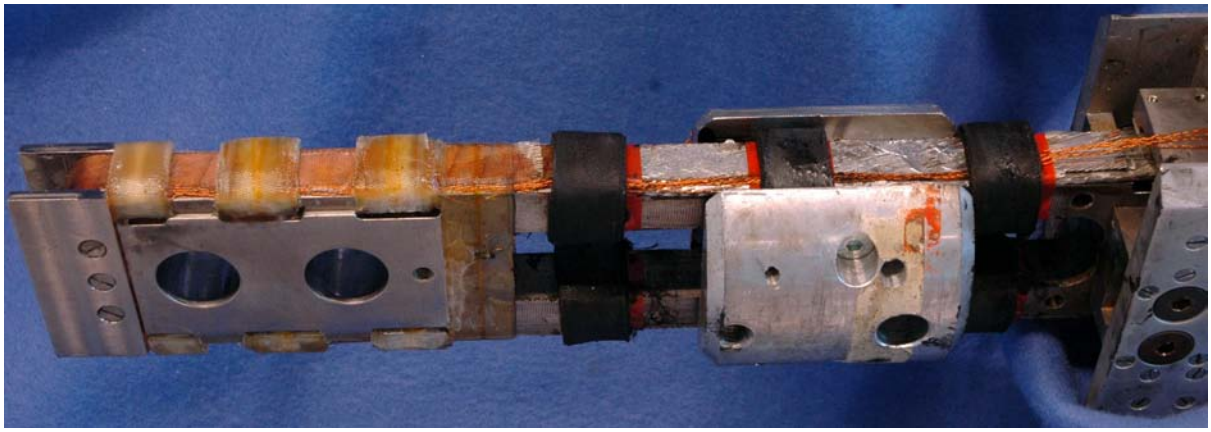

Examination Committee:
Prof. dr. ir. H.J.M. ter Brake
Prof. dr. ir. H.H.J. ten Kate
Dr. ir. H. Wormeester
Dr. M. Dhallé

Abstract

A full-sized state-of-the-art superconducting Nb_3Sn Rutherford cables was tested in terms of its critical current up to a magnetic peak field of 12 T and transverse stress levels up to 270 MPa. Also its thermal stability was assessed as function of magnetic field and test current over a field range of 2 to 11 T and currents from 7 to 20 kA. These measurements were preformed on a cable intended for the DS magnet, which constitutes an important first step in the LHC upgrade program. The samples were tested over a length of 45 mm on a U-shaped sample holder powered by a superconducting transformer. The cable was validated for the application in the DS magnet, both in terms of cabling degradation and in terms of operational transverse stress. Irreversible reduction of the critical current only occurs at transverse stresses far above the maximum coil stress expected in the DS magnet. The transition in thermal stability between the single strand- and the collective cable regime, which is reported in NbTi cables and sub-sized Nb_3Sn cables, is not clearly seen in the magnetic field dependence of this full-sized cable and only a weak transition is found in its current dependence.

Acknowledgements

This report concludes my work performed on the DS cable and with which the final part of the master program of the study Applied Physics at the University of Twente is finished. I have learned a lot during this last year, not only about being a researcher, but also practical experience and skills gathered in the lab and workshop. I had a very nice time at the EMS chair at the University of Twente and I like to thank everyone of the EMS chair for the pleasant work environment.

I want to thank Herman ten Kate and Marc Dhallé for the opportunity to do my master assignment within the research chair EMS and to perform research on this great project. I enjoyed working on this experiment and with this unique set-up. I am satisfied with the results, especially because a poster of this research was presented at the Applied Superconductivity Conference 2012 and a journal paper will be written.

I specifically want to thank my supervisor Marc Dhallé for all the discussion and meetings we had. Those discussions contributed a lot to the final result. I also thank him for correcting this report in the evenings and during night, so it could be finished on time.

The lab can not be operated without its lab engineers, who make everything possible in the lab. Specifically I would like to thank Sander Wessel for all the work he helped me with in the project and all the practical skills I learned from him. I also like to thanks to the rest of the people in the lab for their help when needed.

The PhD student Michiel de Rapper performed similar measurements at the FRESCA test facility at CERN. During his fourth year of his PhD, he helped me a lot with my experiments. I like to thank Michiel for his help, the discussions we had and for sharing his knowledge about these type of measurements.

Contents

Chapter 1

Introduction

This report describes the results of a Master Assignment within the MSc. Program of Applied Physics at the University of Twente. The assignment was to investigate the critical current and the thermal stability of a state-of-the-art superconducting Nb_3Sn Rutherford cable that was produced by CERN within the framework of the LHC upgrade program. CERN has requested the chair Energy, Materials and Systems (EMS) at the University of Twente to determine the magnetic field and transverse pressure dependence of the critical current of this cable in order to validate it for application in DS-type dipole magnets. At the end of these experiments, it was decided to use the same sample to determine also the thermal stability of this type of cable under application-relevant conditions. The present chapter aims to provide an introduction to the key concepts in the assignment. It starts of with a brief discussion of superconductivity in general and of Nb-based superconducting Rutherford cables in specific. It then moves on to give a concise description of the LHC upgrade program at CERN and of the role of the DS magnets, which form an important first step in this program.

1.1 Superconductivity

Accelerator and fusion magnets need to be built from superconducting cables in order to achieve high magnetic fields. Proper characterization of the superconducting properties of cables made from the best performing materials available is therefore essential to achieve higher magnetic fields. Key aspects of superconductivity relevant to the research assignment are described in this section. More general information about the fundamental aspects of superconductivity can be found in the book of Cyrot [1], while detailed considerations about superconducting magnets is discussed in the book of Wilson [2].

The Dutch physicist Heike Kamerlingh Onnes discovered superconductivity in 1911 in his laboratory in Leiden. After liquefying helium at 4.2 K he measured the temperature-dependent DC resistivity of mercury. The resistivity suddenly dropped to zero when the temperature decreased below 4.2 K. He named this phenomenon superconductivity [3].

In the normal state above the critical temperature T_c, a superconducting material behaves as a normal conductor with Ohmic resistivity, while in the superconducting state below T_c the resistivity is virtually zero. However, this zero-resistance state is only maintained up to a certain current density. The relation between the current I through and the electrical field E across a superconducting sample is usually described with a highly non-linear power-law relation:

$$E = E_c \left(\frac{I}{I_c(B,T)} \right)^n , \tag{1.1}$$

with E_c an electrical field criterion (often chosen as 10^{-5} V/m) and I_c the so-called critical current of the superconductor. The value of I_c depends on the magnetic field B and on the temperature T. The so-called n-value defines the quality of the conductor, a high n-value results in a sharp transition. For superconducting applications it is important that the n-value is high, so that at the operation current (typically a given percentage of I_c) virtually no energy is dissipated in the conductor. In Figure 1.1 a superconductor with a n-value of 10 and one with 40 are compared. The voltage build-up in materials with the lower n-value starts much earlier.

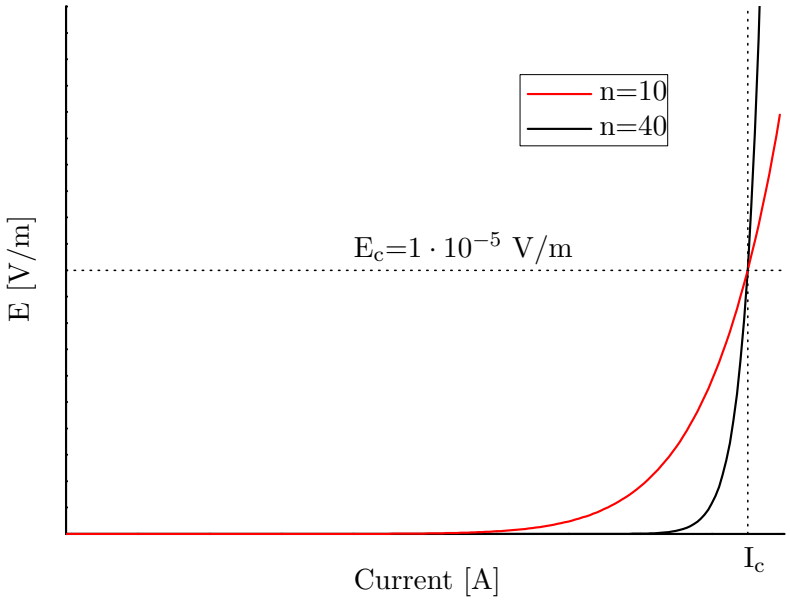

Figure 1.1: Electrical field as function of current for n=10 (red) and 40 (black), both with the same I_c.

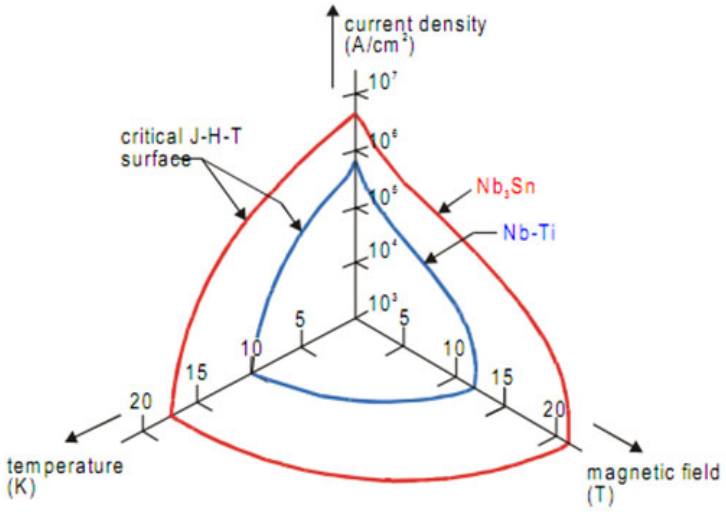

Figure 1.2: The critical surface of Niobium-Titanium and Niobium-3-Tin.

The temperature and magnetic field dependence of the critical current are represented by the so-called critical surface which, for typical NbTi and Nb_3Sn conductors, is shown in Figure 1.2. For each current value above the critical surface, the superconductor is in the normal state while

below the surface it is superconducting. NbTi and Nb_3Sn are the two superconducting materials that are still mostly used for large scale superconducting applications. NbTi is a ductile material and is easy to work with, but is limited by a relative low-lying critical surface. Nevertheless, because of the robustness of the material, most magnets built in the past are made from NbTi. However, it can be seen in Figure 1.2 that the critical surface of Nb_3Sn is higher-lying than that of NbTi and thus Nb_3Sn is a material from which more powerful magnets can be built. For applications that require a higher magnetic field, one has to choose for the brittle Nb_3Sn. Apart from some niche-applications (mainly power cables, cryogenic current leads and some relatively low field magnets), the newer practical superconducting materials (MgB_2, $Bi_2Sr_2CaCu_2O_8$ and $YBa_2Cu_3O_7$) are for technical and/or commercial reasons presently deemed to be not yet ready for large scale superconducting applications.

Superconducting wires cannot be made from a monolithic piece of superconductor. Nb_3Sn needs to be embedded in a normal metal matrix for mechanical and thermal stability reasons. For sufficient stability and low AC loss, a Nb_3Sn wire needs a substructure of fine filaments typically (50 µm in diameter) which must be twisted. Presently, three distinct wire fabrication techniques are used to produce commercial Nb_3Sn wires: the bronze process, the Internal Tin process and the Powder-in-Tube process. The typical wire cross-sections that result are shown in Figure 1.3. For all methods it is important that there is a pure copper part in the wire with a high thermal conductivity and a low electrical resistivity.

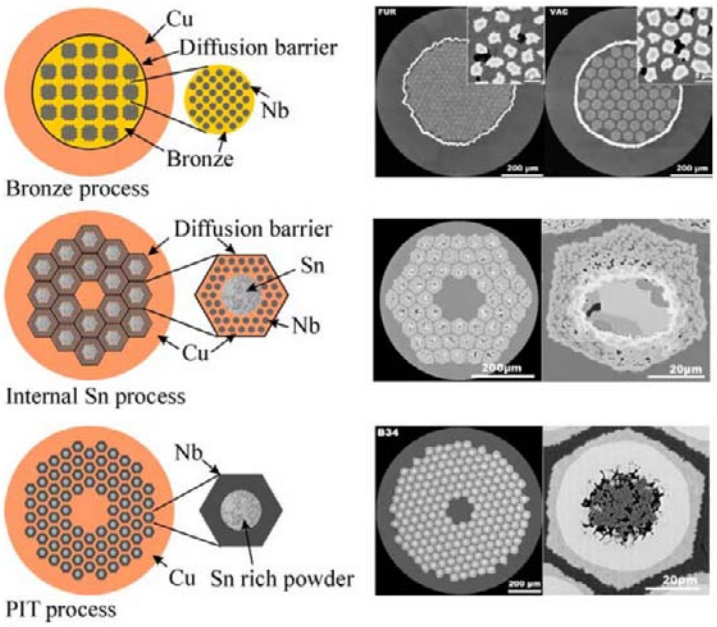

Figure 1.3: Schematic presentation of the three main Nb_3Sn wire fabrication techniques. From top to bottom: The bronze process, the Internal Tin process and the Powder-in-Tube (PIT). The compositions indicated are prior to the heat treatment that converts the Nb and Sn into Nb_3Sn. To the right SEM cross-sections are shown from actual wires fabricated according to these production methods [4].

The bronze process was the first viable wire fabrication process. Niobium rods are inserted in a high-Sn bronze matrix and surrounded by a pure copper sheath for stabilization. A barrier surrounds the bronze to prevent Sn from diffusing into the pure copper. Typically, large starting

billets (with diameter of several tens of cm) are first extruded and then drawn to the final wire diameter (typically below 1 mm). The bronze route is a well-established and still widely used technology, but the maximum non-copper current density obtained in this type of wires achieved is about 1000 A/mm^2 at 12 T and 4.2 K [4]. This value is limited by the relatively slow diffusion of Sn out of the bronze and into the Nb, which leads to undesired Sn gradients inside the final Nb_3Sn filament and sometimes even to incomplete reaction. For this reason, two new processes were developed, aimed at a more mobile Sn distribution.

The Internal Tin process is based on tin cores surrounded by Niobium rods, which are in turn embedded in copper. For the Restack Rod Process (RRP), these rods are extruded to a length of several meters. A diffusion barrier of Ta or Nb is wrapped around them and several of these rods are re-stacked in a pure copper matrix. The diffusion barrier prevents tin from diffusing into the pure copper matrix. This bundle is then extruded to fabricate a wire of several kilometers length. The maximum non-copper current density achieved with this process is about 3000 A/mm^2 at 12 T and 4.2 K [4].

In the Powder-in-Tube method (PIT), hollow Nb tubes are filled with a powder of $NbSn_2$ and additional elements and stacked in a high purity copper matrix. The main advantages of the PIT method are the high tin mobility and reactivity, which results in a very short reaction time at relative low temperatures. As a consequence (and in contrast to the RRP process), the wires can be made with small well separated filaments of 30-50 µm. The maximum non-copper current density achieved is about 2300 A/mm^2 at 12 T and 4.2 K [4].

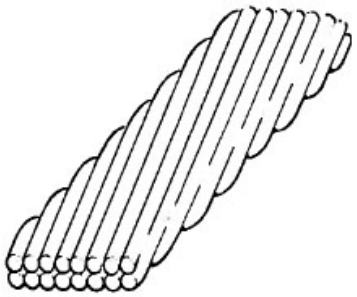

Figure 1.4: Schematic of a Rutherford Cable.

Large magnets need to be built from superconducting cables made from several strands, since single-strand windings schemes would lead to prohibitively large self-inductances. Several superconducting cable designs are possible. For accelerator magnets, mostly Rutherford cables are used. A schematic of such a Rutherford cable is shown in Figure 1.4. The cable is manufactured by flattening a twisted ring of strands into a rectangular cross-section with four cylindrical rollers. Sometimes a Rutherford cable has a small keystone which allows the cable to be stacked more naturally around the aperture of the magnet. A keystone means that one side of the cable is a little thinner than the other one. To ensure a homogeneous current distribution throughout the cable, the strands need to be transposed so that each wire 'feels' the same environment. In practice this is done by twisting them around each other prior to the cable rolling step. The twist pitch of a cable is the length measured along the cable between two successive equivalent positions of a strand. The current density over the whole cable cross-section is much lower than the non-copper current densities cited in the discussion of the fabrication processes, since in the cable there is also copper, insulation and voids between the strands. Note that the combined twisting/rolling step in the cabling process involves considerable material deformation, especially at the cable edges where the strands are forced to bend round over a small radius of

curvature. Despite the fact that this deformation is imposed prior to the heat treatment during which the brittle Nb_3Sn is formed, the filamentary cross-section can be pinched off or the thin barrier layers can locally rupture, leading to a reduction of the critical current. Indeed, one of the important questions in this assignment is whether the new cabling process developed at CERN for RRP strands maintains the high current density which is achievable with this type of wires.

For magnet designers it is also important to know the thermal stability of the cable. Small disturbances (such as movement of the current-carrying cable in a background magnetic field, flux jumps, crack formation and specifically for accelerator magnets the impact of high energetic particles) may increase the temperature locally within a single strand. If the temperature rises above the critical current, the strand locally becomes resistive and generates Joule heating. The area where the temperature is above the critical one is called the normal zone. Due to the Joule heating the normal zone grows and propagates along the strand. However, if the initial normal zone is small enough, cooling at its ends is larger than the heat generation throughout its length and the strand will recover from the local disturbance. Moreover, Rutherford cables consist of several strands and the current inside the normal zone can redistribute to neighbouring strands and so that less current flows through the normal zone, resulting in less Joule heating and thus easier recovery. If the disturbance is too large or the current cannot be redistributed, the whole cable will go to the normal state. The loss of superconductivity in the whole cable is called a quench. During a quench all energy stored in the cable or magnet will be turned into heat that will be deposited in the magnet and resistors parallel to the magnet. To prevent quenches, the smallest amount of heat needed to quench the cable needs to be known: it is called the Minimal Quench Energy (MQE).

There are three types of propagation of the normal zone. The zone propagates in the longitudinal direction along the strand or it can propagate in the transverse direction to neighbouring strands. The propagation in the transverse direction may occur in two ways. The first is to adjacent strands running parallel to the normal zone, while the second is cross propagation to the strands on the other side of the cable. The propagation of heat to other stands will increase their temperature and thus lowers the critical current of those strands. Adjacent propagation is the primary mode of transverse propagation.

The recovery of a strand inside a Rutherford cable depends on several parameters. The current from the strand that is in the normal state redistributes to the neighbouring strands. If these strands can sustain the extra current, the cable can operate with one normal strand and the strand can recover. If the neighbouring strands cannot sustain the extra current and also become normal, the whole cable will quench. This later case is the so-called single strand regime (regime I) where the quench behaviour of the cable is essentially determined by the quench behaviour of a single strand. If the neighbouring strands can sustain the extra current, the cable is much more stable since also the neighbouring strands must quench. This is called the cable regime (regime II) where the quench behaviour depends on the heat propagation through the cable and whether or not more stands will quench.

The current in the neighbouring strands will increase as each takes over about half the current sent through the quenched stand. In principle the cable is thus in the cable regime for currents below 66% of the critical current. However, heat propagated to these adjacent strands reduces their critical current and thus less current can be transferred to these strands. The current at the transition between the single strand and cable regime is called I_{kink}. If the neighbouring strands also quench but their neighbouring strands can take over the current (i.e. the next-nearest neighbours of the originally disturbed strand), the cable can sustain three

normal strands and still recover. This goes on to higher order regimes where each time two extra strand will quench [5, 6].

Willering [6] experimentally demonstrated these regimes in NbTi Rutherford Cables. These cables are not impregnated and are in good thermal contact with the helium bath. An impregnated cable has comparatively limited cooling power, since the superconductor is not directly in contact with the helium bath. Nevertheless De Rapper [7] proved on sub-sized LARP and SMC cables that the different stability regimes also occur in impregnated Nb_3Sn Rutherford cables. In this work, we had the opportunity to test these quench scenarios for the first time in a full-sized state-of-the-art Nb_3Sn cable. Even if CERN did not commission this experiment, we deemed this opportunity too important not to attempt this extra experiment at the end of the $I_c(B)$ and $I_c(\sigma)$ measurements.

1.2 LHC upgrade

1.2.1 CERN

The European Organization for Nuclear Research (CERN) is home to the Large Hadron Collider (LHC), the biggest particle accelerator in the world. CERN is a large international collaboration of many nations and institutes. The LHC is a ring-shaped accelerator with a circumference of 27 km where protons are accelerated to almost the speed of light. A schematic of the LHC is shown in Figure 1.5. In two tubes protons move in opposite direction to collide at four locations where the beam pipes meet. At each of the four locations, a detector (ATLAS, CMS, ALICE or LHCb) is present to measure various data from the collisions. A well-known example one of the things the ATLAS and CMS detector are looking for is the Higgs particle. During these proton-proton collisions many sub-atomic particles are created. The maximum energy the protons have at the moment of a collision is 4 TeV, so an energy of 8 TeV per collision. The LHC is designed to accelerate the protons to an energy of 7 TeV and thus a collision energy of 14 TeV, but that will be achieved after the shut-down of 20 months at the end of 2012.

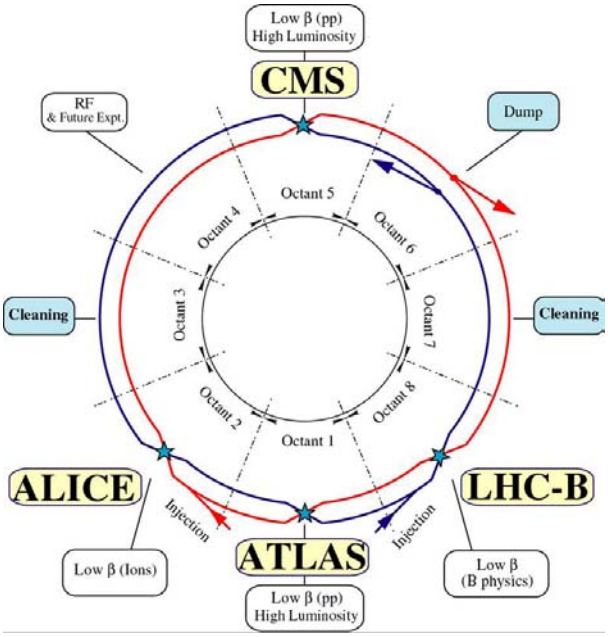

Figure 1.5: Schematic of the Large Hadron Collider at CERN.

Scientists are looking for rare particles created during the collisions, so that many collisions are needed. To achieve this, there will be 2808 bunches in each beam pipe with $1.15 \cdot 10^{11}$ protons per bunch once the LHC operate at full capacity. The luminosity $\mathcal{L}$ is the number of particles passing down the line per unit time, per unit area. The maximum luminosity achieved by the ATLAS experiment at this moment is $7.73 \cdot 10^{33}$ $\mathrm{cm}^{-2}\mathrm{s}^{-1}$ with a collision energy of 8 TeV [8]. More information about particle physics can be found in the book of Griffiths [9].

The ring of the LHC contains 1232 dipole magnets of 15 m length and 392 quadrupole magnets of 5-7 m long. The dipole magnet keeps the beam on a circular trajectory by generating a magnetic field of 8.33 T perpendicular to the particles and thus bending the beam by the Lorentz force. The quadrupole magnets are used to squeeze the beam together in order to keep it focused.

The proton bundles are not perfectly focused in the center of the beam pipe. A small part will move out and hit the superconducting magnet and release a small amount of energy. If too many particles hit the superconducting windings of the magnets, a quench will occur. Collimators are used to clean the proton bundles and thus reduce the number of particles colliding with the superconducting magnets and to prevent a quench. However, the present collimators do limit the maximum beam intensity. The second phase of the LHC collimation upgrade consists of installing two additional collimators in the dispersion suppressor (DS) region of points 2, 3 and 7 of the LHC and will enables proton and ion beam operation at nominal and ultimate intensities.

The LHC is entirely constructed with NbTi magnets, which at the time of its conception were conceived as the more robust technology. Meanwhile, plans are made for a luminosity - and, in a later stage, energy upgrade of the machine. This will require higher magnetic fields, initially in the quadrupoles that focus the beams just before the experiments (luminosity upgrade) and later in the bending dipoles along the entire tunnel (energy upgrade). Since NbTi is intrinsically limited to fields of about 10 T (Figure 1.2), these magnets will need to be Nb_3Sn-based. As a first step in this process, aimed at gaining experience with Nb_3Sn magnets constructed with the newer PIT and RRP high-current strands, a number of Nb_3Sn DS magnets will be installed to achieve the collimation upgrade discussed above. The cable investigated in this assignment is designed to be used in these magnets.

1.2.2 DS Magnet

The necessary longitudinal space of about 3.5 m for the additional collimators is provided by replacing some of the 15 m long 8.33 T NbTi dipole magnets by a pair of 5.5 m long 11 T Nb_3Sn magnets. The new magnets are placed in the DS region and are therefore called DS Magnets. They are connected in series with the rest of the ring and are therefore operated at a current of 11850 A at 1.9 K with 20% operation margin [10]. The degradation of the critical current due to cabling has to be 10% or less to provide the required operation margin [11]. These magnets are straight instead of having the shape of the curvature of the ring, which means that a wider coil aperture is needed (60 mm). A cross-section of the DS magnet is shown in Figure 1.6. This design results in a homogeneous magnetic field in the center of the magnet.

The stress distribution in the DS magnet is simulated by Karppinen et al. [10]. Two designs are simulated, one with a removable pole and the second with an integrated pole. The azimuthal stress distribution of both designs is shown in Figure 1.7 for room temperature, after cool-down and at 12 T generated field. The maximum coil stress is below 145 MPa for the removable pole and below 150 MPa for the integrated pole. The maximum coil stress occurs transverse to the cable, on the midplane of the magnet as can be seen from Figure 1.7. Just like with other superconductors, the properties of Nb_3Sn changes when the material is mechanically loaded.

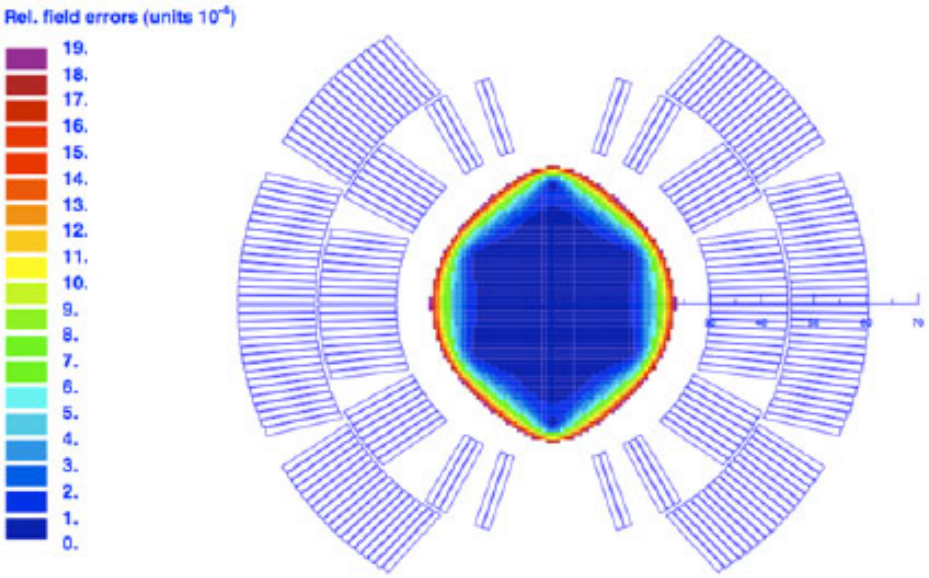

Figure 1.6: DS magnet cross-section with geometrical field errors

For relatively low strain levels (below the so-called irreversible strain limit), deformation of the crystal lattice changes both the electronic band structure of the material and its phonon spectrum. This leads to a gradual 'shrinking' of the critical surface, i.e. a reduction of I_c [12]. However, as soon as the strain is released, the original properties are recovered. At higher strain, the composite wires yield and the brittle Nb_3Sn filaments start to crack. The resulting I_c reduction is not recovered when the strain is released and hence it is called irreversible. Since the magnet will be ramped up and down often, it is essential that the degradation due to the operational transverse stress is reversible. It is therefore important that the margin on the cable is such that it will not reach the irreversible degradation regime, thus preventing damage to the cable. As will be described in the following chapter, the University of Twente developed a unique facility to test the I_c sensitivity to the transverse stress in Rutherford cables continuously and in situ. At CERN and other accelerator labs around the world, this important property can also be measured, but there it requires pre-stressing of the cable prior to cool-down so that a full $I_c(\sigma)$ characterization involves a cumbersome and complicating sequence of cool-down and warm-up cycles. Therefore, CERN asked the University of Twente to test their DS cable also under transverse stress.

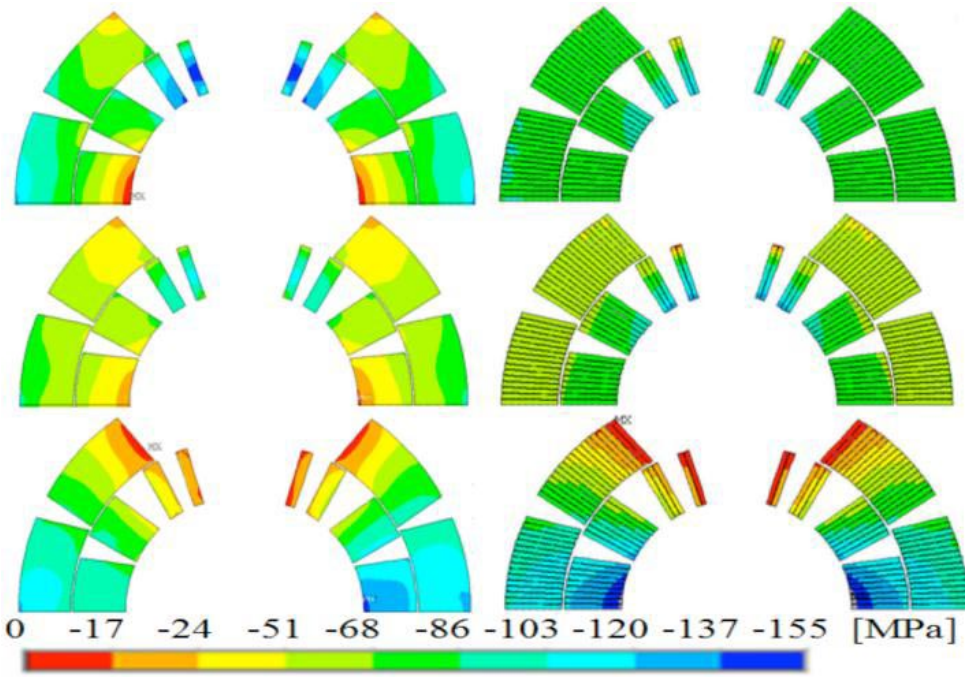

Figure 1.7: Azimuthal stress distribution in the coils after the cold mass assembly at room temperature (top), after cool-down (middle) and at 12 T (bottom) for removable (left) and integrated pole (right) designs.

1.3 Overview report

The first goal of this assignment was thus to measure the field and transverse stress dependence of the Rutherford cable that will be used in the DS magnet. The second goal was to measure the thermal stability of this cable. Both goals have been achieved and the results are included in this report. In this section a summary of the work performed and the outline of the report is given.

The experimental setup had not been used on full-size cables for many years and since then the critical current and properties of Rutherford cables have changed a lot. Present cables have a much higher critical current density compared to the cables measured previously on this set-up. In the course of the LHC upgrade program, it is foreseen that several different cables will be measured at the University of Twente for CERN. At the start of this experiment, it was expected that the first cable to be measured was the so-called FRESCA II cable, which is needed for the upgrade of the FRESCA test facility for superconducting cables at CERN. This cable has strands of 1 mm diameter resulting in a big and relative stiff cable. To test whether this cable could be bent around the sample holder without internal damage, experiments were performed to validate the sample holder, by searching for damaged filaments in the cross-section. The sample holder itself and the results of this initial micro-structural characterization experiment are discussed in Section 2.2.1.

The DS and FRESCA II cables have a much higher current density compared to samples measured previously on this set-up, which results to much higher currents and therefore higher Lorentz forces. Simulations were performed to determine the Lorentz forces and the self field of the FRESCA II cable and of the DS cable. These calculations are described in Section 2.5.

CERN eventually decided that it was more important that the DS cable was measured first, so that the rest of the research in this assignment was performed on this cable. The FRESCA II cable will be measured in the future and is no further part of the master assignment. Before measurements could be performed, the setup had to be modified and the control unit repaired. A vacuum chamber and attributes for impregnation had to be constructed and a new support structure for the MQE measurements had to be designed. The experimental details are found in Chapter 2. The sample preparation is found in Section 2.2. The measurement setup of the transformer, the press and the MQE measurements are described in Section 2.3. The measurements are performed following the protocols described in Section 2.4.

Three samples from the same batch of the DS cable were measured. The first two were not successful since the samples became damaged during the measurements. The first sample was damaged due to the Lorentz forces of the selffield of the cable (see §2.2.1). Press measurements were nevertheless performed on the first sample to test the press set-up. The second sample was damaged because the impregnation was unsuccessful, as was found during the experiments (see §2.2.3). However, from these two sample a lot was learned and the preparation procedure was modified to prevent future problems. The modifications to the sample preparation procedure, set-up and experimental procedure due to the first two sample on the set-up are discussed in the relevant sections in Chapter 2.

The third DS cable sample was successfully measured with respect to the critical current as function of the peakfield and transverse stress, as described in Sections 3.1 and 3.2 respectively. During the first experimental run the press measurements went wrong due to a short circuit over the magnets that energize the press, but the cable sample was not damaged. The problem with the press was fixed, but the setup had to be warmed up to room temperature. Then the critical current was measured at applied fields of 10, 10.5 and 11 T and press measurements were performed with transversal stresses up to 270 MPa. Since the cable was only degraded 2% irreversibly, it was decided that this sample could also be used for the MQE measurements, the results of which are found in Section 3.3. All results for sample 3 are discussed and compared with other measurements in Chapter 4. The conclusions of the measurements are found in Chapter 5.1. Recommendations for future measurements with this set-up are found in Section 5.2.

Chapter 2

Experimental Details

Measuring the critical current in long samples of full-sized Rutherford cables under application-relevant conditions requires a considerable infrastructure in terms of current, and, especially, magnetic field. In order to apply a uniform magnetic field over a straight ∼1 m long cable sample, a wide-bore dipole magnet is needed. When materials become better-performing (as described for Nb_3Sn in the previous chapter), one is faced with the general problem that existing test facilities, constructed with 'older' technology, are stretched to their limits when called upon to investigate 'newer' technology.

A typical example of this dilemma is the FRESCA facility at CERN, which was constructed with a 1.9 K NbTi 10 T magnet for the investigation and quality control of the NbTi cables used in the LHC magnets [13]. Since the LHC upgrade requires Nb_3Sn magnets operating above 10 T, FRESCA results need to be extrapolated to higher field in order to gauge the behavior of the modern Nb_3Sn cable now under development. Indeed, this is exactly the motivation behind the FRESCA II project mentioned before, which seeks to replace the NbTi dipole with a more modern Nb_3Sn one [14]. This explains why not many long-sample experiments are performed on Rutherford cables world-wide.

In order to circumvent this problem, short-sample experiments were designed and realized at the University of Twente already in the run-up to the late eighties and early nineties. A transformer-powered [15] U-shaped cable sample can be fitted in the bore of a relatively simple solenoidal labmagnet, eliminating the need for a high-current power supply and a large-scale high-field dipole. A compact but powerful electro-magnetic press [16] furthermore allows to test the cable samples under magnet-relevant transverse pressure levels.

Even if this infrastructure was constructed many years ago, some of it had not been used for a long period and needed revision, while all of it needed modifications in order to accommodate the present Nb_3Sn cables. The short-sample MQE experiments is new and the instrumentation for these measurements needed to be designed and realized. This chapter describes all these experimental aspects. Section 2.2 gives a description of the investigated cable, while Section 2.2 explains how samples of it are prepared and mounted in the set-up. The measurement set-up itself is described in Section 2.3. The measurements are performed following the protocol described in Section 2.4. Finally, necessary self field corrections and mechanical considerations are found in Section 2.5.

2.1 Sample Description

The DS cable is a Rutherford cable of 40 strands with a keystone of 0.75°, cabled at CERN. The strands are 0.7 mm in diameter and are manufactured by the RRP process by Oxford Superconducting Technology (OST) with a strand configuration of 108/127. This means that 108 of the 127 rods are Nb_3Sn and the center 19 rods are pure copper rods. The cable is optimized for achieving both mechanical stability and minimal damage to the delicate internal configuration of the strands. Figure 2.1 shows a cross-section of the DS strand and of the DS cable. Also a top view of the cable is shown. Tables 2.1 and 2.2 present the key parameters of the strand and cable, respectively.

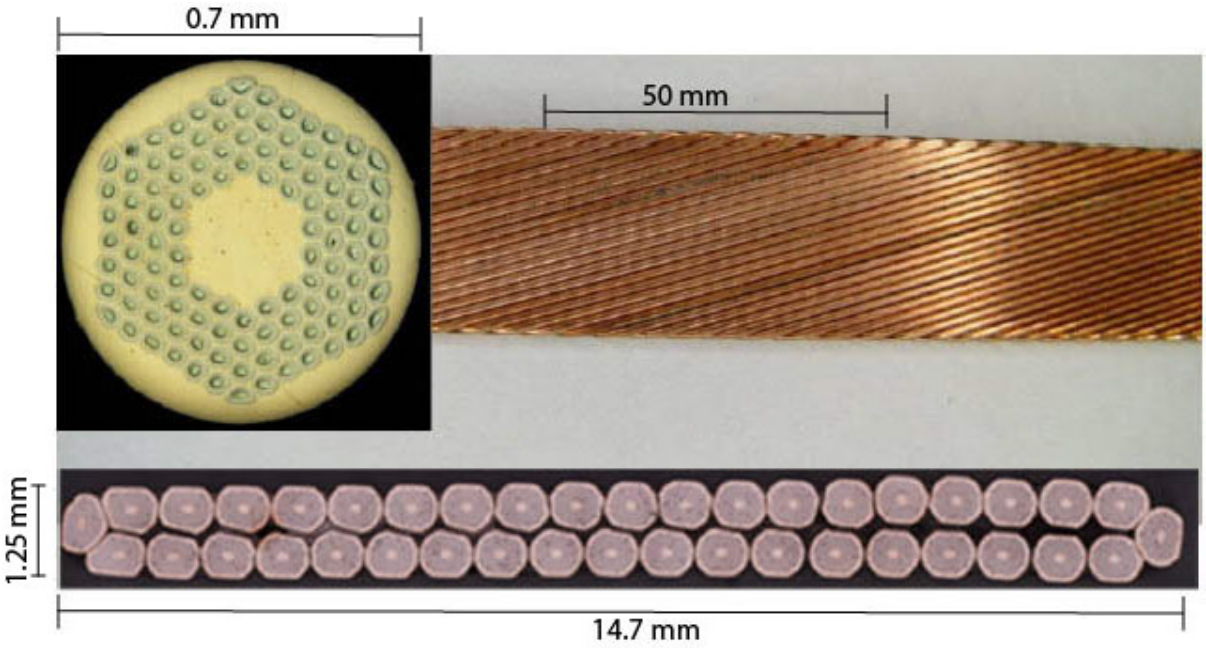

Figure 2.1: The cross-section of the DS strand (top left) and of the DS cable (bottom) as well a top view of the DS cable (top right) [17].

Table 2.1: DS Strand Parameters, RRR is the 'residual resistance ratio', the ratio between the normal-state resistance of the strand at room- and cryogenic temperature. The other parameters are discussed in Section 1.1.

Parameters	Value
Manufacturer	OST
Design	RRP-108/127
Strand diameter	0.700±0.003 mm
Cu fraction	53±3 %
Effective sub-element diameter	<60 µm
Critical current I_c(12T, 4.2K)	>475 A
Critical current density J_c(12T, 4.2K)	>2650 A/mm^2
RRR (after heat treatment)	>60
Twist pitch	14±2 mm

Table 2.2: DS Cable Parameters, the parameters are discussed in Section 1.1.

Parameters	Value
Manufacturer	CERN
Number of strands	40
Width	14.7 mm
Height	1.25 mm
Keystone	0.75°
Twist Pitch	100 mm

2.2 Sample Preparation

2.2.1 Sample Holder

The sample (1) is mounted on a stainless steel U-shaped sample holder (2) as shown in Figure 2.2. The 46 mm long flat 'bottom' of the U-shaped sample holder is in the middle of the high field area of the solenoidal lab-magnet. The 90° bends of the U-shaped holder have a radius of 10 mm. The cable is impregnated on the sample holder (see §2.2.3) and is kept in place by epoxy clamps (3) on the straight 'legs' of the U and by two lateral support plates (4) in the high field area. The ends of the sample are soldered to the secondary loop (5) of the transformer (6) with a resistance of typically 1 nΩ (see §2.3.1). The cable is fixed along these joints by Stycast clamps (7). The epoxy and Stycast clamps protect the cable against the electromechanical forces generated by the magnetic field. The sample holder is fixed to the magnet by the halve circles (8) attached to the sample holder. It was found during the initial experiments that this fixation of the sample is required because the main magnet quenched after a sample quench at an applied transversal pressure of 20 MPa. The exact reason for these magnet quenches remains unclear, but fixing the sample holder to the magnet solved this problem.

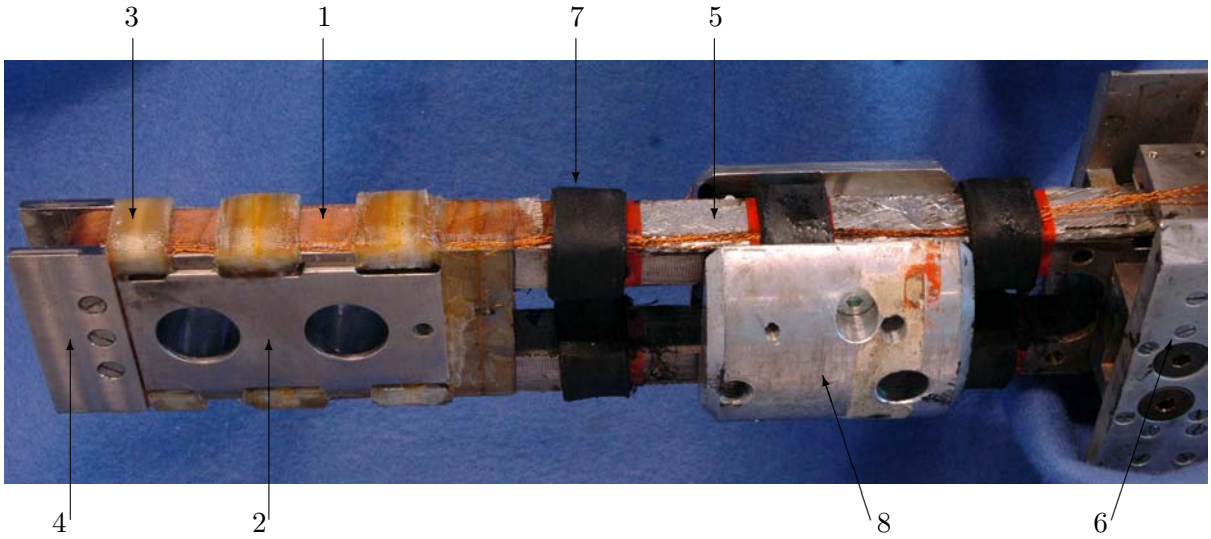

Figure 2.2: The second sample (1) fully mounted on the U-shaped sample holder (2). The cable is fixed in place by epoxy clamps (3) and lateral support plates (4). The joint (5) connects the sample to the transformer (6) en is fixed to the sample holder by Stycast clamps (7). The halve circles (8) fixed the magnet to the sample holder.

All samples show some training quenches before the cable finally reaches its 'true' critical current (i.e. the current level at which a gradual and reproducible voltage build-up is observed instead of a sudden thermal runaway) and is ready for measurements. This well-known trainings phenomenon is caused by energy releases due to Lorentz-force driven movement of the cable or individual strands in the applied magnetic field, which results in inductive voltages. As the sample gradually 'settles' against it supports, its performance will gradually increase over the training quenches, until the cable reaches its final position. The training behavior depends on the preparation quality of the sample. During the training of the cable the quench current I_q is measured by reading out the shunt resistance (§2.3.1). The normalized quench current of the three samples is shown in Figure 2.3. Sample 1 and 3 have a layer of polyimide tape of

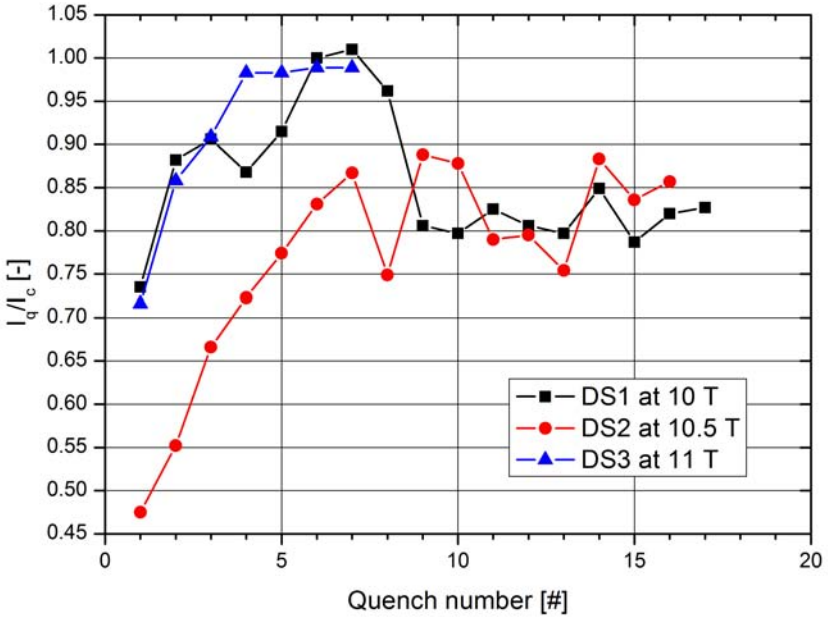

Figure 2.3: The current levels at which the training quenches of the three samples occured, normalized to the critical current of sample 3.

25 µm between the sample and the sample holder, while sample 2 was partially bonded to the sample holder. The difference is clearly seen in the number of training quenches required before I_c measurements can be performed.

The decrease in quench current of sample 1 after the eighth quench is where this sample 'bulged out' under influence of its self-field, as discussed in Section 2.2.3. Sample 2 increased slowly until I_q/I_c value of 0.85-0.90 after which the quench current fluctuates a lot. These fluctuations clearly indicate that the cable does not quench because it exceeds its critical current, but due to random disturbances such as movement of or crack formation in the cable/epoxy sample pack. These might be caused by the ill-defined bonding with the sample holder, which results in local stress build-up caused by the differential thermal contraction between the sample holder and the sample.

Sample 1 became damaged, but nevertheless a critical current could still be determined. The training quench currents before the sample was damaged at 10 T applied magnetic field and after the damage at 11 T applied magnetic field and the critical current afterwards (at 10.5 and 11 T applied magnetic field) are shown in Figure 2.4. It can be seen how the sample reached the expected critical current (i.e. 40 times the critical current measured on a virgin witness strand, see §2.2.2) during the training quenches. However, after quench number 7 the cable was significantly degraded.

From these observations on sample 1 valuable lessons were learned with respect to the fixation of the long current leads (the legs of the U) against the sizeable Lorentz forces, as will be discussed further in Section 2.2.3. At the beginning of the assignment, when the FRESCA II cable was still expected to be the main focus of the experiments, some preliminary tests were performed on the possible influence of sample deformation around the U-shaped holder. The

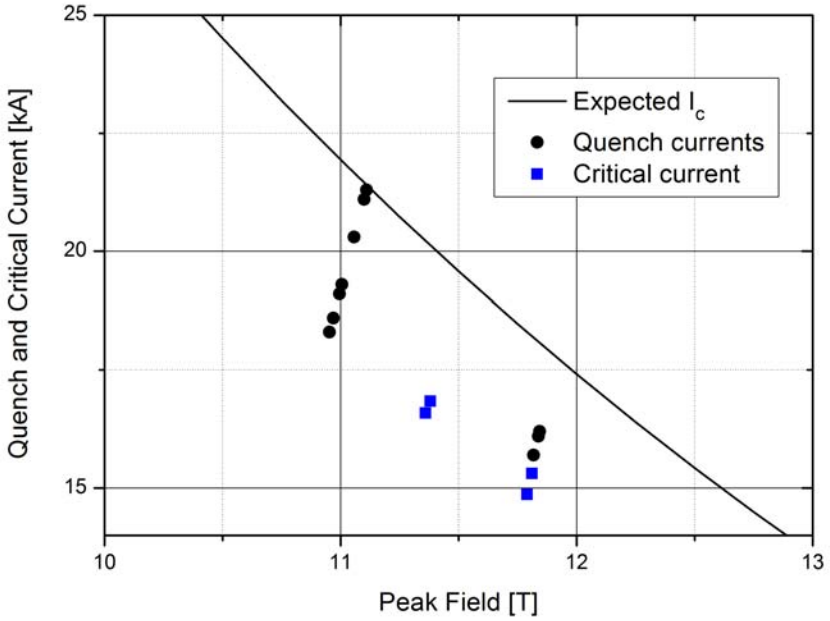

Figure 2.4: The quench currents of sample 1 (black circles) for the training quenches before the cable became damaged at 10 T applied field and quench currents at 11 T after the damage. The blue squares are the measured critical currents. All data are at T=4.2 K.

sample is bent around the corners of the sample holder, which results in compressive strain on the inside of the cable and tensile strain on the outside. This might cause filaments to break. If the strands are damaged in the bending process, the current will redistribute to undamaged strands, causing some strands to carry more current than others and thus influencing the critical current measurements. It is therefore imperative that the cable is not damaged by the bending process.

The Fresca II cable has a cross-sectional area of 21x1.8 mm^2 and is wound from 40 strands of 1 mm diameter. This is a large and stiff cable, which might give problems during preparation. The Fresca II sample will be tested on transverse stress and therefore the question was whether the sample can be bent around a bending radius of 10 to 20 mm so that 46 to 26 mm long straight section remains available in the high field area for transverse pressure tests. To test this, the cable is bent, partially reacted and cross-sectional cuts are made and polished to be examined under a microscope for broken filaments. Broken filaments in PIT wires are known to result in copper diffusing into the strand and tin diffusing to the copper matrix. This will result in the formation of bronze in the filaments and the copper matrix. The bronze is found by the color difference compared to the niobium or copper. Since the fabrication of a new stainless steel holder is costly and the optimal dimensions are not yet certain, a wooden mock-up of the holder is made with a bending radius of approximately 20 mm. It is known that the elastic part of the deformation of the wire does not damage the filaments. The plastic part of the deformation, on the other hand, can result in broken filaments. To find broken filaments by tin leakage, only the plastic part of the deformation is required. Therefore, the sample could be taken off the mock-up mold and put in the oven without support. A quick reaction program

of 12 hours at 650 °C, with a ramping speed of 50 °C/h, is given to the sample. In this time possible diffusion of the copper and tin is already visible if present [18]. The cable is now only partially reacted, but the possible diffusion already occurred, so a full reaction process is not necessary.

Cross-sectional cuts are made in both bends (the corners of the U), the straight part of the high field area (the bottom of the U) and of the current lead (the legs of the U). The current lead is not bent and all damage found in this part is due to the cabling process and not to the deformation of the sample on the holder. To fix all strands during polishing, the cable is fully soldered before the pieces of the cross-section are cut and then embedded in Stycast 2057 under vacuum. The cross-sections are abraded and polished to achieve a micrometer resolution with the microscope.

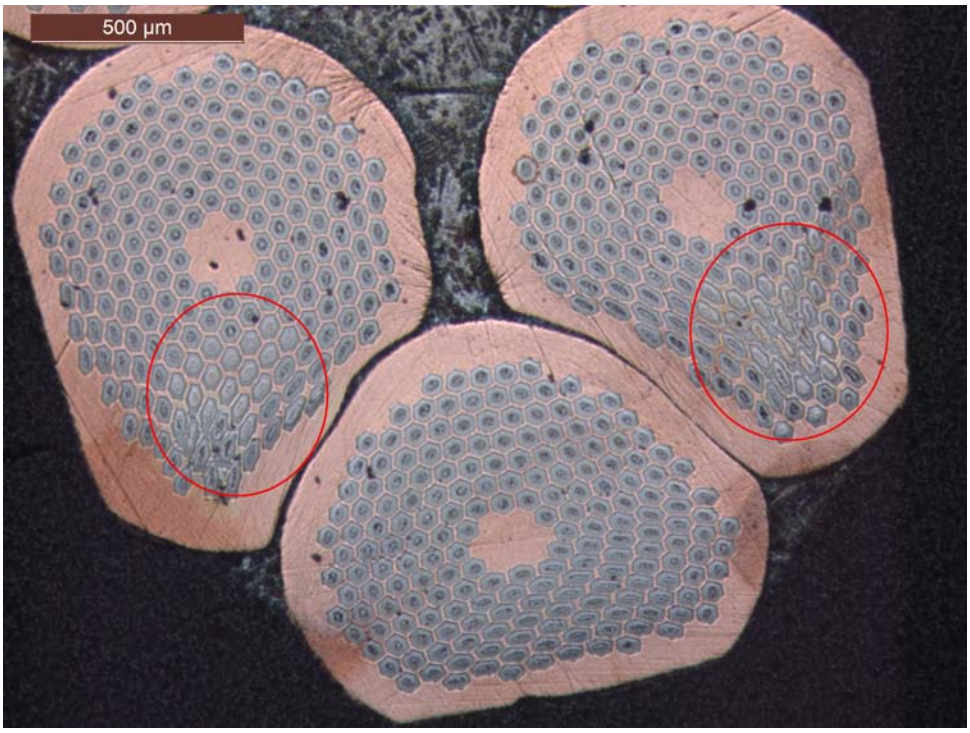

Figure 2.5: Cross-section at the unbent part of the current of the edge of Fresca II cable. The damage to the filaments (seen by the bronze in the filaments), due to the cabling process, is marked with the red circles.

The strands at the side of the cable have many broken filaments, since at this location they are strongly deformed during the cabling process. Damage and deformation at the edge of the unbent part of the current lead is shown in Figure 2.5. The damage that shows up as bronze between and in the filaments is the same over all cross-sections that have a single strand at the edge. The rest of the strands (i.e. those not at the edge of the cable) sporadically have a broken filament, but only a few are found as shown in Figure 2.6 with one bronze filament. The filaments are a little deformed in the bending, but this did not cause broken strands.

The conclusion of the analysis of these cross-sections is that the Fresca II cable can be wound on a U-shape sample holder with a bending radius of 20 mm or larger without broken filaments. In the future, same experiment will have to be performed on a reaction holder with a well defined bending radius of exactly 10 mm. Since no damage at all is found after 20 mm

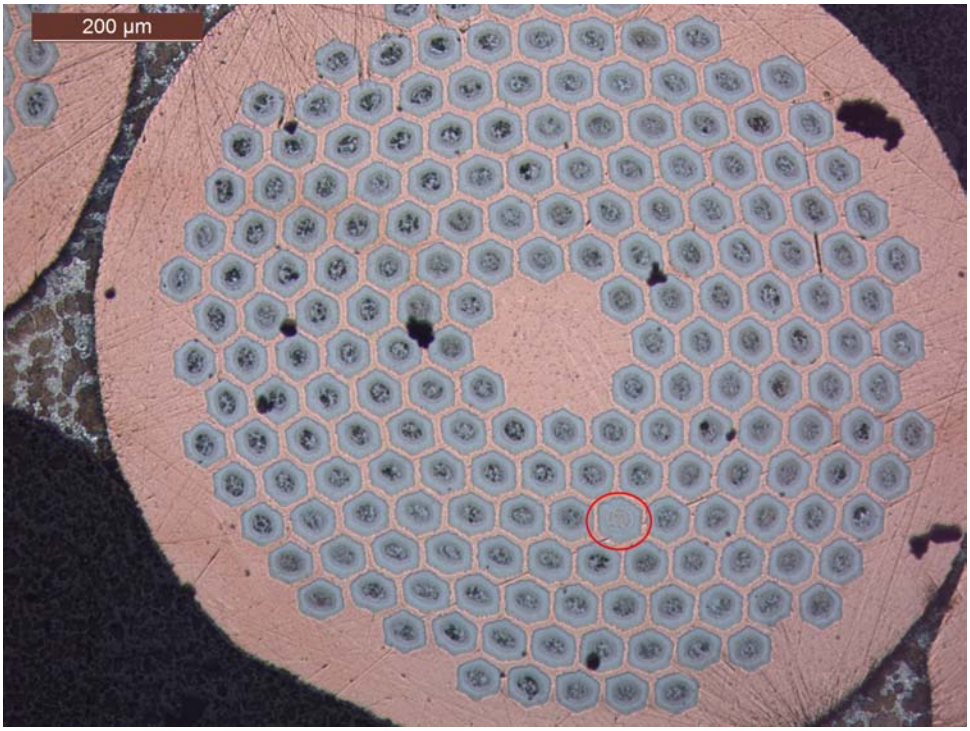

Figure 2.6: Cross-section of a strand at the middle of the high field area of the center of the Fresca II cable. This is one of the few strands in the cross-sections that has a bronze filament (red circle).

bending, the bending radius can be made smaller. During this assignment, the 10 mm bending radius test is not performed because the measurements on the DS-cable had a higher priority. No further reference to the FRESCA II cable is therefore made in the remainder of this report.

2.2.2 Heat Treatment

Nb_3Sn is a brittle material and therefore strands, cables or even entire magnets have to be wound of bent into their desired shape before the heat treatment, when the Nb and Sn is still unreacted and the material is ductile. The cable is reacted on a reaction holder and after the heat treatment mounted on the sample holder. The clamps and supports of the reaction holder keep the cable in the desired shape during the heat treatment, when the Cu is soft and might flow otherwise. Before mounting the sample on to the reaction holder, it is wrapped in two layers of 0.15 mm thick glass fiber matting, which prevents the sample from sticking to the holder.

A virgin witness strand is wound on a standard ITER barrel, shown in Figure 2.7, to be reacted together with the sample. A 'virgin strand' is the term for a strand from the same batch as wires with which the cable was made, but with which nothing happened. This witness strand is used for comparison with the cable sample. Due to the large deformation involved in the cabling process (Figure 2.5), Rutherford cables may suffer a reduction in critical current compared to un-deformed wires and such degradation of the cable can be gauged by comparing the I_c-value of the cable to that of the witness strand. The witness strand will allow to predict the 'ideal' value of the critical current for an undamaged cable by multiplying the I_c of the witness strand with the number of strands. The witness strand is soldered to the current

Figure 2.7: The witness strand on the I_c barrel.

terminals (the Cu rings on either end of the cylindrical holder in Figure 2.7) and by standard I_c measurements its critical current as function of magnetic field is determined.

'Extracted strands' are taken from a piece of unreacted cable. Single strands of 15 cm long are carefully pried loose from the cable and several of them are put in between two stainless steel plates wrapped up in glass fiber matting. These strands will be used to measure the Residual Resistivity Ratio (RRR) on the thick edge, on the thin edge and in the center of the cable. The RRR value is defined as ρ_{300K}/ρ_{20K}. The RRR value gives information about quality of the strands (the Sn leakage in damaged strands discussed above leads to increased impurity scattering in the Cu matrix and hence to a lower RRR value and will also turn out to be relevant for the thermal stability of the cable.

The sample, witness strand and extracted RRR samples are reacted together in a vacuum tube oven. The heat treatment of the DS cable has three plateaus at 210, 400 and 650 °C for 48, 48 and 50 hours respectively. The heat treatment recommended by the strand manufacturer OST prescribes a third plateau of 50 hours at 665 °C, but the RRR resulting from this recipe is around 60, which is too low for stability purposes. Therefore it was recommended to use 650 °C for the third plateau to reach higher RRR values [19].

2.2.3 Impregnation

Nb_3Sn Rutherford cables need to be impregnated to prevent conductor movement and to protect the cable against electro-mechanical stresses applied to the cable. A press experiment on a cable that is not impregnated would result in prematurely damaged filaments and the performance of such a cable would quickly degrade, since the stress in bare Rutherford cables is concentrated at the points where the strands cross each other and can locally reach much higher levels than the overall pressure exerted on the cable. In the case of an impregnated cable the stress is transmitted through the filling material, resulting in a more uniform stress distribution [20].

As seen in Figure 2.2, part of the sample (the bottom of the U and about 1/3 of the legs) is wrapped in glass fiber and two extra layers of glass fiber are added on top of the cable. These 2 extra layers of glass fiber are added to achieve a more hydrostatic stress distribution in the cable. The glass fiber is drawn full with epoxy and hardened in a vacuum oven. The result is a strong layer that forms around the cable to protect it from the forces that will be applied during handling and during the experiment. The Lorentz force due to the combined applied and self-magnetic field must be absorbed by the epoxy. Furthermore, the thermal stability of the cable is also increased since the cable cannot move.

The first and third sample were not bonded to the sample holder. A 25 µm thick polyimide foil was inserted between the impregnated cable and the sample holder. The foil does not stick to epoxy, so the cable can move on the sample holder. It is kept in place by the clamps during the impregnation around the cable and by an anvil and support flanges in the high field area. The second sample did not have polyimide foil between the cable and the sample holder and was therefore partially bonded to the sample holder. Since the stainless steel sample holder shrinks less than the cable when cooled, thermal stresses build up. After removing the second sample from the sample holder it could be clearly seen that the cable was only bonded at a few places, which furthermore resulted in local stress concentrations. As a result, the second sample required a lot of training quenches, while the samples with polyimide foil needed only four to seven training quenches as shown in Figure 2.3.

The sample is transferred from the reaction holder to the sample holder. Voltage pairs are connected to the cable, each time spanning a given length on a single strand and the glass fiber clamps on the legs of the U are made. A flat surface on the bottom part of the U between the support plates is ensured by gently pushing the sample against the holder with a Teflon block. Impregnation is performed by lowering the sample holder with cable slowly and under a small angle in a rectangular recipient of epoxy. This is performed in a vacuum chamber in order to remove all bubbles from the epoxy. After venting the vacuum chamber, any bubbles that remain in the epoxy will shrink under normal pressure and become very small, further drawing epoxy in the glass fiber. Afterwards the epoxy is hardened in an oven. All details of the impregnation can be found in the impregnation protocol included in this report as Appendix A.3.

The impregnation process changed somewhat from sample to sample. The first sample was impregnated adequately, but after one of the quenches during the measurement the cable became damaged on the current lead, due to the electromechanical forces generated by the self field. In Figure 2.8a the damage is shown from the top side. The epoxy cracked open and the the cable was bent outwards. The bending of the cable is even more clearly visible in a side view as shown in Figure 2.8b. The epoxy is locally removed to examine the cable further and the bending is also clearly seen on the un-covered cable. Bending occurred only to the strands at outside of the cable, while those on the inside remained unbent. To prevent this 'bulging out' of the cable in future measurements, the clamps are made wider. The distance between clamp two and three is too large and in the new design the third clamp is made bigger. Also the thickness of the clamps is increased by increasing the width of the anchoring slits in the stainless sample holder. The result is a cable which is better supported with stronger clamps.

For the first two samples, the temperature of the sample holder was regulated. Whereas the first sample was impregnated well, the second one showed many bubbles in the epoxy. During the start of the impregnation there were some issues which needed unforeseen attention and meanwhile the epoxy cooled down to much. The feedback loop of the heaters on the sample holder was not fast and powerful enough to warm it up again. Since the temperature was too low, the viscosity went up and the epoxy could not be drawn in all cracks. Furthermore, a lot of bubbles stayed in the epoxy since the viscosity was too high for them to move out the epoxy.

The inside of the first impregnated cable is shown in Figure 2.9a. It can be seen that there are only a few bubbles between the strands. The impregnation was performed well. The inside of the second cable is shown in Figure 2.9b. There are a lot of bubbles in the epoxy. Between the strands are series of interconnected bubbles (1). Along the edge of the glass fiber, bubbles and pores are found on the surface (2). Finally, large pores are observed between the cable and the lateral support plates. If the viscosity of the epoxy was too low, the bubbles cannot get out

of the epoxy and the gas voids are not pumped. When the pressure in the vacuum chamber is increased to standard pressure, the epoxy is pushed in the holes as the bubbles shrink. This happens in the direction where the epoxy flows and any bubbles remaining will form along the cable (3).

(a) front

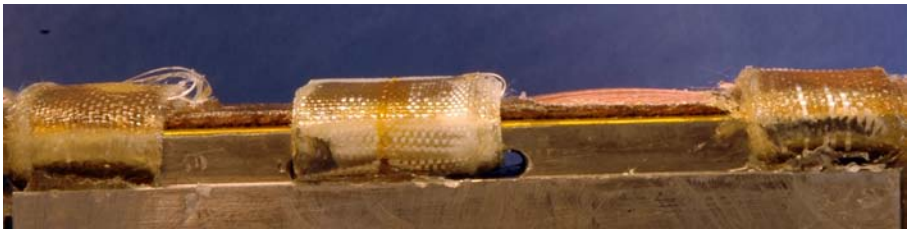

(b) side

Figure 2.8: The damage to DS cable 1.

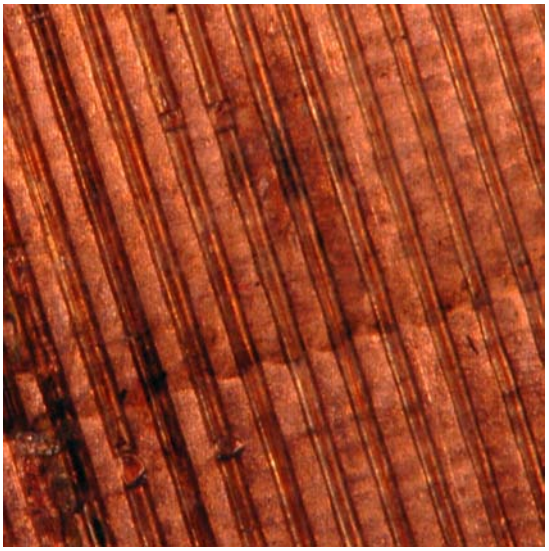

(a)

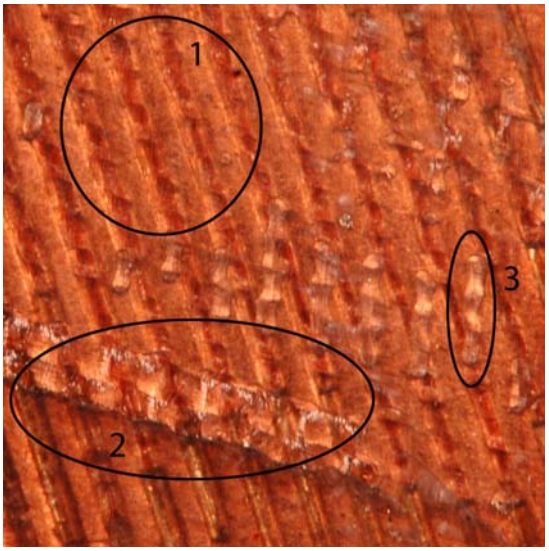

(b)

Figure 2.9: a) Adequate impregnation and b) poor impregnation as visible in pictures from the inside of the cable, where (1) are the interconnected bubbles between the strands, (2) the bubbles at the edges of the glass fiber and (3) the bubbles stretched in the direction of the cable. The strand diameter is 0.7 mm.

No 'proper' critical current (with gradual and reproducible voltage build-up) could be determined of the second sample due to disturbances. By increasing the transverse stress to 20 MPa, the cable might be better fixated. However, the measurement of sample 2 at a transverse stress

of 20 MPa resulted in a degradation of 17-23% of the quench current. It may be assumed that this degradation is caused by the bad impregnation in combination with the local bonding of the sample to the sample holder.

The problem with the impregnation is fixed by adding a second temperature control to the bucket filled with epoxy. Heaters are placed on both sides of the recipient with an extra temperature sensor. Now both the recipient and the sample holder have an individual feedback loop to regulate the temperature. This improved control allows the temperature of the epoxy to be kept constant within a few degrees. This resulted in a proper impregnation for the third sample.

2.3 Measurement Setup

2.3.1 Superconducting Transformer

A superconducting transformer is used to power the cable samples to currents up to 50 kA. The transformer is designed and built at the University of Twente [15] and there are only a few superconducting transformers in the world. The benefits of a superconducting transformer compared to a conventional power supply are:

- The transformer is considerably less costly.
- A conventional power supply needs sizeable copper current leads from room temperature to 4.2 K. Helium consumption will very high due to the large thermal leak and to Joule heating in the current lead. The high-current secondary of superconducting transformer is already fully submerged in liquid helium, while the primary needs only to be powered by a room-temperature power supply of 50 A. The helium consumption of the transformer is therefore negligible compared to a conventional supply.
- The superconducting transformer is small and fits above the magnet in the cryostat. The required room-temperature instrumentation next to the cryostat is small compared to the large conventional supplies.

All the components of the superconducting transformer are shown in Figure 2.10. The transformer consists of a multi-turn primary coil (1) with around it 1.5 turns of the secondary coil (2). Both primary and secondary coils are superconducting and made from NbTi. The secondary coil is soldered to the sample. The primary is connected to the current leads going out of the cryostat to an external power supply. Normal conducting transformers are fully resistive and have a step-response that decays directly. Therefore they can only be operated at AC current. Since the transformer used in the experiment is superconducting, the only resistance lies in the current leads to the power supply in the primary loop and the joint resistance of the connections to the superconducting sample in the secondary. In the ideal case this joint resistance can be neglected and the current induced in the secondary by a step change of the current in the primary will flow forever. In practice, there is a joint resistance of typically 1 nΩ and the secondary current will eventually decay. With a joint resistance of $\sim$1 nΩ and a self inductance of 0.8 μH, the decay time constant of the transformer is about 800 s. Therefore to perform measurements at a stationary current level or to ramp the current at a constant speed, a feedback loop is required that increases the primary current such that the secondary current is at the desired level.

The simplified electrical scheme illustrating the essential principle of the feedback loop is shown in Figure 2.11. A more detailed scheme including the modifications that needed to be made to the electronics is discussed in Appendix E. Both for the experiment itself and the proper

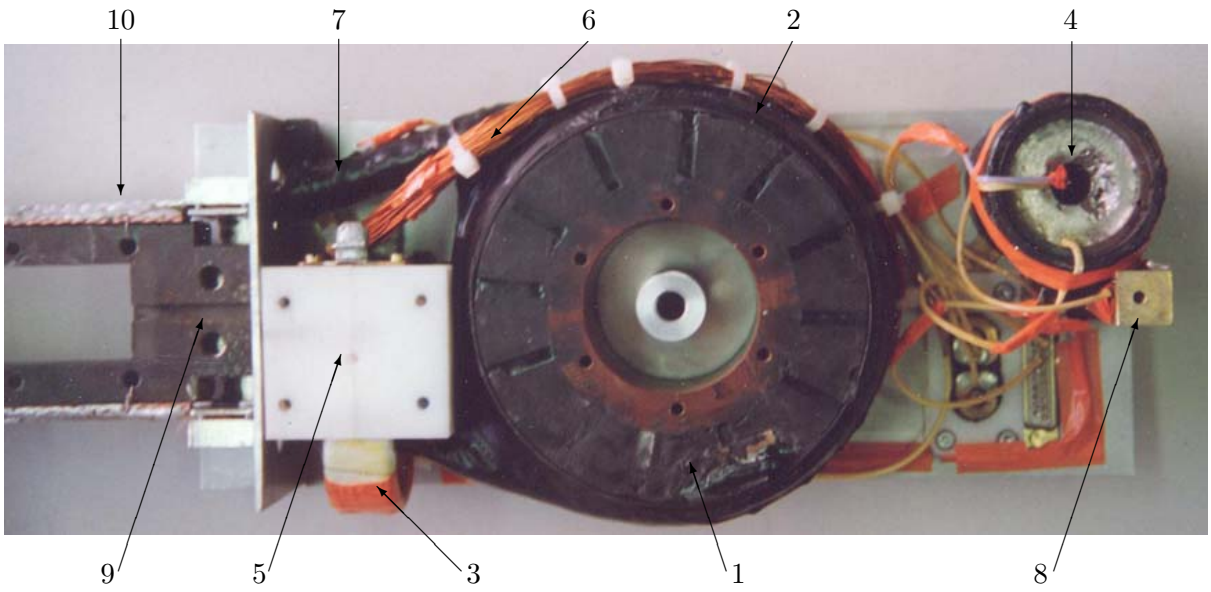

Figure 2.10: The components of the superconducting transformer: (1) the primary coil, (2) the secondary coil, (3) Rogowski coil, (4) Superconducting Shield of Lead-Bismuth with a Hall-sensor in the center, (5) Correction Coil, (6) Calibration Coil, (7) Heater of secondary coil (8) Heater of integrator circuit, (9) Sample Holder and (10) Joint with the sample.

operation of the feedback loop, the current through the sample must be measured accurately. A shunt resistance is not an option, because currents up to 50 kA will cause too much Joule heating and the decay of the current in the secondary circuit will be too fast. Therefore a Rogowski pick-up coil is used to measure the current through the sample. The superconducting Rogowski coil is connected in series with a second superconducting coil with a Hall element. The second coil and the Hall element are placed within a superconducting lead-bismuth shield to eliminate any influence of the stray field of the main magnet on the Hall probe(4). The voltage over the Rogowski coil is given by

$$V_{rog} = M\frac{\delta I_s}{\delta t}, \tag{2.1}$$

where I_c is the current through the secondary coil, t is the time and M is the mutual inductance between the Rogowski coil and the secondary of the transformer. The induced current in the superconducting circuit is then given by

$$I_{cir} = \frac{\int V_{rog} dt}{L_r + L_h}, \tag{2.2}$$

where L_r is the self-inductance of the Rogowski and L_h is the inductance of the coil at the Hall-sensor. Combining Equation 2.1 with 2.2, one sees that I_{cir}, which is measured directly by the Hall-sensor, is in principle always proportional to I_s. In practice, there is an extra motivation. The high-sensitivity Hall probe has a limited dynamic range and therefore the current in the pick-up circuit is compensated back to zero. To achieve such a null-measurement, the signal from the Hall sensor drives a voltage-controlled current supply that powers an extra compensation coil (5) which is coupled to the Rogowski coil and cancels out the current in the pick-up circuit induced by the current (changes) in the secondary circuit. The current needed for the compensation coil is given by

$$I_{comp} = \frac{I_s}{N} \tag{2.3}$$

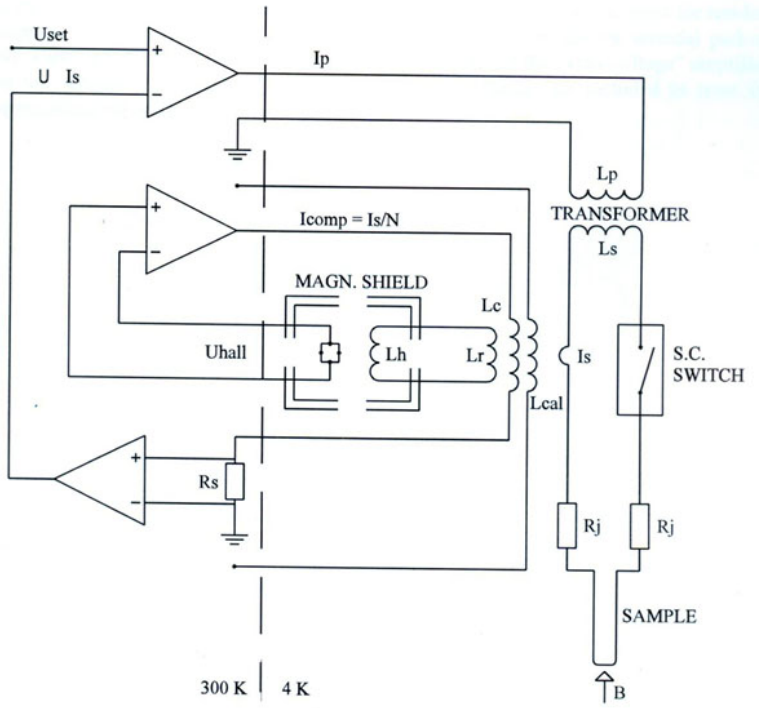

Figure 2.11: Schematic of the feedback loop of the superconducting transformer.

where N is the number of turns in the compensation coil. This way the pick-up circuit can be made very sensitive and this time the current through the compensation coil is proportional to the secondary current. By connecting a shunt resistance in series with the compensation coil, the current through the compensation coil can be measured and thus the secondary current can be measured. In the setup a 10 mΩ shunt resistance is used, resulting in a ratio between the shunt voltage and the secondary current of 1 mV/kA. This voltage is used in combination with the 'set' current to regulate the current in the primary coil. The decay due the joint resistance is in the secondary circuit compensated by this feedback-loop by gradually increasing the primary current, so that the current in the secondary coil stays constant with a fluctuation less than 1 A. By slowly increasing the 'set' voltage, the current in the sample can be ramped.

Due to the joint resistance, the current in the primary slowly rises in order to keep the current in the secondary stationary. The maximum allowed primary current is 50 A for this transformer. The measuring time is thus limited by the maximum current through the primary coil. The faster the decay in the secondary coil, the faster the current will increase in the primary coil. A low joint resistance is therefore important. Also measuring at high currents decreases the measuring time, since most of the primary current (for typical measurements on the DS sample about 30 A) is already 'used up' to ramp the secondary current to the desired level.

In order to achieve longer measuring times a switch is used to reverse the polarity of the primary. This would also work with a voltage-controlled bipolar power supply, but since no bipolar power supply available in the lab was compatible with the control unit, the method with the switch is used for all measurements described in this report. First the transformer is negatively powered while repeatedly quenching the secondary circuit at low negative currents. These quenches are invoked with the aid of a heater attached to this circuit (7). Note that the negative sample current is kept low in order to avoid 're-training' of the sample in the opposite

direction (see §2.2.1). This procedure is repeated until the primary current is at the desired level. Due to the forced quenches, the secondary current is zero at this point, next the primary power supply is turned off. The change in the primary current will induce a sizeable current in the secondary loop. Once the current in the primary coil is zero, its polarity can be commuted, the control of the primary supply is switched from manual to feedback mode and the feed-back loop can pick up the current. With this polarity reversal method, the primary current starts at 0 A while the secondary current is already for example at 15 to 18 kA, resulting in a much longer measuring time. A detailed manual with proper protocols for operating the superconducting transformer is included as Appendix B.

A calibration coil (6) is used to calibrate the pick-up circuit and to make an estimate of the measuring error. Heaters are added which allow to decay the current through the secondary coil (7), the pick-up circuit (8) and to heat the superconducting shield. Below the transformer different sample holders can be connected. All samples must be soldered to the transformer to ensure the low joint resistance.

A control unit which automates the feedback loop contains all amplifiers that control the power supplies. The control unit that was used in the past did not work anymore. This is fixed by replacing the feedback electronics from the control unit with a spare one that was manufactured together with the control unit for MIT [21]. The testing of the electrical unit is performed on a NbTi cable which was already on the transformer and it was verified that with the new electronics the same currents were measured on this sample as previously [22]. As an added complication, the current in the primary coil of the transformer also induces a current in the Rogowski (ideally the mutual inductance between the primary and the Rogowski should be zero. In practice it is small, but non-negligible). This undesired effect can only be partial compensated by the new control unit. In the calibration, an extra compensation factor of 4.73 mV/A between the primary and secondary current is measured for the new control unit to compensate for the coupling between the primary and Rogowski. The electronics are calibrated as described in Appendix E. Further details about the transformer can be found in [21, 23].

Due to the high Lorentz forces acting on the cable, the setup must be well-supported inside the magnet. A new aluminum support structure is designed that can be used for $I_c(B)$ and MQE measurements (§2.3.3) in the 15 T magnet. This support can also be used for the big Fresca II cables. The new support structure transmits the Lorentz forces only to the flanges of the magnet and not to the magnet itself. The stainless steel anvil supporting the measurement section is kept in place by three bolts on each 2 disk springs to apply adequate stress to the sample during the cooling down and during the measurements at 4.2 K.

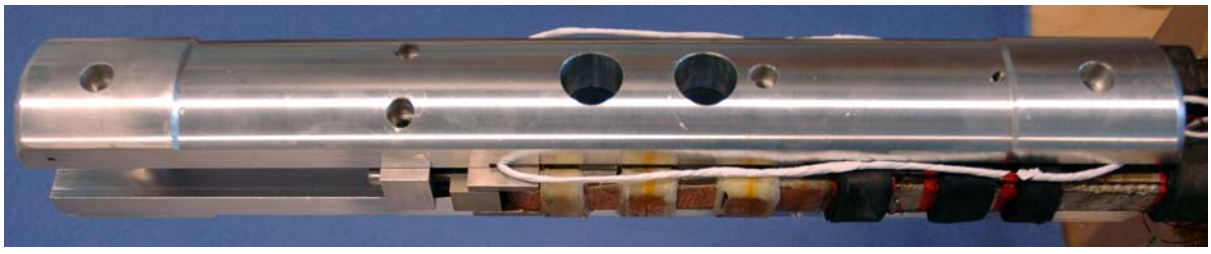

Figure 2.12: The sample holder with aluminum supports for MQE measurement.

2.3.2 Cryogenic Press

The cryogenic press consists of two superconducting NbTi pancake coils which are connected in series to generate a repulsive force between the coils. The press can generate a maximum force of 240 kN perpendicular to the high field area of the cable. The anvil is custom-made for the DS cable from stainless steel. The area over which the anvil presses is 45x15.2 mm^2 which results in a maximum transverse stress of 350 MPa. The corners are rounded to prevent stress concentration at the corners of the anvil. On top of the anvil, there are four layers of 50 µm polyimide tape for a good contact between the anvil and the cable, resulting in a more homogeneous stress distribution over the sample. Both the anvil as the cable have some roughness which smoothened by the polyimide tape.

A schematic of the press is shown in Figure 2.13. The two pancake coils are made from a Niobium-Titanium wire which is wet wound (with alumina-filled Stycast 2850 epoxy) around stainless steel formers. The bottom coil firmly connected to the sample holder by a thick steel cylindrical sleeve assembly which fits smugly around the holder and is attached to it with two thick fixation pins. The top coil is therefore pushed upwards when a current is passed through the press coils. A piston transmits this force to the anvil which pushes on the sample.

For the third DS sample, the press setup is modified so that the epoxy clamps can be made bigger and no epoxy has to be removed from the clamps to make it fit inside the outer sleeve that transmits the reaction force. This modification will also allow for larger samples such as the Fresca II cable to be well-supported inside the cylinder.

The force generated by the press is given by

$$F_p = I_p^2 \frac{dM_{12}}{dz} \pm I_p I_A \frac{dM_{1A}}{dz} - mg, \tag{2.4}$$

where F_p is the force generated by the press, I_p the current through the press, I_A the current through the background magnet, M_{12} the mutual induction between the press coils, M_{1A} the mutual induction between the upper press coil and the main magnet, m the mass of the upper press coil and the inner cylinder, g the gravitational acceleration and z_2 is the position of the upper press coil. The plus sign is when I_p and I_A are in the same direction and a minus sign for opposite direction. The correction for the main magnet depends on the field direction of the press and magnet. For the experimental configuration used in this assignment, this is determined by Verweij [24] as

$$F_d = I_p \left[I_p(82.47 - 2.71 z_2) \pm 0.23 I_A \right] - 110. \tag{2.5}$$

I_A and I_p can be determined with an accuracy < 0.1 A. The error in the force is mainly determined by the error in z_2 and a systematical error in dM_{12}/dz due to imperfections in the press. The estimations for the error are $\Delta I_p < 0.1\%$, $\Delta I_A < 0.1\%$, $\Delta z_2 = 0.1$ mm and $\Delta(dM_{12}/dz) = 0.2$ follows $\Delta F_p/F_p \ < 2\%$ [24].

The extensometer that was used in the past had to be rebuilt. A new design is made from titanium and is shown in Figure 2.14. A pin positioned on the upper press coil sticks through the cover against the extensometer. By reading out the extensometer, variations in the distance between the two coils can be monitored and the force between them can be calculated.

The extensometer is made from a strip of titanium alloy (6Al-4V) with four strain gauges bonded to it. These four strain gauges are connected in a full Wheatstone Bridge configuration with two of them in tensions and the other two in compression. The full bridge configuration is very sensitive and linear to the extension. More information about the design and the

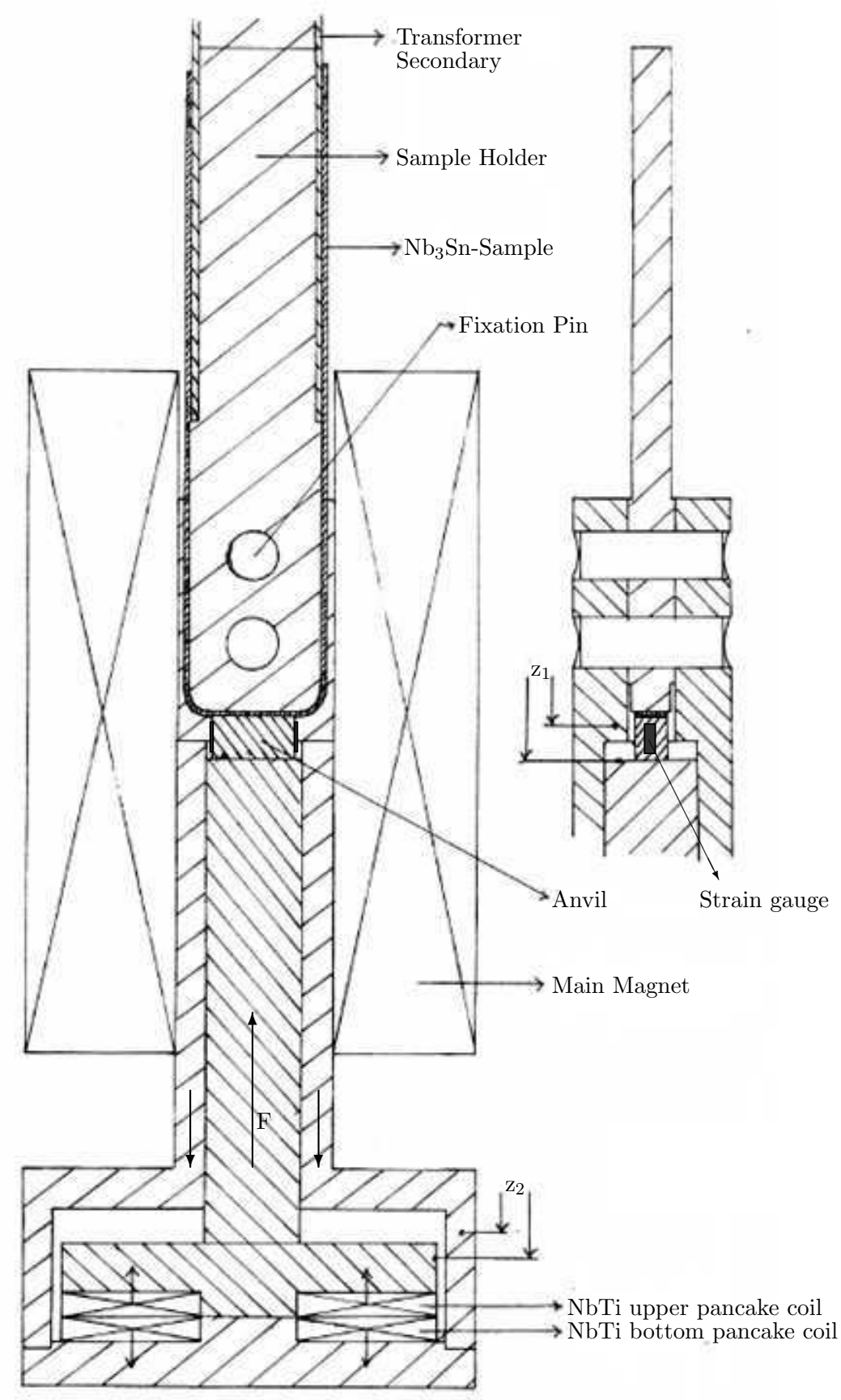

Figure 2.13: Schematic of cryogenic press.

Figure 2.14: The extensometer mounted on the press.

calibration of the extensometer is found in Appendix C. The extensometer can measure with an accuracy of 1 µm within a range of a few millimeters and a sensitivity of 1.046 mV/mm. While the extensometer might be very accurate so that small extensions such as creep can be measured with micrometer accuracy, the systematical error on the absolute position value is much larger (estimated to be 0.1 mm). The systematical error comes from the positioning of the extensometer since the length of the arm might be slightly off. The whole system is under tensile and compressive strain due to the forces generated by the press. Most of the increase in distance between the press coils is due to this as shown by Verweij [24].

Even if the first sample was damaged due to the bulking out of the current lead, it was nevertheless decided to submit it to transverse stress in order to test the press set-up and to get some preliminary results for this type of cable. The reduced I_c of the two half twist pitch voltage pairs is shown in Figure 2.15. When the transverse stress is increased the critical current reduces immediately. I_c at 100 MPa is approximately 3% lower than the one initially observed without pressure, but repetition of the 'unstressed' measurements once the force is brought back to zero shows that this reduction is fully reversible. It can be concluded that irreversible damage is absent at least up to 100 MPa.

However, the cable is only damaged at the current lead and not in the high field area. Therefore a critical current in the order of the quench currents of the training quenches before the damage occurred is expected in the high field area. However, since about half of the current lead has many broken filaments, the current has to be redistributed trough the other strands. The effect of this is that in the high field area the current trough some strands is much higher than the current through other strands (i.e. the strands, which are damaged in the current lead, have a lower current). Since the voltage pairs were connected to the strands that were not damaged, the critical current could still be measured. However, when one strands is already at its critical current, while the other still has a low current. Therefore the current in the total cable is much lower than the expected current determined from the witness strand. Voltage pairs 1 and 2 have a different critical current reduction as function of transverse stress compared to each other. Since only a part of the strands are at the critical current, the current in some strands can be redistributed to other strands. This might cause the difference in the critical current degradation as function of transverse stress between voltage pair 1 and 2.

In principle the force and thus the transverse stress can be calculated if the current in the press as well the position indicated by the extensometer are read out. The third sample showed no degradation up to 150 MPa, which is above expectation. Therefore, in order to double-check these measurements the setup is warmed up and additional strain gauges are glued to the short sides of the anvil, providing an independent measurement of the stress on the sample, as

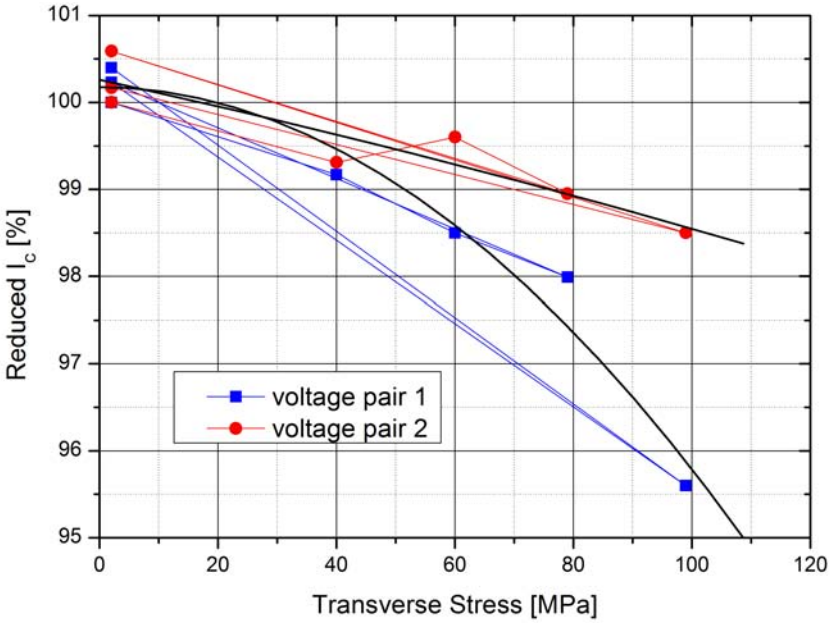

Figure 2.15: The critical current reduction as function of transverse stress recorded with the half twist pitch voltage pairs of DS sample 1. The red and blue solid lines connecting the data points indicate the order of the measurements (∼0; 40; 60; 80 and 100 MPa and then an additional measurement once the force has been brought back to 0). The black lines are polynomial fits to the data points.

described above. The data from the extensometer is analyzed in Appendix D and compared to the data from the anvil deformation with as conclusion that the press worked properly.

2.3.3 Minimum Quench Energy Setup

The minimum quench energy (MQE) of NbTi [6] and some (sub-sized) Nb_3Sn [7] Rutherford cables was already studied in large-scale facilities such as FRESCA, but for the reason meantioned in the introduction to this chapter there were no measurements up till now on modern full-size Nb_3Sn magnet cables. After the press measurements the sample only showed a 2% irreversible reduction of the critical current due to filament cracking. since this type of damage is not expected to influence thermal stability issues significantly, it was decided to attempt a MQE experiment on sample 3 of the DS cable. For this experiment, basically the same instrumentation was used as in the FRESCA experiment, adapted to the short-sample set-up and to the present cable geometry. This adapted experiment is described below.

For the MQE measurements the goal is essentially to deposit a controlled amount of energy into a single strand and to see whether the current-carrying cable will recover from this local disturbance. A 100 µs heat pulse is sent through a resistive heater which is in direct contact with the single strand. To do this, a heater array of nine heaters is attached to the middle of the flat high field region of the cable sample, as shown in Figure 2.16. Three heaters are placed at 1 mm from the thin edge, three are placed in the center of the cable and three are placed

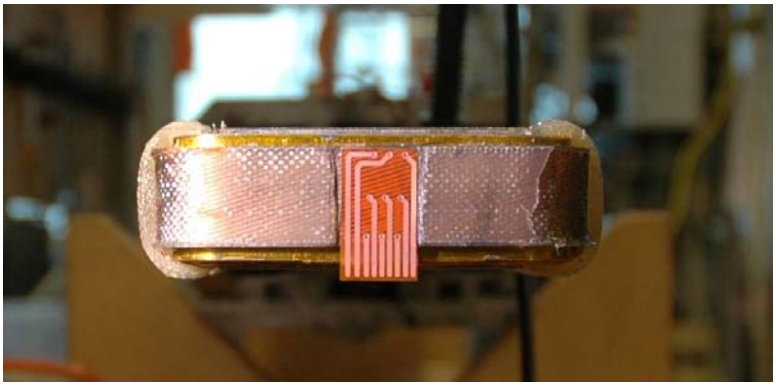

Figure 2.16: The point heaters placed on the cable sample.

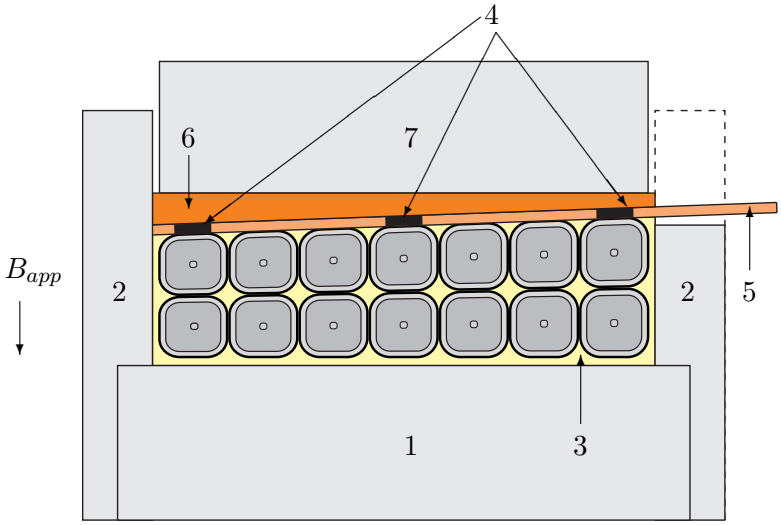

Figure 2.17: Cross section of the sample at the location of the heaters. As described earlier, the cable is placed on the sample holder (1), enclosed by two plates (2), and impregnated with epoxy resin (3). At the location of the MQE experiment, the top layer of epoxy is removed over the whole broad side of the sample to fix the heaters (4) integrated in a polyimide foil (5). Several layers of extra polyimide foil (6) are used to create a flat surface on which a stainless steel anvil is placed (7). The number of strands in the cable is reduced for illustrative purposes.

at 1 mm from the thick edge. This allows to test the MQE on three qualitatively different locations within the cable, each with a redundancy of three.

A schematic of the MQE heaters is shown in Figure 2.17. The outer layer of epoxy is locally removed by a high speed abrasive tool to make place for the heater assembly. The assembly consist of a polyimide foil with copper tracks on it and small holes for the actual resistive heaters. The lateral support plate on one side of the cable is modified to make space for the electrical connections. The heaters are prepared from a mixture of graphite and epoxy which is used to fill up the holes of the polyimide foil. Once hardened, these filled-epoxy heaters are directly on the stands and the heat from the pulse will quickly be transferred to the strand, without a layer of insulation between the heater and the cable. On top of the heater assembly, a key-stoned spacer consisting of several extra layers of polyimide foil is used to reconstruct the same surface as before the insulation was removed and separates the heaters from the helium bath. On top of the whole a stainless steel anvil is placed to apply adequate stress and thus to

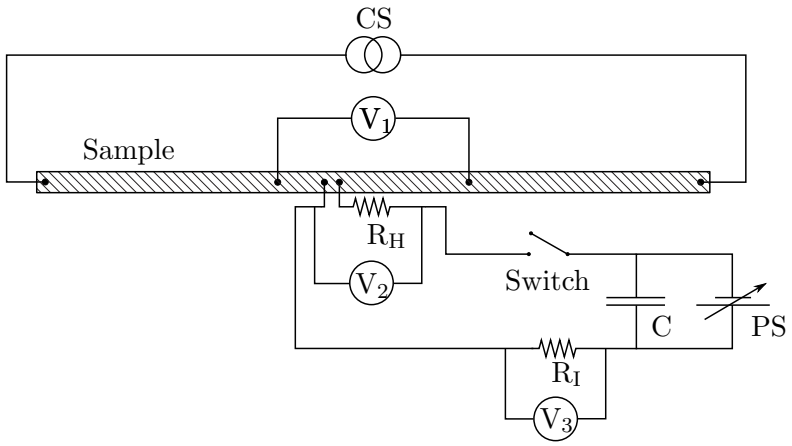

Figure 2.18: A simplified scheme of the MQE heater. With the capacitor C fully charged by the power supply PS, the switch can be closed to discharge C through the heater R_H. The voltage $V_1$is then monitored with a digital oscilloscope (triggered by the same switch) to determine whether the cable recovers (Q<MQE) or not (Q>MQE). The voltage V_3 across the reference resistor R_I is used to determine the heater current. Together with the voltage V_2 across R_H, this allows to work out the exact amount of heat Q deposited during the pulse.

counteract the electromechanical forces and to push the heaters against the sample, ensuring good electrical contact.

A schematic of the electronics controlling the MQE heaters is shown in Figure 2.18. The current is passed through the heater and uses the superconducting strand as current return path. Note that the heater current is sufficiently small (I_H ∼1-6 A) compared to the strand current (I_s ∼500 A for a test current of 20 kA and 296 at 11.85 kA) and has therefore no effect on the stability of the cable other than by heating R_H. A four point measurement is performed over the heater and the cable to determine the amount of heat deposited by the pulse. Note also that part of the heat deposited in the heater is cooled away by the helium bath or will not transfer to the heater before the cable quenches or recovers. Only a part of the heat actually contributes to the effective quench energy. De Rapper [7] calculated this so-called heater-efficiency to be 0.52 for these graphite epoxy heaters used in other MQE experiments. Further details about the MQE heater preparation can be found in Appendix A.5.

2.4 Experimental Protocol

2.4.1 Critical Current

The voltage pairs span one half, one and two transposition pitches (50, 100 and 200 mm) of the cable to measure the critical current. All voltage pairs are twisted and connected twice with 2.5 mm transposition for redundancy. The voltage pairs are soldered to individual strands, ensuring that each tap within a pair contacts the same strand. Extra voltage taps are connected across the joint to measure the joint resistance directly and to determine the quench location. Each voltage pair is monitored with a nanovoltmeter. The secondary transformer current is measured over the shunt resistance and the primary current with a zero flux measuring system.

When performing measurements on a Rutherford cable with a small bending radius, the current will redistribute between the strands and therefore needs to cross the copper matrix. (the flat measurement section experiences the highest perpendicular field and therefore has the

lowest critical current. Due to their transpositoin, the strands do not 'enter' this high field zone simultaneously so that in the bends neighboring strands may be on different potentials. These lateral potentials differences drive a current redistribution.) In the measurements, this is observed as a small linear resistance R which is commonly called a the resistive foot. Taking also into account the instrumental offset on the nanovolt meter E_{offset}, the measured electrical field will be

$$E = E_{offset} + IR + E_c \left(\frac{I}{I_c}\right)^n . \tag{2.6}$$

Only the last term in this equation stems from the actual superconducting transition that we are interested in (see §1.1). In order to determine I_c the resistive foot must be subtracted from the measured electrical field to negate the voltage built-up due to the current redistribution. The correction for the resistive foot is illustrated in Figure 2.19. The critical current is determined as the current value at the point where the fit crosses the criterion of E_c=10^{-5} V/m. The n-value is the slope on the loglog plot. To find the best fit to the measurements, the root mean square (RMS) deviation of the fit is minimized by a minimalisation function of Matlab. The RMS deviation between equation 2.6 and the measured data is given by

$$RMS = \sqrt{\frac{1}{N}\sum_N \left(E_{offset} + IR + E_c \left(\frac{I}{I_c}\right)^n - E_m\right)^2}, \tag{2.7}$$

where N is the number of data points and E_m are the data points of the measured electrical field.

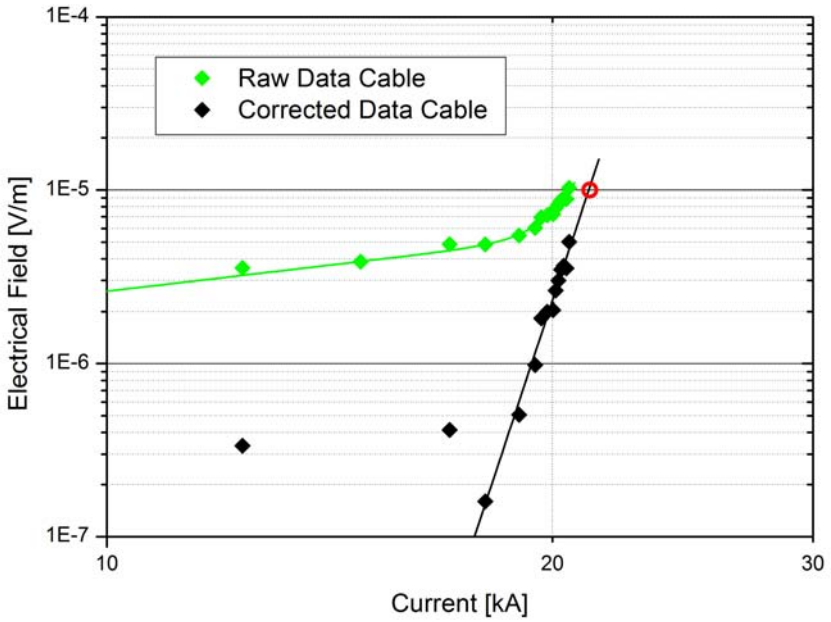

Figure 2.19: Illustration of the I_c-extraction method. the green symbols represent the as-measured $E(I)$ data (in this case at 10 T applied magnetic field), while the black symbols represent the power-law terms in equation 2.6. I_c is determined by extrapolating this power law to the voltage criterion $E_c = 10^{-5}$ V/m (red circle).

The procedure of the measurements starts with measuring two data points at zero current to determine E_{offset}. Then the current is ramped up (by changing the polarity of the primary power supply as described in Section 2.3.1) to a starting current of typically a few kA below the expected I_c. Smaller current steps are taken closer to I_c, ending with steps of 100 A. This continues until a voltage is measured which belongs to a current just below the quench current. Then points are measured at 15, 10 and 5 kA for an accurate estimate of the resistive foot. These points are taken last while lowering the current back to zero, in order to have enough measuring time with the transformer at high current levels. At each current level, the nanovoltmeters are allowed to settle for 30 sec before the voltage is recorded.

2.4.2 Transversal Stress

The critical current dependence on transverse stress is determined by first measuring the critical current at a certain transverse stress level and then repeating the measurements at 'zero'-stress. (Note that this 'zero-stress level corresponds to a relatively low but finite transverse stress level (50 MPa) chosen to be adequate to support the high field area of the cable without causing degradation to the cable significant I_c reduction). Each time the transverse stress is reduced back to this 'zero'-level, the reversible part of the I_c-reduction is thus removed and the remaining reduction at this stress level is purely due to irreversible degradation. By cycling the transverse stress in this way, the transition to the irreversible part of $I_c(\sigma)$ curve can be determined. When a reduction of 1% is determined, the transverse stress will be increased by steps of 50 MPa, where at each stress level I_c is determined to validat that the 1% reduction is irreversible over the whole range of stress levels.

2.4.3 Minimum Quench Energy

For accurate measurements, the resistance of the MQE heaters should stay approximately constant. A large change in the resistance means the contact resistance between the strand and the heater has changed and the heat transfer between them will most likely also be changed. In order to reach a constant resistance, the heaters have to be 'trained' to bond well with the stands. Before heater training, the resistance of the heaters was in the range of 16 to 136 Ω.

The training procedure is carried out during cool-down of the setup. The cryostat is filled with liquid nitrogen to a level above the heaters. All heaters are trained by sending the same 100 µs pulses as for the MQE measurement. Each time pulses are sent with a given voltage level across the capacitor C (Figure 2.18) until the heater resistance settles and a new series of pulses is started at a higher voltage. This is repeated until the deposited energy is larger than the energy levels used in the measurement. The training procedure is performed both at 77 K and 4.2 K. After training, the heaters typically have a resistance between 3 and 11 Ω.

During each measurement, the current in the cable is increased with 200 A/s. When the next desired current level is reached, a heat pulse is delivered with one of the heaters. The cable will either quench or recover. If the cable recovers, the current will redistribute so that less current will be in the target strand than before the pulse (the strand has become effectively more stable). However, for accurate measurements the current distribution in the cable should remain the same. Therefore the sample current has to be reset after each measurement. In order to keep the overall measurement time and He consumption within reasonable limits, the step size between successive quench energies is chosen in such a way that MQE is determined with an accuracy of 5%.

2.5 Correction factors & Mechanical consideration

2.5.1 Magnetic Self Field Correction

A 3D model is created with the finite element program COMSOL to simulate the self field of the cable. From the self field, the peak field on the windings can be estimated as the superposition of the applied background field and the sample self-field. For the MQE measurements on the two edges or in the middle of the cable, it is important to determine the peak field on individual strands.

In the model, the whole U-shaped cable including the keystone is simulated. The detailed current distribution in a Rutherford cable is complicated to simulate, since its strands are twisted. In the simulation this is simplified by assuming a homogeneous current density throughout the cable. Around the filamentary zone within each strand (and thus around the whole cable) is a copper layer through which no current flows below I_c. This layer is excluded from the simulation, so that the simulated peak field (which will be found at the edge of the cable), is the field experienced by the filaments themselves.

The cable has a keystone which means that one side is more compressed than the other side. The compaction factor of the cable thus varies over its width [25]. Therefore the strands are packed more closely together on the thin edge than on the thick edge. This implies that the current density at the thin edge is a little higher ($\sim$8%) and on the thick edge somewhat lower ($\sim$-7%). Compared to the self field determined assuming a homogeneous current density, the magnetic field on the thin edge will thus be slightly increased while the magnetic field on the thick edge will be a little lower (these corrections were not taken into account).

The correction factor for the magnetic peak field of the DS cable on the windings due to the self field is 0.0521 $\pm$ 0.0019 T/kA.

For the MQE measurements the peak field is simulated at the heater location, so either in the middle or at 1 mm from both sides of the cable. For accuracy, the mesh density at these locations is increased and the peak field correction is determined over an area of a single strand. The correction factors for the MQE measurements are shown in Table 2.3.

Table 2.3: Peak field correction factors for the MQE measurements on the DS cable.

Heater number	Location	B_x [T/kA]	B_y [T/kA]
1	Thick edge	0.025	0.036
2	Center	0.032	-0.004
3	Thin edge	0.025	-0.034

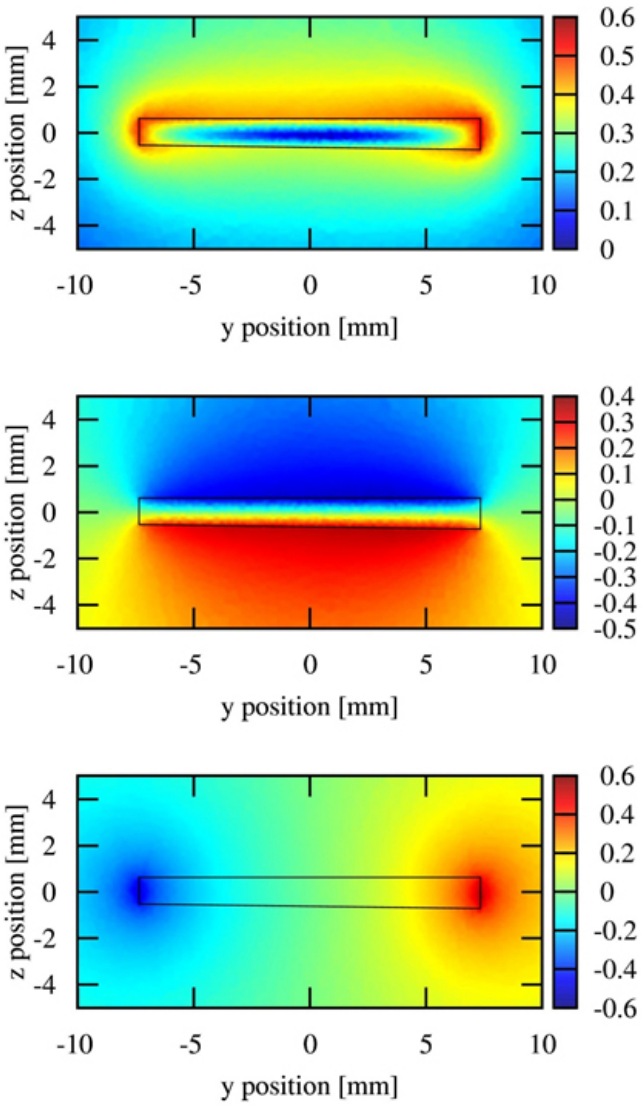

Figure 2.20: Self-field of the U shaped sample powered with 10 kA, expressed in tesla. From top to bottom; total magnetic field magnitude, horizontal field component and vertical field component. The cross-section is taken through the middle of the high field sample section.

2.5.2 Mechanical Considerations

The high current flowing through the sample in a high magnetic field generates large Lorentz forces. The cable is protected against these forces by the impregnation, by the lateral support plates and by clamps. Nevertheless, these forces still need to be supported by the sample holder and are eventually transmitted to the superconducting magnet. An estimate is made of these forces with the same model as used for the magnetic field corrections. The forces are calculated for the DS cable and for the Fresca II cable and are shown in Tables 2.4 and 2.5 respectively. The simulations are performed for the I_c and MQE measurements in the 15 T magnet for magnetic peak fields up to 14 T. From the simulated forces, it can be seen that the Lorentz force decreases with magnetic field in the range from 10 to 14 T (i.e. the critical current decreases faster than the field increase).

The forces in the high field area are calculated over the entire high field area, including the sample bends. The two straight current leads of the sample have a length of 40 cm. In this section, the largest part of the force comes from the radial component of the applied magnetic field above the magnet. The current that can flow through the cable is estimated from witness strand data measured at CERN with the aid of a scaling law [4] (i.e. a accurate numeric description of the critical surface that allows to inter- or extrapolate measured data to other magnetic field values, see Section 1.1). The current will be a little lower in the experiment due to the cabling degradation. So the forces calculated form the worst case scenario.

The field change $\delta B/\delta t$ generated by the sample during a sample quench is high and may trigger a quench of the main magnet surrounding the experiment. Unfortunately the risk of quenching the 15 T magnet with these samples was deemed too high and therefore I_c measurements were only performed in the 11 T magnet, which results in a maximum magnetic peak field of around 12 T.

Table 2.4: Forces simulated on the DS cable.

Peak field [T]	Current [kA]	$F_{y,highfield}$ [N]	$F_{z,highfield}$ [N]	$F_{y,currentlead}$ [N]	$F_{x,currentlead}$ [N]
10	26.1	-14948	-400	3733	834
11	22.2	-14614	-289	3648	598
12	18.8	-13799	-207	3443	424
13	15.9	-12926	-148	3224	299
14	13.3	-11819	-104	2947	205

Table 2.5: Forces simulated on the Fresca II cable.

Peak field [T]	Current [kA]	$F_{y,highfield}$ [N]	$F_{z,highfield}$ [N]	$F_{y,currentlead}$ [N]	$F_{x,currentlead}$ [N]
10	47.1	-26573	-1148	6581	2682
11	40.1	-25951	-832	6437	1944
12	34.0	-24824	-598	6164	1397
13	28.7	-23145	-426	5752	996
14	24.1	-21275	-301	5291	702

Chapter 3

Results

The first sample became damaged by the electromechanical forces and the second sample was poorly impregnated. The results from these measurement were used to improve the measurement setup for these high-J_c Rutherford cables, as is described in Chapter 2. This chapter therefore presents only the results obtained with the third sample. The magnetic field dependence of the critical current is shown in Section 3.1. The transverse stress dependence of the critical current is given in Section 3.2. In Section 3.3 the thermal stability measurements are shown.

3.1 Magnetic field dependence of the critical current

For the critical current measurements, the current in the sample is ramped at 100 A/s. Only four training quenches were needed for the third sample (§2.2.1, Figure 2.3). the sample is initially trained in an applied magnetic field of 11 T. After measuring the critical current at 11 T, the field is lowered to 10.5 T and 10 T. As discussed in Section 2.5.2, the Lorentz forces on the cable increase with decreasing field and at both fields the cable required one additional training quench before I_c could be determined.

Press measurements were initially performed on the cable up to a transverse stress of 150 MPa without any degradation. However, during these measurements a sudden change in resistance suggested that there was a short circuit somewhere in the press set-up. Since it was uncertain whether the press operated correctly and the sample really was under this transverse stress, the setup was warmed up. At room temperature no fault could be discovered, but a cryogenic contact could not be excluded. Therefore, to be completely sure that the press works properly, two stain gauges are now added to the short side of the anvil as discussed in Section 2.3.2, while extra insulation is added to the circuit powering the NbTi press coils to prevent any chance on a short.

After the cooling down following these adaptations, two additional training quenches are needed before critical current measurements could be performed. The critical current is again determined at 10, 10.5 and 11 T applied magnetic field. Only voltage pair 3 and 4, each spanning one twist pitch length, could be used for critical current measurements. The other voltage pairs gave no clear signal. The critical current values measured before and after the thermal cycle are shown in Figure 3.1, together with the optimal critical current as expected from the witness strand measurements. The blue diamonds represent the data obtained before the thermal cycle. They show a degradation of 6% compared to the witness strand. The green triangles correspond to the critical current measurements performed after the thermal cycle and show an increase of 3% in the critical current compared to the critical current measured before the thermal cycle.

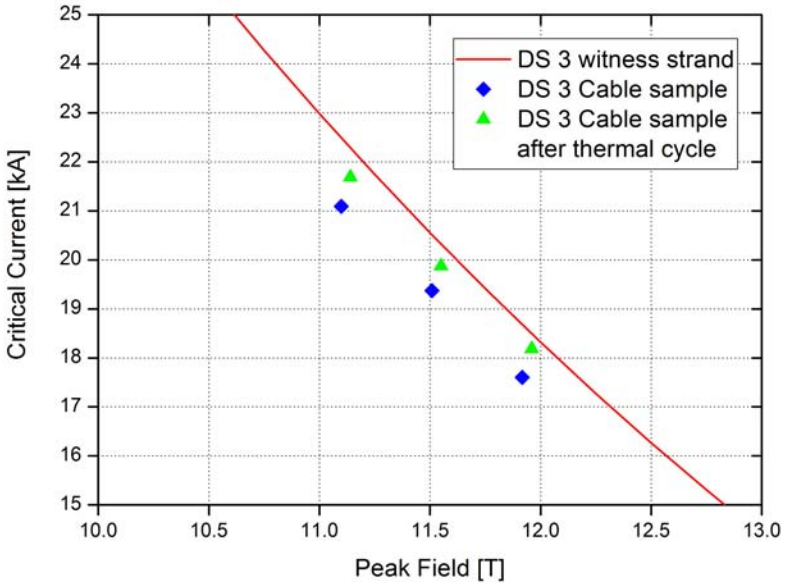

Figure 3.1: The critical current of the DS cable at T=4.2 K (symbols) plotted as function of peak magnetic field and compared with 40 times the critical current of the witness strand. The cable critical current is measured before and after a thermal cycle.

The degradation of the cable is also evident when comparing electrical field versus current data of the cable and the virgin witness strand, as in Figure 3.2. Here the data of the virgin witness strand measured at a peak magnetic field of 11.28 T on the filamentary zone is compared the cable data measured at a peak magnetic field on the windings of 11.10 T. Both the raw data and the data corrected for the resistive foot (see §2.4) of the cable is shown together with the power-law fit to the data. The raw measurements (blue dots) of the witness strand are shown with the current multiplied by 40 (the number of strands) for accurate comparison, while the red dots represent these same data, but decreased by 6% in current in order to compare the degradation directly. Since the magnetic peak field on the witness strand is a little higher than that on the cable, the expected critical current derived from the witness strand should be a little lower than the critical current of the cable. Taking this into account, it can be seen from Figure 3.2 that there is indeed a degradation of approximately 6% compared to the virgin witness strand.

The n-value of the cable and of the virgin witness strand is shown in Figure 3.3 as function of peak magnetic field are shown. It can be seen that the n-value determined from the cable data is close to that of the witness strand and thus almost no change occurred in the n-value due to the cabling process. However there is more scatter in the n-value of the cable, since the $E(I)$ window that can be sampled in these measurements is smaller than the one measured with the strand.

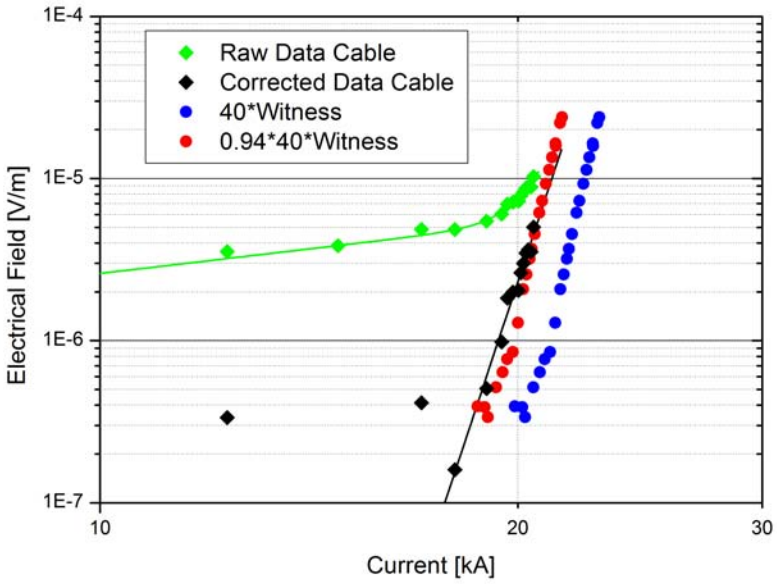

Figure 3.2: The electrical field - current data measured at a peak field of ∼11.2 T on both the cable sample (green diamonds) and the witness strand (blue circles, current scale multiplied by 40). The ohmic foot in the cable data is corrected for (see §2.4.1), yielding the black diamonds, while the strand data is further multiplied by 0.94 (red circles) for direct comparison with the cable data.

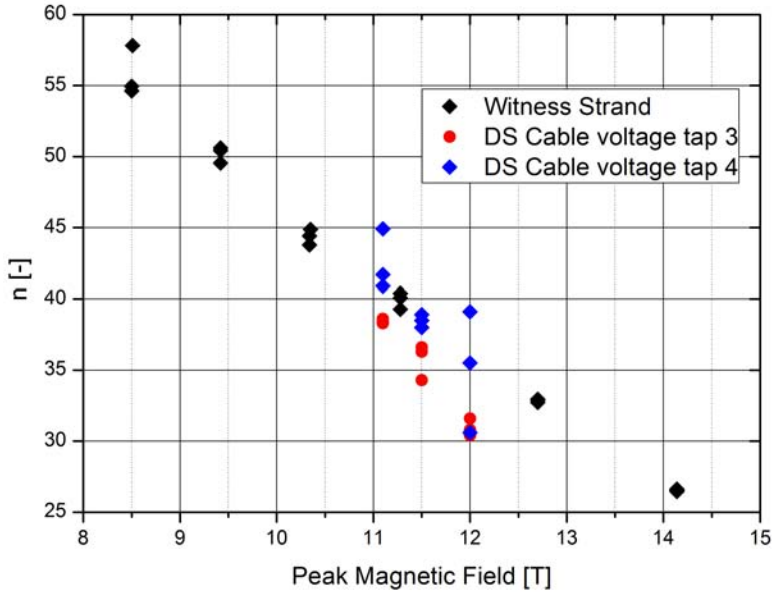

Figure 3.3: The n-value of the witness strand and the cable as function of peak magnetic field on the filamentary zone of the strand or the windings in the cable.

3.2 Transverse stress dependence of the critical current

The critical current is measured at transverse stresses up to 270 MPa at an applied magnetic field of 10 T. After each measurement at a certain transverse stress level, an extra measurement is performed at 'zero' stress to determine the irreversible stress degradation. The 'zero' stress level is chosen to be 2 MPa for transverse stress measurements up to 210 MPa. At that point 1% irreversible degradation was observed when the stress was reduced to 2 MPa. However, at 50 and 100 MPa no degradation was measured, so the 'degradation' measured at 2 MPa was actually not irreversible at 50 and 100 MPa. The strain gauges on the side of the anvil indicate that for transversal stresses below 20 MPa, only one side of the anvil makes contact with the sample as shown in Figure 3.4. The transverse stresses calculated from the strain gauges on either side of the anvil are compared to the values calculated from the current through the press and voltage over the extensometer. From this figure it can be seen that at a certain transversal stress the strain gauges no longer sense any deformation of the anvil. The strain gauge on the side that remains in contact with the sample the longest shows no strain until a transverse stress of 7.5 MPa is applied to the sample. The error on the transverse stress measurements is therefore taken to be this value of 7.5 MPa.

It was concluded that the 'reversible degradation' at the 2 MPa level is most likely caused by a local and ill-defined stress build-up since the anvil only touches the sample at one side. To measure the irreversible degradation in the remainder of the measurements, the 'zero' point is chosen at 50 MPa where the cable has no degradation and is in full contact with the anvil. The average of the first measurements between 40 and 80 MPa is taken as the I_c value without degradation.

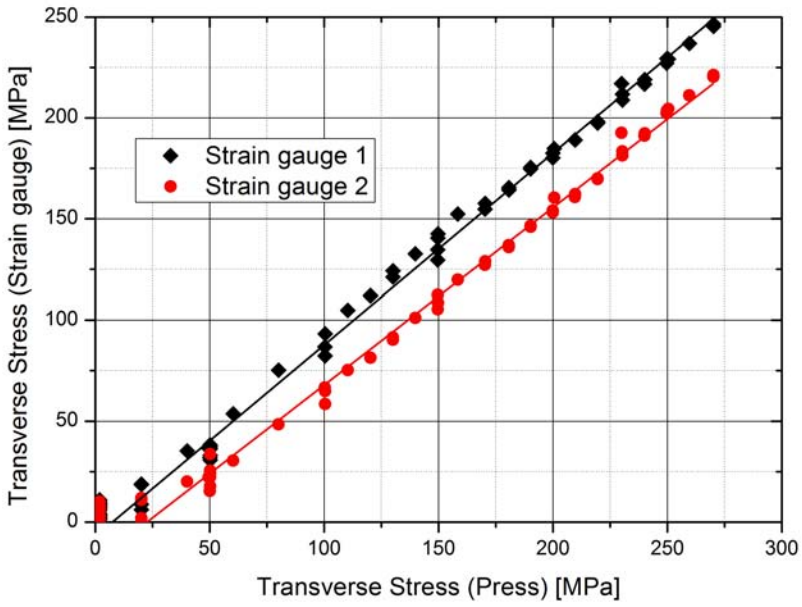

Figure 3.4: The transverse stress calculated from the strain gauges on the side of the anvil, plotted against the transverse stress calculated from the current in the press and the extensometer.

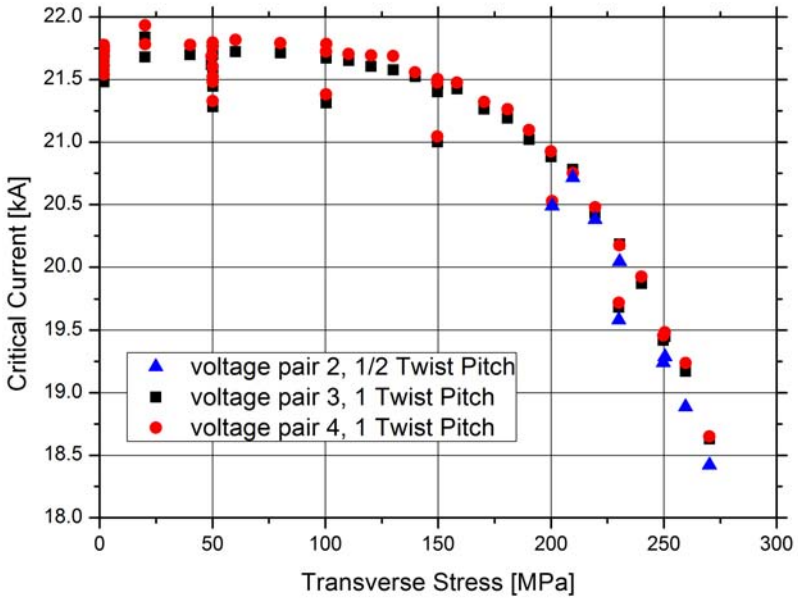

Figure 3.5: Critical current deduced with voltage pair 2 (1/2 twist pitch) and voltage pair 3 and 4 (1 twist pitch) as function of transverse stress at 10 T applied magnetic field.

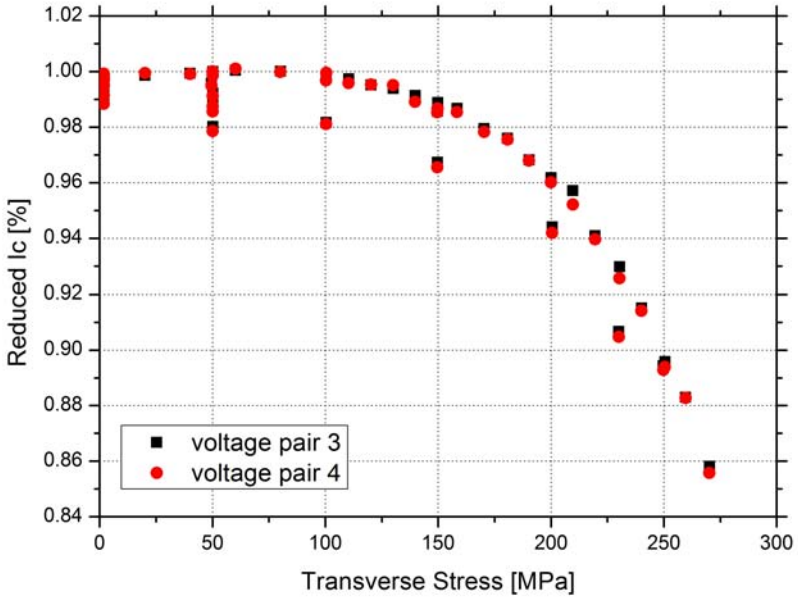

Figure 3.6: Reduced critical current measured with voltage pair 3 and 4 as function of transverse stress at 10 T applied magnetic field.

The critical current as function of transverse stress is shown in Figure 3.5. Voltage pair 3 and 4 could be measured over the whole range, with voltage pair 4 yielding a slightly higher critical current than pair 3. Above 200 MPa, voltage pair 2 (which previously indicated just noise) started to record reproducible V-I curves from which the critical current could be determined. There is no clear difference found between the 1/2 twist pitch measurement with voltage pair 2 and the 1 twist pitch measurements with pairs 3 and 4.

The reduced critical current values measured with voltage pairs 3 and 4 are shown in Figure 3.6. Both pairs show the same reduced critical current as function of transverse stress and thus the same degradation. The results from voltage pair 2 could not be normalized, since no points under the 200 MPa were recorded.

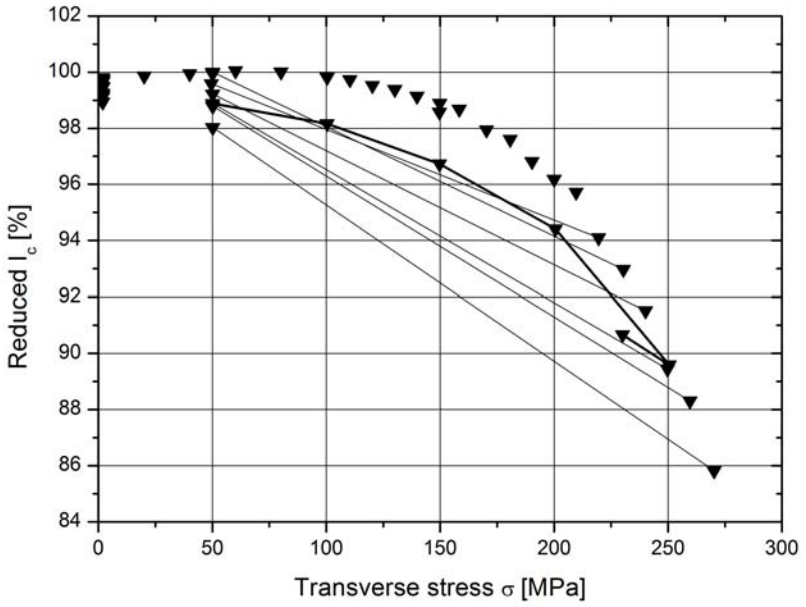

Figure 3.7: Reduced critical current measured at T=4.2 K and B=10 T with voltage pair 3 as function of transverse stress. The thin lines connect a high stress measurement to the low stress measurement measured directly after it. The thick lines belong to the points measured after a maximum stress level of 250 MPa, which results in a 1% irreversible degradation. All measurements are at T=4.2 K and B=10 T.

In Figure 3.7 all measurements of voltage pair 3 are shown. The thin lines show the return lines from a measurement at a high transversse stress back to the 'zero' point. It can be seen that the irreversible degradation gradually increases when the maximum transverse stress is increased. The thick line connects a series of measurements taken after 1% irreversible degradation was measured at 250 MPa.

The reduced critical current is shown together with the irreversible degradation of the DS cable in Figure 3.8. Only the first point measured at any given stress level is plotted. A fourth order polynomial is fitted through the points. In gray, the irreversible part of the degradation is shown as function of transverse stress. At 250 MPa there is an 11% degradation of which 1% irreversible. At 270 MPa there is a 14% degradation of which 2% irreversible.

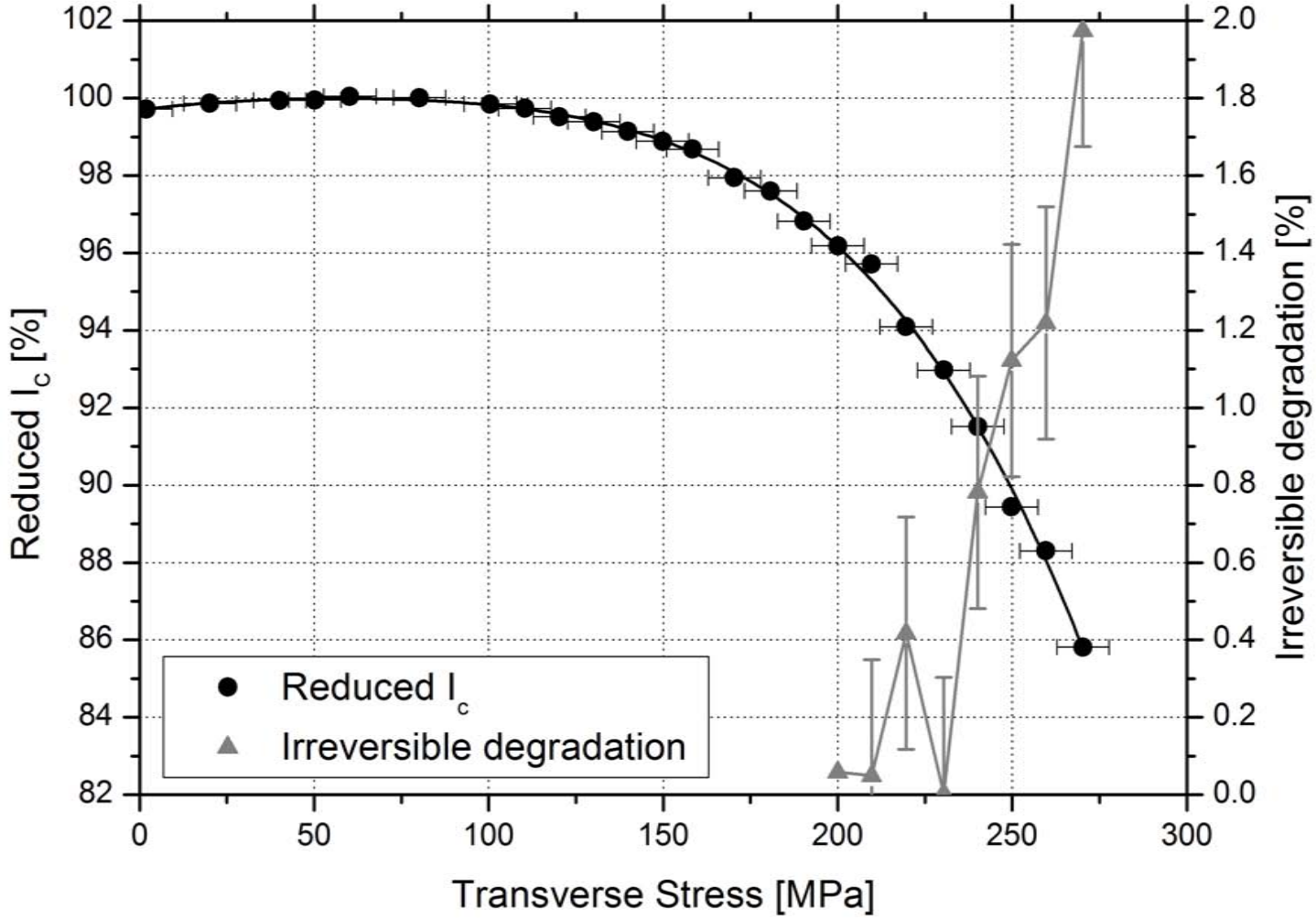

Figure 3.8: Transverse stress sensitivity of the critical current and irreversible degradation as function of transverse stress. All data are recorded with voltage pair 3 at T=4.2 K and B=10 T.

3.3 Thermal stability

For the minimum quench energy experiments the same cable sample is used as for the press measurements. The cable is 2 % irreversibly degraded during the transverse stress measurement, but it is expected that for MQE measurements this is not a problem. After preparation of the heaters (see §2.3.3) and cool-down the critical current is re-measured to see if the cable is further degraded due to mounting procedure of the heater assembly. The critical current measured is 0.5% higher than the initial critical current measured prior to the press experiment (§3.1). This implies that during the thermal cycle the sample not only recovered from the 2% irreversible degradation caused with the transverse stress measurement, but even increased 0.5% further in critical current. However, the sample did become unstable close to I_c and many sample quenches were required to obtain the data points needed to calculate the critical current. The cable even quenched sometimes at stationary current levels while the voltmeters were settling. Since the MQE is not measured close to the critical current, this high-current instability is no problem.

3.3.1 Field dependence

In Figure 3.9 the MQE as function of magnetic peak field is shown. The MQE is determined with three different heaters: one in the center, one on the thin edge and one on the thick edge. The open symbols show the thermal stability at the nominal current (11.85 kA) that will be used in the DS magnet. The closed symbols show the thermal stability at a higher test current of 20.00 kA. Unlike in previous measurements on NbTi and Nb_3Sn cables (see §1.1), there is no clear transition shown between the single strand- and the cable regime. At all the applied magnetic fields in the range from 2 to 10 T the cable is stable at a test current of 20 kA and therefore a magnet with a nominal current of 11.85 kA can be expected to be stable at all field within its operating range.

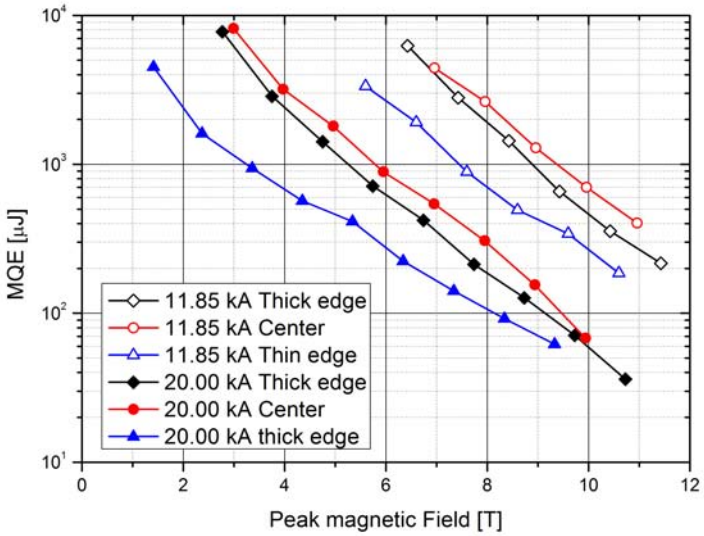

Figure 3.9: The minimum quench energy measured as function of the local peak magnetic field at three different representative locations. The open symbols are data gathered with a test current of 11.85 kA and the closed symbols with a test current of 20.00 kA.

The thick edge has a slightly lower thermal stability than the center of the cable. The thin edge, however, yields a thermal stability that is a factor 2 lower than the center. The RRR-measurements on the extracted strands reveal a RRR value of 80 for the center and thick edge part of the sample, but only of 40 at the thin edge, presumably due to diffusion barrier damage resulting from a higher deformation during cabling (see also §2.2.1). A lower RRR implies a lower thermal conductivity and higher electrical resistance, both of which lead to a lower thermal stability. (Note that only one RRR measurement is performed on the extracted strands, so that this conclusion is tentative. Nevertheless, the results are in line with those of the MQE measurements).

3.3.2 Current dependence

The thermal stability tested with the center heater as function of the test current at three different applied magnetic fields of 7, 9 and 11 T is shown in Figure 3.10. Note that at the center of the cable, the peak field is approximately equal to the applied magnetic field. The local magnetic field at the edge heaters is current-dependent due to the magnetic self field corrections and thus cannot be used to determine the 'pure' current dependence of MQE. The magnetic self-field corrections at the location of the center heater, on the other hand, are negligible.

The transition between the steeper cable- and less steep single strand stability regimes is less clear-cut than in previous measurements performed on Nb_3Sn Rutherford cables [26], but it is nevertheless visible. At 11 T, I_{kink} is approximately 10 kA, at 9 T it is approximately 13 kA and at 7 T approximately 14 kA. When comparing these data to the magnetic field dependence shown in Figure 3.9, it suggests that at a test current of 11.85 kA there is a transition between 9 and 10 T applied field, but that it is too weak to be noticeable.

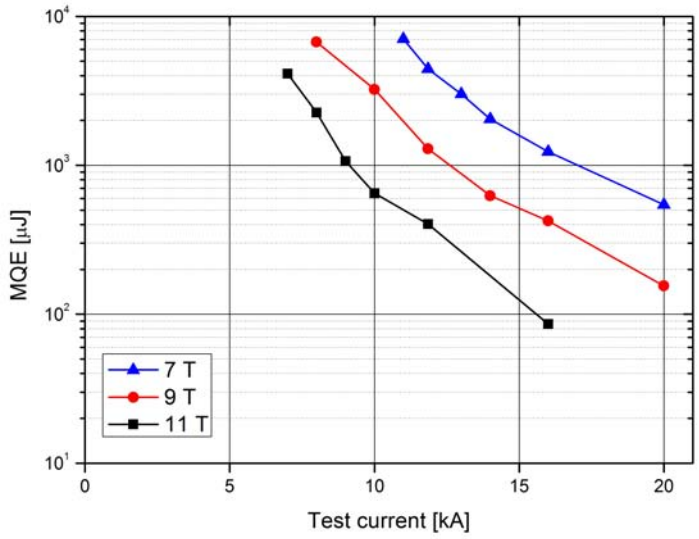

Figure 3.10: The minimum quench energy in the center of the cable as a function of the test current, measured at 4.2 K at three different magnetic fields.

Chapter 4

Discussion

The experimental results that were obtained in this assignment are presented in Chapter 3. They are further discussed and put in context in this chapter. In Section 4.1 the measurements over short samples are reviewed. The voltage build-up along the sample is only over the high field area, while the voltage pairs span a larger length. The experimental magnetic field dependence of the critical current of the DS cable is compared to the design criteria of the DS magnet.

The transverse stress sensitivity depends strongly on the precise stress distribution over the sample. Therefore it is important to discuss the results in terms of different pressure components. A stated goal of the assignment was to validate this cable for the application in the DS magnet for the LHC upgrade, as discussed in Section 4.2. At LBNL, CERN and Fermi lab, related research is performed into the transverse stress sensitivity of Nb_3Sn cables. These literature data are compared to the results of the DS cable.

The results of the MQE measurements are discussed in Section 4.3. They are compared to other MQE experiments on Nb_3Sn and NbTi Rutherford cables. From the MQE and the RRR measurements, the damage due to the cabling process is discussed also in terms of stability. The DS cable displays only a weak transition between the single-strand and cable stability regimes. The differences between our measurements and literature results on similar cables are discussed and possible reasons are suggested.

4.1 Magnetic field dependence on the critical current

Short sample measurements on Rutherford cables can involve complications caused by unequal current distribution among the different strands within the cable [27]. In our case, the straight sample section between the bends in the high magnetic field region is 45 mm long. Furthermore, the total magnetic field is non-uniform across the width of the cable with the peak magnetic field at the thick edge. Only half of the strands cross the thick edge in the high magnetic field area and thus the peak magnetic field on the filaments within a strand is not the same for all strands in the cable. The strands on which voltage pairs 3 and 4 are connected cross the thick side of the cable in the high field area and thus experience the magnetic peak field. Note that both critical current and n-value are magnetic field dependent.

In previous experiments on this type of sample holder measurements were performed where I-V curves were recorded from different strands. A distribution was demonstrated in the U-I curves collected on different strands. Weijers [28] demonstrated experimentally that this distribution is only marginally influenced by the transverse stress or by the selffield of the cable. The distribution is mainly caused by the changing orientation of the background magnetic field

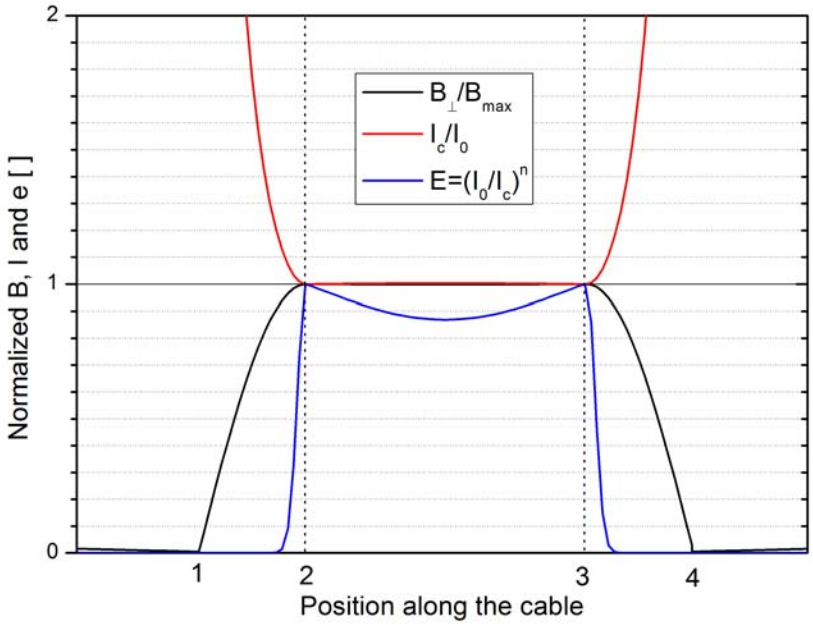

Figure 4.1: The normalized magnetic field component perpendicular to the cable (black), the critical current normalized to the critical current in the high magnetic field area (red) and the local electrical field (blue), as a function of the position along the cable. The small gradient in the magnetic field calculated by Soleno, causes a decrease in the local electrical field. The electrical field is calculated with a n-value of 40. The bending of the cable is between positions 1 and 2 and between 3 and 4. The high field area is between position 2 and 3.

as one moves along the 'bends' in the U-shaped sample (from longitudinal on the straight 'legs' to transverse on the flat 'bottom').

The critical current of NbTi and Nb_3Sn strands is limited by the magnetic field component perpendicular to the strand [2] (since flux due to longitudinal field component does not interact with the current). In the bending of the sample the magnetic field perpendicular to the cable changes from transverse to longitudinal. Thus the current in the sample is limited only at the high field area and the measured voltage build-up comes from the high field area. In Figure 4.1 the perpendicular field, the critical current and the electrical field are shown along the sample. The ends of the bent sections are marked with the numbers 1 to 4. It can be seen that the electrical field quickly drops in the bending. The half-twist pitch voltage pairs span a length of 5 cm, thus covering the high field area and a small part of the bent sections. The one-twist pitch voltage pairs span a length of 10 cm of which a large part does not contribute to the total voltage drop. By measuring the voltage drop over a voltage pair and dividing the results with the length that is spanned, the average electrical field between the voltage taps is determined. Since there is no electrical field in a sizeable part of the one-twist pitch contacts, the average electrical field goes down if the voltage is divided by the full length of the contact. This shifts the measured E values down with respect to the electrical field criterion. However, in view of the steepness of the current voltage characteristics (the large n-factors), the critical current will only be off a little. Nevertheless, this constitutes a systematic error on the critical

current. As can be seen from Figure 3.5, the critical current measured with voltage pair 2 is a little lower than the one recorded with pair 3 and 4. If a shorter effective length of the voltage pair 3 and 4 is used, the critical current of pair 3 and 4 will decrease to the level of voltage pair 2.

The measurements performed with voltage pair 3 are as expected by Equation 2.6 (a power-law transition superimposed on a gradual ohmic foot). Voltage pair 4, however, displays an anomalous offset at the start of the measurement and sometimes at the end. An extra offset is measured on the voltage pair at zero current and during the initial part of the measurements until it disappears at a current around 15-17 kA. The last point of the I-V curves is taken at a current of 5 kA, at which the offset sometimes returns. Also if extra points at zero current are taken afterwards, the offset returns. No explanation was found for this behaviour. However, apart from the points with the extra offset, the rest of the I-V curve can still be used to calculate I_c and n.

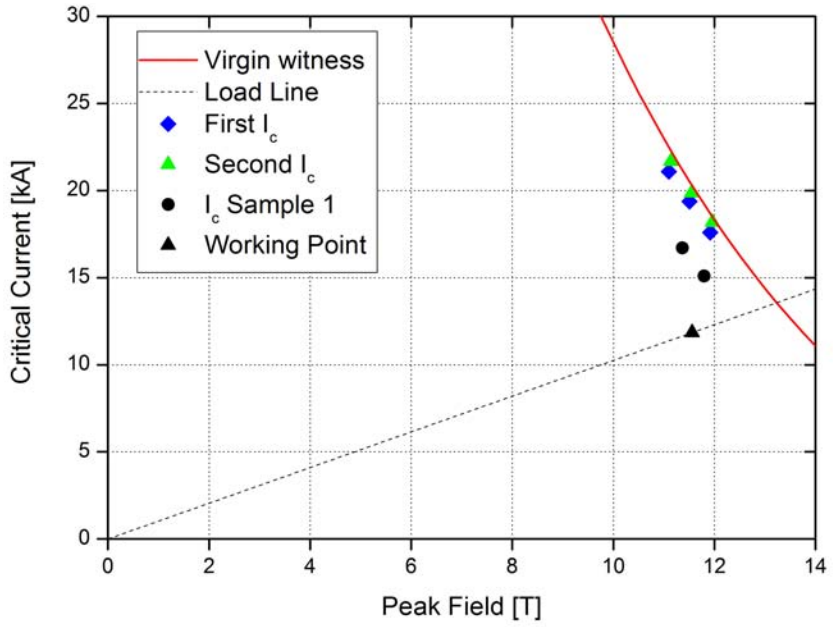

Figure 4.2: The critical current of sample 3 (blue diamonds are before the thermal cycle and green triangle after) as function of peak magnetic field in the windings. The black circles are the critical current measurement obtained with the damaged sample 1. The work point of the magnet is at a current of 11.85 kA in a peak field of 11.56 T. The dotted load line indicates the current versus peak field trajectory that the magnet will follow during ramp-up. All data are at T=4.2 K.

The DS magnet requires a minimum critical current to provide the required operation margin. The design calls for a degradation due to cabling which has to be lower than 10% [11]. Our experiments clearly show that the DS cable is only degradaded 6% and is therefore suitable for the DS magnet. After a thermal cycle the critical current even recoverd 3%. From this it can be concluded that the cabling process developed at CERN is amply adequate, causing less critical current degradation than is maximum permitted. In Figure 4.2 the critical current of

the third DS cable sample is compared to the working point and the load line of the magnet. Also the critical current of sample 1 with a degradation of 23% due to the damage in the current lead is shown for comparison. The DS magnet is designed to operate at 80% of the maximam achievable current with the given load line [11]. However, we observed experimentally on the DS cable, that the work point of the magnet is at 87% of the load line. The work point is also compared to the critical current that magnetic field and is 61% of the critical current of the DS cable.

4.2 Transverse stress dependence on the critical current

To measure the influence of transverse stress on the critical current, the stress distribution over the sample must be homogeneous. In order to achieve this, the anvil should be placed perfectly parallel to the surface. However, in practice this is not possible. The anvil was not perfectly aligned with the sample according to the strain gauges on the sides of the anvil. This implies that at low transverse stress levels, the anvil presses only locally the cable. At the start of the measurement there is enough elastically deformation in the epoxy and polyimide foil to distribute the stress more homogeneous. After the measurements at 210 MPa, a degradation of 1% was observed after reducing the pressure back to 2 MPa, but no degradation was noticeable at 50 and 100 MPa. It may be assumed that after the high-stress excursion, most creep is out of the polyimide foils and the measurements at 2 MPa have only one side of the anvil supporting the cable. The polyimide foils can no longer distribute the stress as before because they are plastically deformed and can no longer elastically deform to distribute the stress homogeneously. The force applied to the anvil causes a local stress build-up, resulting in a 1% reversible degradation to the critical current. Further study is required to understand the stress distribution in more details by simulating the effect of the alignment of the anvil.

The poles of the DS magnet remain under compression at all times with a maximum coil stress below 150 MPa [10]. Our results show that the degradation of the DS cable at 150 MPa is only 1% reversible. The DS cable shows no irreversible degradation up to at least 220 MPa. Since the magnet is ramped up and down several times each day, it should not be operated in the irreversible stress regime. This magnet design has a margin of 70 MPa at its operating stress before it reaches the irreversible degradation measured in the DS cable. The DS cable will therefore survive the transverse stresses in the DS magnet.

Barzi et al. [29, 30] measured the transverse stress dependence of a single strand within a Rutherford cable. Only the tested strand is powered during these measurements. To make sure that the current flows only through the strand under test, the rest of the cable is made from copper 'dummy' strands. Strands from several types of production methods including some RRP strands were tested by these authors. All their samples showed more degradation at lower transverse stresses than the DS cable. It might well be that the environment (Cu dummy strands instead of harder Nb_3Sn composite wires) as well as the detailed support of the tested cable is responsible for these deviations.

In our tests, the RRP DS cable only showed 1 and 2% irreversible degradation out of 11 and 14% total I_c reduction at 250 and 270 MPa transverse stress, respectively. These numbers are not too dissimilar from previous work by LBNL and CERN [31] on a quadrupole magnet made from a 27 strand Rutherford cable with 0.7 mm diameter OST RRP 108/127 strands. The magnet showed 12% total I_c reduction of which 5% irreversible at 260 MPa.

Nb_3Sn Rutherford cables are impregnated with epoxy for a more uniform stress distribution. The uniform stress distribution depends on the quality of the impregnation. The extra layers of glass fiber on top of the cable give some extra space to redistribute any stress concentrations. The strain state of the cable is reduced considerably and becomes more uniform when impregnated by epoxy with a moderate Young's modulus [32].

The stress applied to the cable consists of two components, a hydrostatic and a deviatoric stress component. Is has been shown that the critical current does not depend on the hydrostatic stress component and the reduction in the critical current is due only to the deviatoric stress component [12].

Mondonico et al. [33] proved the importance of impregnation on single PIT and Bronze Nb_3SN strands. From their results it is clear that with proper impregnation and adequate sample supports on all sides (for the DS cable, the sample holder, support flanges and the anvil) the reduction in the critical current is reduced and much higher transverse stresses can be applied to the strands before they will plastically deform. Several experiments were performed on bare, soldered and impregnated Rutherford cables which prove that impregnation is a crucial aspect for the performance of Nb_3Sn Rutherford cables under transverse stress [20, 34, 35]. The epoxy distributes the uniaxial stress applied to the cable into a hydrostatic component and only a small deviatoric component.

4.3 Thermal Stability

The DS cable is 6% degraded by the cabling process, as discussed in Section 4.1. As suggested by the microscopy study on the FRESCA II cable (§2.2.1), the cabling damage is situated at the edges of the cable where the strands need to make a sharp turn from one cable face to the other. The diffusion barrier around the filaments might break due to this sizeable deformation, causing tin and copper to diffuse towards each other. Previous research by Sumption et al. [36,37] show that Nb_3Sn Rutherford cables have lower RRR-values at the edges of the cable compared to its center. The RRR-measurement on the extracted strand from the DS-cable has a reduced RRR at the thin edge, but the thick edge has the same RRR as the center. We concluded that the cabling process indeed somewhat damaged the filaments on the thin edge of this cable, but left the thick side undamaged. A lower RRR value implies besides a higher electrical resistance also a lower heat transfer coefficient and these two parameters together cause a lower thermal stability.

The stability measurements show that the minimum quench energy at the thin edge is a factor 2 lower than the one found with the center heater, while the thick edge has a MQE that is only slightly lower than the center. The reduced stability at the thin edge, but less so at the thick edge are in agreement with the RRR measurements. However, only one RRR measurements is performed on both edges and therefore this correlation is only preliminary.

The observed transition from the single strand stability regime to the collective cable regime is weak compared to measurements on NbTi Rutherford cables [6,38] or on other high J_c-Nb_3Sn Rutherford cables [7]. The thermal stability depends on how effective heat can be transported away from the disturbance, allowing the normal zone to shrink and the cable to recover before it quenches. NbTi Rutherford cables are directly surrounded by liquid helium and are thus in good thermal contact with the helium bath. In these cables, the transition between the single-strand and cable regime is sharp and MQE increases by an order of magnitude when one reduces the current of field through the boundary between both regimes. Nb_3Sn Rutherford cables, on the other hand, are impregnated which separates the cable from the helium bath and therefore lessens the benefits of the heat transfer to the helium bath.

For the LARP project two 27-strand Nb_3Sn Rutherford cables made from of 0.7 mm RRP 104/127 OST strands, were tested by de Rapper et al. [26]. Similar MQE values were found as for the DS cable. However on these cables a clear transition between the different stability regimes was measured. However, the stability in the cable regime is difficult to compare between different samples, because the MQE strongly depends on the geometry in general and on the inter-strand contact resistance in specific [26]. There are some differences between the measurements performed on the LARP cable compared to the DS cable. The DS cable has two extra layers of glass fiber over the cable and the high field area is surrounded by stainless steel. Therefore, there is even less heat transfer to the helium bath. A poorer heat transfer from the strand towards the helium bath results in a smaller amount of energy needed to quench a second strand. This might cause the transition between regimes to become weaker in the DS sample.

Another difference between the two experiments is the sample. The LARP and DS cable are both fabricated from (27 or 40) 0.7 mm RRP strands. However, the substructure is different, namely 104/127 for the LARP strands and 108/127 for the DS ones. Also the Cu/non-Cu ratio is different (1.18 and 1.13 for the two LARP cables and 1.13 for the DS cable). More copper results in a higher stability, because the heat is easier transported out of the cable. The quench behavior of these cables is not expected to depend directly on the number of strands when both cables are operated at the same ratio of I_c. When one strand quenches, the neighbouring strands have to take over the current. For this is does not matter is there are 27 or 40 strands in the cable, because the current is taken mostly over by the neighbouring strands [6].

The transition between the two stability regimes at I_{kink} is not directly noticeable from the curves of the current dependence in Figure 3.10. From the test current dependence of the MQE, the transition is expected between 9 and 10 T at a test current of 11.85 kA. When the magnet is at its operational magnetic field, the cable will thus be in the single strand regime. From the critical current measurements the current at the working point is determined to be 61% of I_c, but because also the temperature of the neighbouring strands increases and thereby lowering I_c, these strands cannot take over the current. Therefore the cable still operates in the single-strand regime. The stability of the magnet would increase significantly by changing I_{kink} such that the cable operates in the cable regime. The location of I_{kink} strongly depends on the contact resistance between the adjacent strands [39].

A map of the thermal stability as function of test current and magnetic field can be created by combining the data for each heater. The thermal stability maps of the thick edge, center and thin edge are shown in Figures 4.3, 4.4 and 4.5 respectively. From these figures the stability over the entire cross-section of the magnet can be determined. Note that different parts of the magnet winding pack will experience different magnetic fields. A magnet design with more turns requires a lower current to achieve the same magnetic field. This will also lower the load line, resulting in a higher stability. So the stability of the magnet will increase if more conductor is added. The MQE maps quantify the stability of the conductor for a certain current.

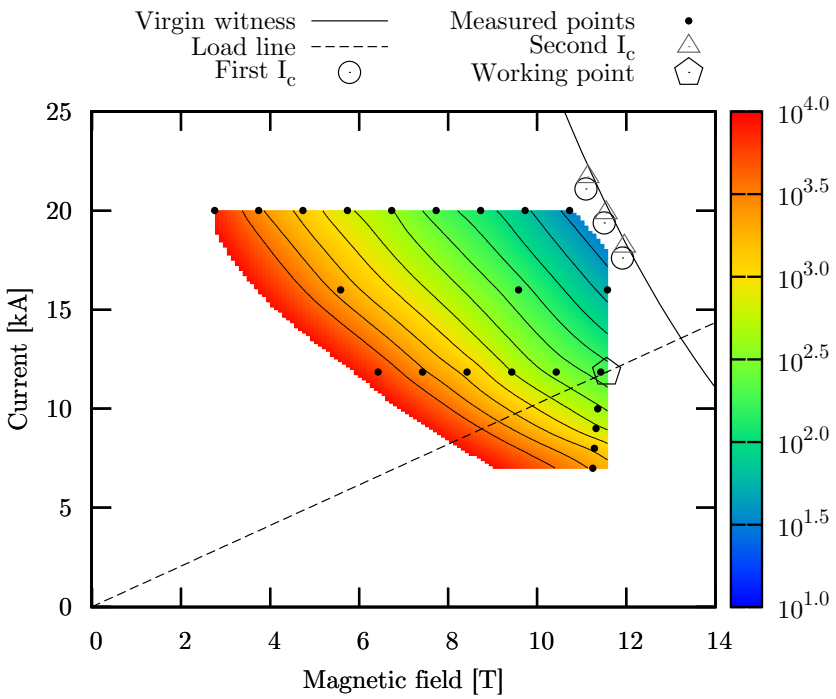

Figure 4.3: Contour plot of the MQE at the thick cable edge (color scale labeled in units of µJ) as a function of the local magnetic field and test current. The black dots indicate the measurements performed during this assignment, from which the contour plot is spline-interpolated. As a visual reference the I_c values and the work point are also shown.

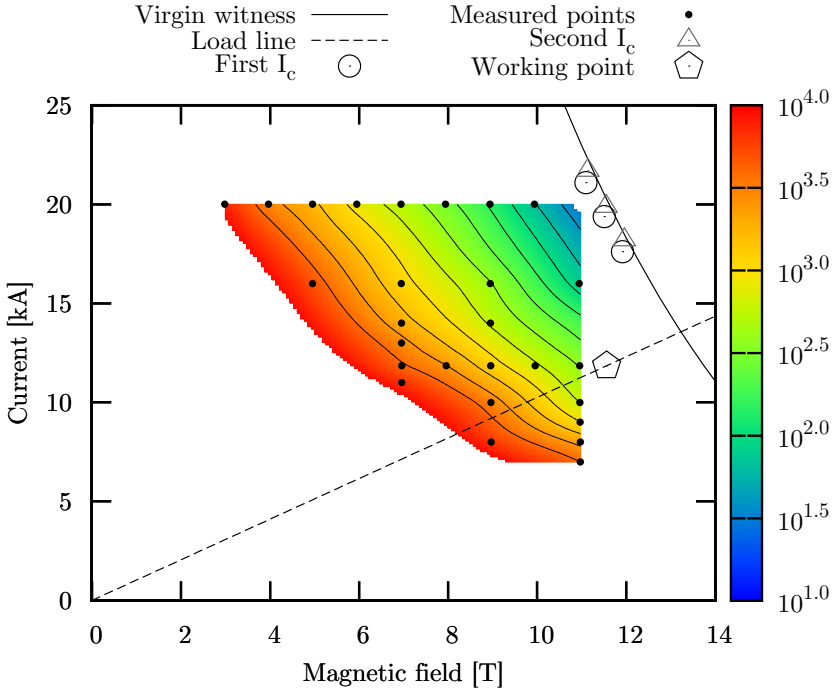

Figure 4.4: Contour plot of the MQE at the center cable edge (color scale labeled in units of µJ) as a function of the local magnetic field and test current. The black dots indicate the measurements performed during this assignment, from which the contour plot is spline-interpolated. As a visual reference the I_c values and the work point are also shown.

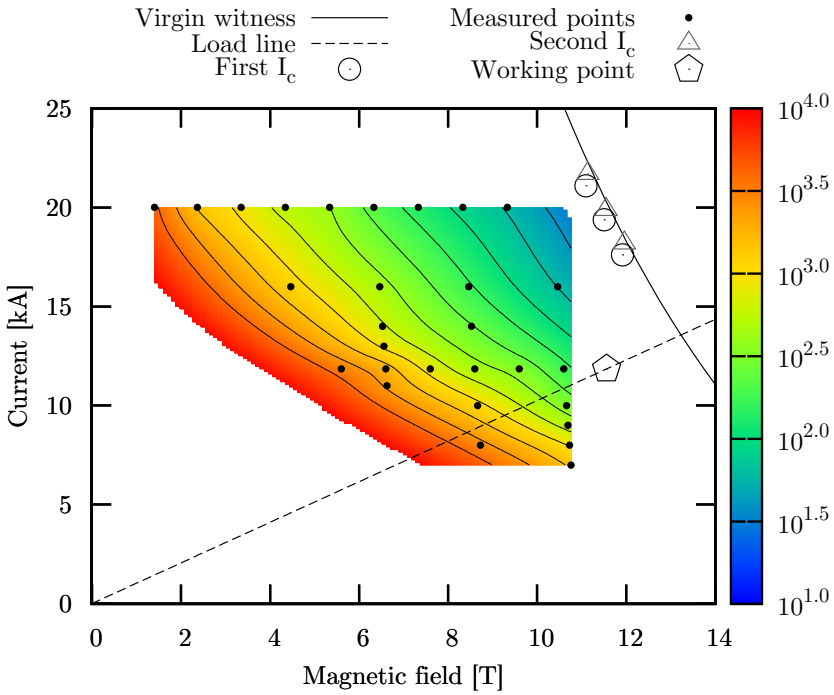

Figure 4.5: Contour plot of the MQE at the thin cable edge (color scale labeled in units of µJ) as a function of the local magnetic field and test current. The black dots indicate the measurements performed during this assignment, from which the contour plot is spline-interpolated. As a visual reference the I_c values and the work point are also shown.

Chapter 5

Conclusion & Recommendation

In this assignment measurements are performed to determine the critical current as function of magnetic field and transverse stress. Secondly, minimum quench energy measurements are performed as function of magnetic field and test current. The main conclusions of these measurements are found in Section 5.1. Recommendations for future measurements with this set-up are discussed in Section 5.2.

5.1 Conclusion

For the first time a full-size RRP Nb_3Sn Rutherford cable for accelerator dipole magnets has been tested for the transverse stress dependence of the critical current and for the thermal stability. The critical current is measured at transverse stresses up to 270 MPa over a length of 45 mm. A map of the minimum quench energy is made as function of magnetic field and test current over a range of 2 to 11 T and 7 to 20 kA.

The critical current as a function of magnetic peak field shows a degradation of 6 % compared to the optimally achievable value, based on the critical current measurements of a single virgin witness strand. This degradation is most likely due to the cabling process but falls well within the margin of the magnet design. The critical current regained 3% of its value after a thermal cycle.

Also from the point of view of stress sensitivity, the DS cable is validated to be applied in the DS magnet for the LHC upgrade. The transverse stress level at which the current reduction becomes irreversible, lies about 70 MPa above the maximum coil design stress of 150 MPa. At the transverse stress level that the magnet will operate at, the critical current is only reduced by 1% and this reduction is fully reversible. The results thus demonstrate that RRP Nb_3Sn Rutherford cables can be used at high transverse stress levels if the cable is properly impregnated. The performance of the DS cable is in good agreement with observations made on magnet built with an RRP cable (with the same strands as the DS cable) by LBNL and CERN.

The MQE is measured at the center and at both edges of the DS cable and the results deviates from previously measured cables. There is no clear transition observed between the single-strand and collective cable stability regime in the magnetic field dependence and only a weak transition in the current dependence. The thermal stability of the thick edge is close to that of the center of the cable. The thermal stability of the thin edge, however, is a about a factor 2 lower than at the center. First results indicate that the reduced stability at this thinner

edge may be correlated with a reduced RRR value, presumably due to rupture of the diffusion barriers around the filaments in this highly deformed and compacted area of the cable.

5.2 Recommendations

In the course of the LHC upgrade program, several different cable samples will be measured at the University of Twente. Some of those cables will be larger than the DS cable and have higher critical current (such as the FRESCA II cable). For the modification of the set-up, it is taken into account that also larger cables must be measured with it. The superconducting transformer is designed for currents up to 50 kA. However, the measuring time was already limited for the DS cable with currents up to 21-22 kA. After several quenches of the primary coil, it was decided to check, whether the transformer is still suitable for the higher current of these larger cables. The DS cable was used to test the transformer at zero background field, where the cable I_c-value is well above 50 kA.

The primary coil of the transformer is not degraded during operation, it still reaches at least 64 A without quenching, while there is no current in the secondary. The performance of the secondary coil, however, seems to have degraded over the years, because a maximum quench current of only 33 kA in the secondary coil is achieved. The quench location is determined and turns out to be located far away from the high field area. This indicates that the cable quenches due to a disturbance in the secondary coil of the transformer or in the joint. The cable might be degraded by repeated soldering to various samples. This might limit the transformer in current.

A second problem for measuring larger samples on this setup is the maximum current of 50 A in the primary coil during the measurements. By changing the polarity of the primary coil, a large current can be initiated in the sample. The joint resistance of around 1 nΩ causes the current in the primary coil to rise rapidly and therefore the measuring time is limited. For accurate measurements on samples with large currents, it might be necessary to reduce the joint resistance or to upgrade the primary coil to a maximum of 100 A or more, to achieve enough measuring points. Replacing the secondary coil might already result in a large gain in measuring time, since the questionable quality of the cable used for the secondary may also be responsible for a higher joint resistance. Smaller joint resistances are measured on previous samples at this setup, down to 0.2 nΩ per joint.

Bibliography

[1] M. Cyrot and D. Pavuna, *Introduction to Superconductivity and High-Tc Materials*. World Scientific Publishing, 1995, vol. first reprint.

[2] M. N. Wilson, *Superconducting Magnets*. Clarendon Press Oxford, 1983.

[3] H. K. Onnes, "Sur les résistances électriques," *Communications from the Physical Laboratory of the University of Leiden*, pp. 1–11, 1911, supplement 29.

[4] A. Godeke, "Performance Boundaries in Nb_3Sn Superconductors," Ph.D. dissertation, University of Twente, 2005.

[5] M. N. Wilson and R. Wolf, "Calculation of Minimum Quench Energies in Rutherford Cables," *IEEE Transactions on Applied Superconductivity*, vol. 7, no. 2 PART 1, pp. 950–953, 1997.

[6] G. P. Willering, "Stability of Superconducting Rutherford Cables," Ph.D. dissertation, University of Twente, 2009.

[7] W. M. De Rapper, "Thermal Stability of Nb_3Sn Rutherford Cables for Accelerator Magnets," Ph.D. dissertation, University of Twente, 2012, unpublished.

[8] CERN, "ATLAS Experiment - Public Results," data from 03/10/2012. [Online]. Available: https://twiki.cern.ch/twiki/bin/view/AtlasPublic/LuminosityPublicResults

[9] D. Griffiths, *Introduction to Elementary Particles*. WILEY-VCH Verlag GmgH & Co. KGaA, Weinheim, 2008, vol. Second, Revised Edition.

[10] M. Karppinen, N. Andreev, G. Apollinari, B. Auchmann, E. Barzi, R. Bossert, V. V. Kashikhin, A. Nobrega, I. Novitski, L. Rossi, D. Smekens, and A. V. Zlobin, "Design of 11 T Twin-Aperture Nb_3Sn Dipole Demonstrator Magnet for LHC Upgrades," *IEEE Transactions on Applied Superconductivity*, vol. 22, no. 3, 2012.

[11] E. Barzi, N. Andreev, M. Karppinen, V. Lombardo, F. Nobrega, D. Turrioni, R. Yamada, and A. V. Zlobin, "Development and Fabrication of Nb_3Sn Rutherford Cable for the 11 T DS Dipole Demonstrator Model," *IEEE Transactions on Applied Superconductivity*, vol. 22, no. 3, 2012.

[12] B. ten Haken, "Strain Effects of the Critical Properties of High-Field Superconductors," Ph.D. dissertation, University of Twente, 1994.

[13] A. P. Verweij, J. Genest, A. Knezovic, D. F. Leroy, J. . Marzolf, and L. R. Oberli, "1.9 K Test Facility for the Reception of the Superconducting Cables for the LHC," *IEEE Transactions on Applied Superconductivity*, vol. 9, no. 2 PART 1, pp. 153–156, 1999.

[14] A. Milanese, M. Devaux, M. Durante, P. Manil, J. C. Perez, J. M. Rifflet, G. De Rijk, and F. Rondeaux, "Design of the eucard high field model dipole magnet fresca2," *IEEE Transactions on Applied Superconductivity*, vol. 22, no. 3, 2012.

[15] L. J. M. van de Klundert and H. H. J. ten Kate, "Fully Superconducting Rectifiers and Fluxpumps Part 1: Realized Methods for Pumping Flux," *Cryogenics*, vol. 21, no. 4, pp. 195–206, 1981.

[16] H. H. J. ten Kate, H. Weijers, and J. M. van Oort, "Critical Current Degradation in Nb_3Sn cables Under Transverse Pressure," *IEEE Transactions on Applied Superconductivity*, vol. 3, no. 1, pp. 1334–1337, 1993.

[17] A. Zlobin, N. Andreev, G. Apollinari, E. Barzi, R. Bossert, G. Chlachidze, V. Kashikhin, F. Nobrega, I. Novitski, D. Turrioni, R. Yamada, B. Auchmann, M. Karppinen, L. Oberli, L. Rossi, and D. Smekens, "Status of a Single-Aperture 11 T Nb_3Sn Demonstrator Dipole for LHC Upgrades." Presented on the International Particle Accelerator Conference, 2012.

[18] W. Neijmeijer, "Microstructural and Kinetic Studies of the Manufacturing of Superconducting Nb_3Sn," Ph.D. dissertation, University of Twente, 1988.

[19] L.-R. Oberli, personal communication, 2012.

[20] J. M. van Oort, R. M. Scanlan, H. W. Weijers, S. Wessel, and H. H. J. ten Kate, "Reduction of the critical current in nb3sn cables under transverse loads," *IEEE Transactions on Applied Superconductivity*, vol. 3, no. 1 pt 2, pp. 559–562, 1993.

[21] H. G. Knoopers, H. H. J. Ten Kate, W. A. J. Wessel, H. J. G. Krooshoop, A. Godeke, and O. A. Shevchenko, "Fast Ramp 50 kA Superconducting Transformer."

[22] M. Dhallé, W. A. J. Wessel, and H. Krooshoop, "Critical Current Measurements on NbTi Rutherford Cables SSC-4-F-00xxx," University of Twente, Research Report, 2010.

[23] A. Kamps, "Simuleren, Bouwen en Testen van een Supergeleidende Kabeltransformator," Master's thesis, University of Twente, 1993.

[24] A. P. Verweij, "De Invloed van Transversale Druk op de Spanning-Stroom Karakteristiek van Nb_3Sn-Kabels tot 340 MPa en tot 11 T," Master's thesis, University of Twente, 1990.

[25] J. van Oort, "Critical Current Degradation in Nb_3Sn Superconductors in Accelerator Magnets," Ph.D. dissertation, University of Twente, 2000.

[26] W. M. De Rapper, "Thermal Stability at 1.9 K and 4.3 K of Nb_3Sn Cables for Quadrupoles for the LHC Upgrade," in *Applied Superconductivity Conference*, unpublished.

[27] A. Verweij, "The Consequence of Self-Field and Non-Uniform Current Distribution on Short Sample Tests of Superconducting Cables," Tech. Rep., 1997.

[28] H. Weijers, "Degradatie van de Kritieke Stroom van Nb_3Sn Kabels door Transversale Druk tot 200 MPa in Magneetvelden van 9-11 T," Master's thesis, University of Twente, 1991.

[29] E. Barzi, T. Wokas, and A. V. Zlobin, "Sensitivity of Nb_3Sn Rutherford-type Cables to Transverse Pressure," *IEEE Transactions on Applied Superconductivity*, vol. 15, no. 2 PART II, pp. 1541–1544, 2005.

[30] E. Barzi, D. Turrioni, and A. V. Zlobin, "Effect of transverse pressure on brittle superconductors," *IEEE Transactions on Applied Superconductivity*, vol. 18, no. 2, pp. 980–983, 2008.

[31] H. Felice, M. Bajko, B. Bingham, B. Bordini, L. Bottura, S. Caspi, G. De Rijk, D. Dietderich, P. Ferracin, C. Giloux, A. Godeke, R. Hafalia, A. Milanese, L. Rossi, and G. L. Sabbi, "Performance of a Nb_3Sn Quadrupole Under High Stress," *IEEE Transactions on Applied Superconductivity*, vol. 21, no. 3 PART 2, pp. 1849–1853, 2011.

[32] B. ten Haken, T. N. Zaitseva, and H. H. J. ten Kate, "Modeling of strain in multifilamentary wires deformed by thermal contraction and transverse forces," *Cryogenics*, vol. 34, no. SUPPL. 1, pp. 513–516, 1994.

[33] G. Mondonico, B. Seeber, A. Ferreira, B. Bordini, L. Oberli, L. Bottura, A. Ballarino, R. Flükiger, and C. Senatore, "Effect of Quasi-Hydrostatical Radial Pressure on I_c of Nb_3Sn Wires," *Superconductor Science and Technology*, vol. 25, no. 11, 2012.

[34] H. Boschman, A. P. Verweij, S. Wessel, H. H. J. ten Kate, and L. J. M. van de Klundert, "The Effect of Transverse Loads up to 300 MPa on the Critical Currents of Nb3Sn Cables," *IEEE Transactions on Magnetics*, vol. 27, no. 2 pt III, pp. 1831–1834, 1991.

[35] G. Pasztor, A. Anghel, B. Jakob, and R. Wesche, "Transverse Stress Effects in Nb_3Sn Cables," *IEEE Transactions on Magnetics*, vol. 30, no. 4 pt 2, pp. 1938–1941, 1994.

[36] M. D. Sumption, V. Nazareth, E. Barzi, D. Turrioni, R. Yamada, A. V. Zlobin, and E. W. Collings, "Measurements of RRR Variation in Strands Extracted from Nb_3Sn-type Rutherford Cables," in *AIP Conference Proceedings*, vol. 986, 2008, pp. 277–284.

[37] M. D. Sumption, M. Susner, E. W. Collings, D. R. Dietderich, E. Barzi, D. Turrion, R. Yamada, and A. V. Zlobin, "Effect of Cable Edge Deformation on RRR and Magnetization of Strands Extracted from Nb_3Sn Rutherford-Type Cables," *IEEE Transactions on Applied Superconductivity*, vol. 19, no. 3, pp. 2481–2485, 2009.

[38] A. K. Ghosh, W. B. Sampson, and M. N. Wilson, "Minimum quench energies of rutherford cables and single wires," *IEEE Transactions on Applied Superconductivity*, vol. 7, no. 2 PART 1, pp. 954–957, 1997.

[39] G. P. Willering, A. P. Verweij, J. Kaugerts, and H. H. J. Ten Kate, "Stability of Nb-Ti Rutherford Cables Exhibiting Different Contact Resistances," *IEEE Transactions on Applied Superconductivity*, vol. 18, no. 2, pp. 1263–1266, 2008.

[40] P. P. L. Regtien, F. van der Heijden, M. J. Korsten, and W. Olthuis, *Measurement Science for Engineers*, 2nd ed. Kogan Page Science, 2004.

Appendices

Appendix A

Preparation of Nb_3Sn Rutherford Cables on the U-shaped holder

In appendix A all protocols can be found to prepare a Rutherford cable sample for transverse stress or MQE measurements on the U-shaped sample holder. Nb_3Sn Rutherford cables have to be properly prepared for successful measurements. First the sample has to be reacted in the desired U-shape, following the protocol described in Section A.1. Then the current lead section of the cable sample have to be pre-soldered, the sample is placed on the sample holder, voltage pairs are connected and the sample and holder are prepared for impregnation. These steps can be found in Section A.2. The impregnation itself is a crucial step of the sample preparation and its protocol is given in Section A.3. After the impregnation the sample has to be connected to the transformer. The rest of the MQE and press set-up preparation steps are described in Section A.5 and A.6, respectively. All steps in these protocols have to be followed for an adequate preparation.

For a proper sample preparation it is important that the following general points are taken into account when working with Nb_3Sn Rutherford samples.

- Work clean, use latex gloves.
- Nb_3Sn is a sensitive and brittle material after the heat treatment. Be very careful with the sample during all the steps. The filaments of the superconductor will break very easily. Once reacted, do not move the sample holder without supports to maintain the U-shape.
- Glass fiber is not healthy to breathe in. It also cause itching reaction when in contact with the skin. When you work with glass fiber use a lab coat, gloves and a dusk mask to avoid contact with the fibers. Also work under air extraction (fume extraction), so a minimum of glass fiber will stay in the air.
- Take your time for the steps and work precisely, because the preparation of Nb_3Sn Rutherford cables take a lot of time and you do not want to make errors that damage the sample or result in an improper preparation.
- Follow the each steps described in the manuals carefully. They are there for a good reason.

A.1 Heat Treatment

Nb_3Sn is a brittle materials once it is reacted. However, Nb and Sn itself are ductile materials and can be plastically deformed. Therefore the Nb_3Sn cable sample has to be bent into shape before the heat treatment is performed. A Rutherford cable may be degraded by the cabling process. Therefore it is useful to compare the cable data with measurements on a 'virgin witness strand', i.e. a strand from the same batch as those used to assemble the cable, but with which nothing happened. 'Extracted strands' are pried loose from the cable after the cabling process, but prior to the heat treatment. They are needed for RRR measurements on the strands. The cable, witness strand and extracted strands need to be reacted together to ensure that all three have had exactly the same reaction process and can thus be compared to each other. In this section the protocol for the heat treatment is described.

- For measurements on the U-shape sample holder, samples are needed with a length of at least 70 cm. If possible, use 80 cm instead for easier preparation. If the sample has to be cut off a larger cable, cut it with a high speed tool (dremel) between two pieces of scotch tape to keep the strands on either side of the cut in place. Clean the cable with alcohol.
- Wrap the sample in glass fiber ribbon (cross-section of 20 by 0.15 mm^2) with 50% overlap. This step is not required if the cable is already wrapped. The easiest way to get a good 50% overlap is by clamping the cable between two places with the desired space in between and wrapping by hand. For this two metal pieces are available that can be clamped to the work table. Do not forget to wear a dust mask to avoid breathing in the fibers.
- Clean the cable in an ultrasonic bath with alcohol for 15 min. This has to be done sequentially for successive sections since the bath is not big enough to accommodate the whole sample in one go. Find a good way to keep the cable stable in a wide glass tray.
- Place the reaction holder with the support flanges in a vise with the U-side up. Put the cable on top. It should fit exactly, if there is a slit on the sides of the wire, you need to adjust the reaction blocks until it fits exactly. Place the top part of the reaction holder to it and place the anvil (with the same keystone as the sample) on the cable. Tighten it so that it keeps it in place. If the cable has a keystone, make sure the anvil is placed correctly. Put a drop of 'graphite with alcohol' mixture on each bolt, this will make it easier to disassemble the reaction holder again.
- Ask someone to help with this step. Add a clamp to the end of the cable. One person needs to pull this clamp down to shape the cable in the U-shape. The other person puts the stainless steel bar on top of it. Use something small and not sharp to position the cable between the bar and the holder. When in place, put two wooden clamps over the bar and reaction holder to keep them in place. Five clamps must be connected on each side. These clamps can be positioned by pushing them into place with a wooden clamp. Use 'graphite and alcohol' mixture on the tips of the bolts.
- Do this also for the other side.
- Clean the reaction holder with the sample in an ultrasonic bath with alcohol for at least 15 min. Since the bath is not big enough, use a big glass beaker to put it in. Also repeat the process with the reaction holder up-side down in the beaker, to clean the whole sample. Use external clamps to hang the reaction holder in. The reaction holder might be to heavy for the basket of the ultrasonic bath. For this remove temporarily the anvil so that the alcohol can clean the bottom of the U properly. A part of the cable should stick out of the reaction holder. This will limit the effect of tin leakage at the end of the cable. Afterwards these parts will be cut off. The sample is now ready for heat treatment and should look like Figure A.1.
- Mount the virgin witness strand on the ITER barrel following the standard procedure.

Add some glass fiber around the coil to prevent the sample from sticking to the other holders.

- A part of the cable is used for the RRR measurements. Cut a part of a length of at least 15 cm of the cable with a high speed cutting tool (dremel). The longer the extracted strand the better. Squeeze the ends of the strands shut to limit the effect of thin leakage at the ends of the RRR samples. From this piece of cable, several strands will be taken and put between two stainless steel plates covered with glass fiber. With iron wire these plates tied together and held into place.
- The reaction holder, the barrel of the witness strand and the RRR samples are inserted together into the vacuum tube oven. Once the vacuum is sufficiently low, below 10^{-2} mbar, the reaction program can be started. Depending on the type of cable a reaction program should be choosen.

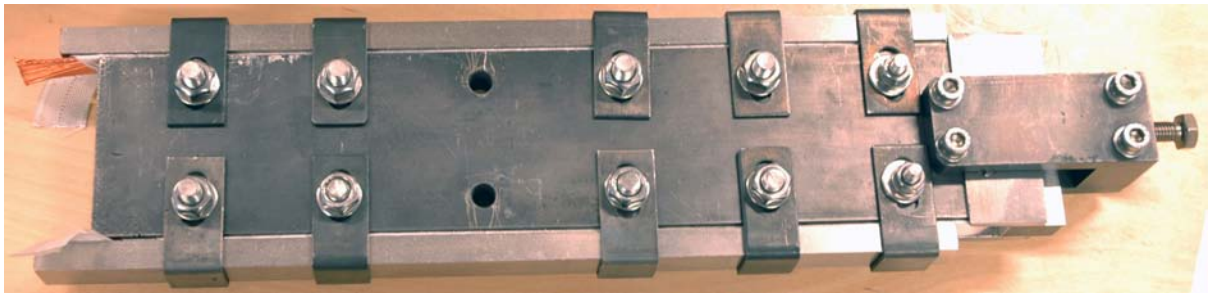

Figure A.1: A mounted reaction holder.

A.2 Mounting the sample to the sample holder

After the heat treatment the sample undergoes several steps to mount it onto the sample holder and to prepare it for impregnation. The current lead section of the sample have to be pre-soldered and the cable has to be mounted on the sample holder. Voltage pairs have to be added and glass fiber clamps have to be wound. Be very careful: in this step the Nb_3Sn cable is most fragile, since it is reacted but not yet supported.

- Remove all remaining traces of epoxy from the sample holder and the support plates. Soaking them in formid acid for a night will help to clean them. A clean and epoxy-free sample holder and supports are required.
- Cover the slits where the epoxy clamps will come with tape and coat the sample holder and support plates with dry Teflon spray. Best way to do this is three thin layers for full cover. The Teflon spray will prevent epoxy from bonding to the sample holder and plates.
- Cut off the ends of the cable that stick out of the reaction holder with a high speed abrasive tool. This will make life easier when performing the next steps.
- Carefully disassemble the reaction holder, starting with the anvil, then the bars at the side, the support flanges and finally the reaction holder itself. If a bolt is stuck, a droplet of alcohol might help to release it. Watch out, the cable is fragile! Work on a clean surface and remove everything around the sample. Do not lift the sample without supports to keep the sample in the U-shape.
- Add a droplet of "Super Glue" at the ends of the section where the cable will be impregnated. Carefully remove the glass fiber from the current lead section with a scalpel.

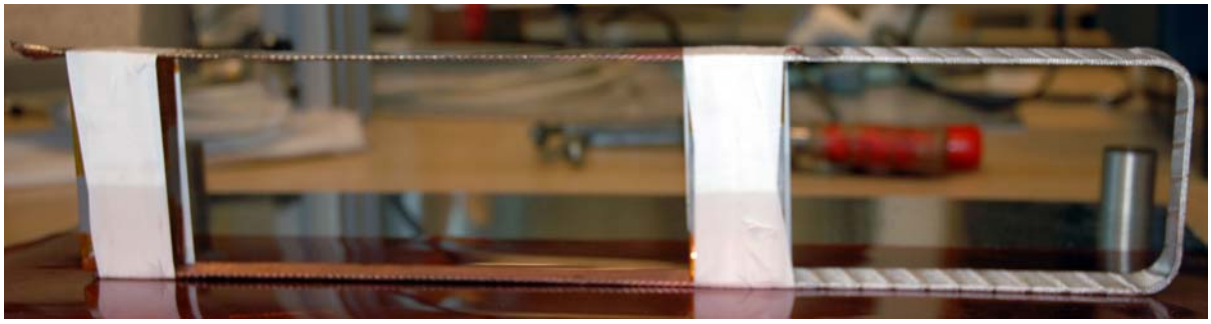

Figure A.2: The sample ready for pre-soldering on the insides. The outside is already fully pre-soldered on the current leads. To pre-solder the whole inside of the cable, move the left block carefully to an already soldered part. A piece of polyimide foil is under the sample to prevent the heat from moving to the aluminum work table.

- The current lead section must be pre-soldered on the inside and the outside. During the soldering it is important that the cable keeps the U-shape and will not twist. To solder the outside, put the reaction holder back in place and fix the cable onto it with Teflon tape. To solder the inside, place two blocks with smooth corners covered with polyimide tape between the cable and fixate it as shown in Figure A.2. It is then ready for soldering. In two steps each side of the current leads can be soldered. Before the soldering gently polish the sample surface with "Scotch Brite" to remove the oxide layer and apply soldering flux "S-39 Cu" for better bonding. The final solder surface has to be smooth so that the sample can be connected to the transformer.
- Put the sample around the sample holder with one of the support plates in place. Put a piece of G10 plates with the same thickness as the transformer secondary cable between the current lead sections of the sample and the sample holder. Fix the cable with Teflon tape. Cut the cable to the exact desired length (an integer number of twist pitches) with a high speed cutting tool. Since the cable ends are soldered, the strands will stay in place.
- Connect the voltage pairs to the cable. These pairs are easiest soldered at the side of the cable to a single strand. Remove the glass fiber from where you want to place the voltage taps by scratching it away with a scalpel. For soldering the contacts to the cable, the surface of the cable must be clean. Pre-solder the cable by putting a small soldering iron with a fine point along the strand and after a few seconds add a little solder. A small layer of solder should stick. Pre-solder the voltage lead, put it on the strand and tip it with the soldering iron. Test the mechanical connection by pulling softly to the voltage tap. Use some tape to keep the voltage leads neatly along the sample holder.
- Check the resistance of the voltage taps. Only once that all connections are good, continue with the next steps.
- If the sample is to be used in the press, add two layers of glass fiber over the cable.
- Wind the glass fiber clamps. You need for each clamp about 2 meters of glass fiber ribbon. Glue the end of the glass fiber with super glue.
- Add heaters and Pt100 sensor to the sample holder, roll up the voltage leads and connect them to the sample holder with some "tie-wraps". The Pt100 is best added in the hole just above the large holes for the press fixation pins.
- Add a Teflon block (or the stainless steel block covered with dry Teflon spray) against the high field area to ensure a flat surface. A Teflon block will not have perfectly sharp edges, which during the impregnation will result in epoxy in the corners with the support plates. Keep the block in place with a tie-wrap. Make sure there are no cracks around

the anvil. The surface of the cable needs to be aligned with the anvil.
- Now the sample and sample holder are ready for impregnation.

A.3 Impregnation

Materials needed:

- Vacuum chamber (specifically made for the U-shaped sample holder)
- Vacuum pump (18 Two Stage, Edwards)
- Vacuum level detector (Piezovac PV20)
- Brass recipient (which fits closely around the sample holder) with heaters and Pt100 sensor added.
- 100 mass units Resin MY 740
- 90 mass units Hardener HY 906
- 0.2 mass units Accelerator DY 062
- Two 30 V/3 A power supplies
- Two Pt100 temperature controls
- Wooden pieces to put the vacuum chamber under an angle
- The fume hood and the oven for two days
- Two warming plates, one of them with stir option
- Stir magnet
- Two flasks marked as "Hardener" and "Resin"'
- Two plastic corks that close the flasks
- One big funnel
- A 250 mL measuring cup
- Acetone
- Paper towels
- Thermal sensor

Before beginning with the impregnation, read carefully the rest of the impregnation protocol. It is best when you have everything already in place where you need it. Do not let the epoxy cool down because you did not fetch everything beforehand and waste time looking for things.

- Heat the oven to 60 °C and pre-heat the sample holder, the brass recipient and the measuring cup in the oven. They need to be at the desired temperature when you need them.
- Put the required amount of resin and hardener in their flasks. Take a margin in the amount, since some epoxy will stay in the flasks. In the brass recipient you will need approximately 170 mL of epoxy. To be sure, prepare about 250 g of resin.
- Preheat the resin to 40 °C and the hardener to 45 °C.
- De-gas the hardener at approximately 25 Torr for 1/2 hour. Do not evacuate below the vapor pressure of 20 Torr.
- Add the Hardener and Accelerator to the resin. Do not "overshoot" with the accelerator, since this might limit the pot time of the epoxy. Stir everything thoroughly with a stir magnet for 20 min and de-gas the mixture at 25 Torr.
- Heat the mixture to 55 °C. The mixture is ready for impregnation when it reaches this temperature and has a pot life of 6 hours.
- Take the sample holder from the oven and hang it in the vacuum chamber with the heater and Pt100 contacts connected. Then take the brass recipient and place it at the bottom of the vacuum chamber and connect its contacts. Next take the measuring cup and measure

the required amount (170 mL for the DS sample) in the cup and pour it into the brass recipient. Do this by opening the vacuum chamber from the bottom, the cables are long enough that the recipient will be out of the vacuum chamber. Close the vacuum chamber again. Watch out for the wire and make sure the sample holder is inside the recipient. Do not drop the sample holder in the epoxy.

- Once the vacuum chamber is closed, connect the vacuum pump, vacuum level detector and cables. Evacuate the vacuum chamber to approximately 30 mBar on the vacuum gauge. Connect the cables on top of the vacuum chamber and turn the power supply of the heater on together with the temperature controls. Set the temperature controller to the requested temperature of 55 °C. The heaters will turn off if their pt100 gives a temperature of 55 °C and turn on again at 54 °C. The heater on the recipient will switch on every few minutes.
- Once vacuum is reached, let somebody check the vacuum chamber and lower the sample about 5 mm every 5 min. Meanwhile you can clean the fume hood, flasks etc with acetone and put the oven in the fume hood. Add a thermometer in the oven and connect it to the computer. Turn the oven on at 85 °C, check the temperature a few times, since the temperature of the oven is hard to set precisely. This way you know for sure that the first phase in the oven is at the correct temperature.
- Keep lowering the sample 5 mm every 5 min until it attains its maximum depth in the recipient. The depth is reached once the sample holder reached the bottom of the recipient or once the epoxy level reaches the edge of the recipient. Wait another 20 minutes. Vent the vacuum chamber a few times and pump it off again. This may help remaining bubbles to escape.
- Disconnect everything from the outside of the vacuum chamber. Move the vacuum chamber next to the fume hood.
- Disconnect the sample holder from the top part and remove the top and center part of the vacuum chamber. The sample holder now stands in the brass recipient. Take the sample holder out of the recipient and place it on a plate of stainless steel covered with Teflon Tape. Use small blocks covered with Teflon tape to support the sample holder on the plate. Put the plate with the sample holder in the oven. Put the tip of the thermometer in a hole in the sample holder, so that it detects the temperature of the sample holder instead of that of the oven.
- Put the remaining epoxy from the recipient in small trays. Clean the recipient thoroughly with acetone. Place the trays with epoxy and the brass recipient in the oven. Clean the perspex vacuum chamber with alcohol if necessary. Do not use acetone on the perspex!
- Heat the sample to 85±2 °C and keep it there for 4 hours. Then heat it to 110 °C for 16 hours (check the temperature a few times). Finally let it cool down slowly by simply switching off the oven.
- Carefully scrape away excess epoxy till the sample holder fits easily in the outer cylinder of the press. If it still does not fit and the support flanges are a little to wide, you can mill the outside of the support flanges away in the workplace. Watch out for the cable when supporting the sample under the mill.

A.4 Connecting the sample to the transformer

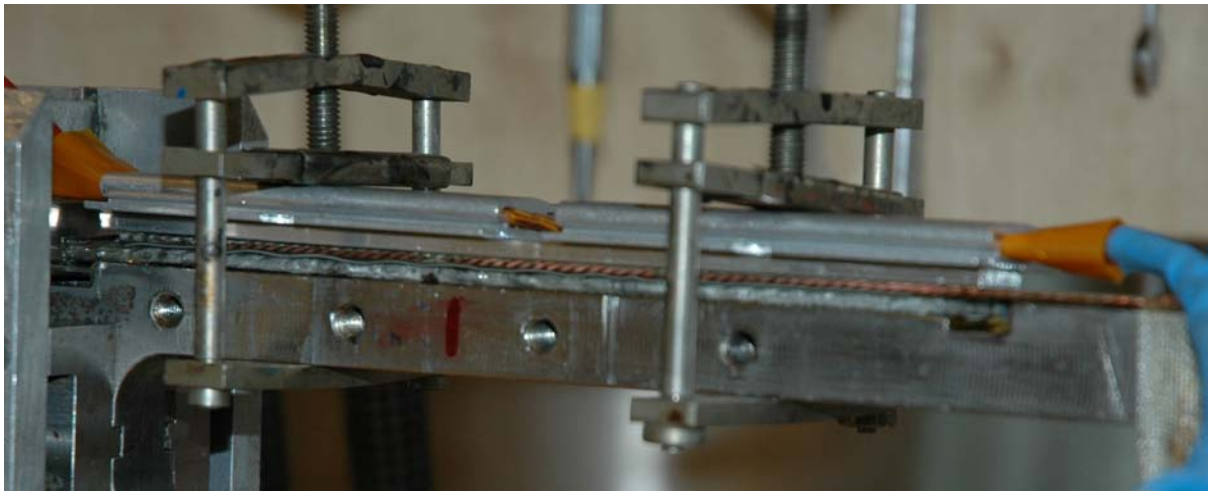

Figure A.3: Set-up used to solder the cable to the transformer with between the two cables two strips of flat-rolled solder and flux. On top of the sample is an aluminium strip on which the heaters are clamped. Each heater has a power of 225 W.

Materials needed:

- Two aluminium bars with a width of at least the cable width.
- Two 225 W flat rectangular heaters
- A largest soldering iron with a flat head
- Flux S-39 Cu
- Small soldering wire
- Fabric gloves so you don't burn yourself with the heaters
- Flat-rolled solder
- Two clamps

After the impregnation, the sample needs to be connected to the transformer. Follow the following steps for a good joint connection. A low joint resistance will result in a lower decay time constant of the secondary.

- The current leads from the transformer needs to be flat. If necessary add the aluminium bars on each side of the cable with the heaters and clamps. Let all the excess solder fall off the cable.
- Slowly move the sample holder in position. Be careful with the sample, it can break very easily. You might use a lab jack to lift the sample holder to the correct height and slowly moved the sample into place. This way the sample moves as little as possible. Add the bolts to fix the sample holder. Don't apply force when the sample holder get stuck. You either hit a droplet of solder sticking out or the transformer needs to be turned 180°. One side has more flexibility when moving the sample holder in position.
- Add flux between the cables where you can reach.
- For each joint cut two pieces of flat-rolled solder of the length of the joint. Smear both sides of these solder strips with flux and add them between the connection.
- Add the aluminium bar on top of the sample. Make sure that it does not end above the edge of the sample holder. If you press too hard in this step, the filaments may break

inside the cable, so take some margin. Add both heaters and the clamps. Now you should have the situation as in Figure A.3.

- Plug in both heaters and let a soldering iron warm up.
- The solder in the joint will melt and as a result the cables can be moved closer to each other. Tighten the clamps to fill up the slack (Carefull, still screw the clamps to tight, you might damage the cable). Check during the whole soldering process if the clamps are tight enough.
- Both ends of the joint will not melt by the heaters. To get a good solder connection here, add extra heat to these areas with the soldering iron. Add more solder or flux when required.
- When the connection is ready, turn off the heaters and soldering iron.
- When the sample has cooled down far enough, remove the heaters and the aluminium bar. Clean the cable, heaters and the aluminium bar with alcohol, the grease is easier removed when the cable is still warm.
- Do the same for the other joint.
- If necessary solder the extra voltage taps used to determine the quench location and to measure the joint resistance. These can be connected to the 24 pins connector on the side of the transformer case.
- Add Stycast clamps by wet winding procedure. Make sure the half-moons clamps and/or the insert for the 15 T magnet/MQE measurements still fits. Put a piece of tape below the clamps so that the Stycast will not stick to the cable. This makes it easier to remove it afterwards.
- Add the half-moons (with the tapped holes below) to the sample holder.
- The sample should now look like the sample shown in Figure A.4.

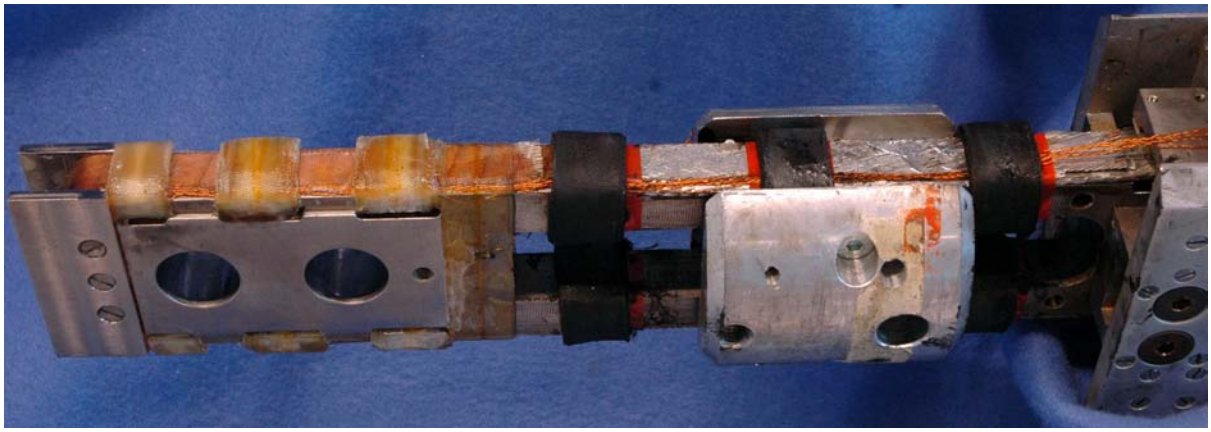

Figure A.4: A fully mounted sample.

A.5 MQE heater

If you want to perform minimum quench energy measurements on the cable, you start with the sample as prepared for the press measurements and make changes in the high field area. A strip of nine heaters is placed on the cable. Some heaters will not survive the cool-down and heater training so redundancy is important.

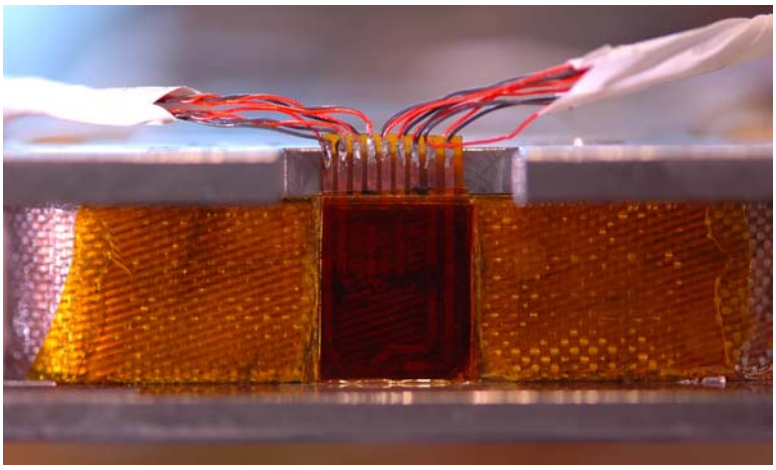

Figure A.5: The point heaters placed on the cable sample with extra layers polyimide foil on top of the heater strip. On top a layer of polyimide tape is added for good pressure contact with the anvil. On each heater a twisted pair is soldered.

- Remove the lateral support plates from the high field area. Since these are coated with dry Teflon spray, they should come of easily. Mark the plates so that you do not interchange them and they can be returned to the right side of the sample. Let someone modify the plate on the side that the heater assembly foil will stick out.
- Remove the epoxy only from the area where the heater will be placed. The rest of the sample needs no modification. Start with removing the epoxy with a high speed abrasive tool and abrasive paper until only a thin layer of epoxy remains on the cable. The last part of the epoxy has to be removed by careful scraping with a scalpel. The surface where the heater will be positioned needs to be epoxy-free.
- Glue the heater strip with "Super Glue" on the clean surface of the cable. Make sure the holes are positioned on single strands. Remove the glue from the holes with acetone and a small brush.
- Prepare the graphite-loaded epoxy by the recipe of M. de Rapper (Graphite loaded epoxy à la Michiel). It is made from commercial grade graphite powder for dry lubrication purposes and poly-pox expoxy (2:1 Resin:Harder) (In this experiment resin 700 and harder 355 are used).
- Fill the holes of the heater with the graphite loaded epoxy using the tip of a scalpel.
- Add a layer of polyimide tape and put the whole under pressure by adding a clamp with silicon rubber in between. Let it dry for a night. From now on the heaters need to stay under pressure except when modifications are performed, but leave the pressure on it as much as possible. Check the resistances of the heaters and also when dried. If the resistance is below 200 Ω, the heaters should be fine. If the heaters are not good, remove them, clean the surface again and try again.
- Add the support plate at the side where the heater sticks out.
- Connect a twisted pair to each heater track.

- Connect two twisted pairs to the joint as a return path.
- Bundle the pairs in two bundles with Teflon tape.
- Solder the pairs to the 24 pins connector on the side of the transformer.
- Solder a green LED to two taps of the 24 pins connector. Place the green LED in the opening in the sample holder between the joints. This LED is needed to measure the nitrogen level during the heater training. A sudden voltage increase occurs when the liquid nitrogen level reaches the LED. Power the LED at a current of 20 mA.
- Connect one side of the support plate on the side of the heater wires. Be careful not damage the heater strip. Turn the sample holder over.
- Remove the clamp attached to the heaters and add several layers of polyimide tape to fill up the space on top of the heater to a thickness a little larger than the epoxy. In that way, after the anvil presses against the sample, the polyimide will be pressed together and transmit about the same stress as the rest of the cable at the high field area. On top op the whole high field area , a layer of polyimide film must be added to smooth the contact between the anvil and the epoxy.
- Add the anvil and the rest of the support structure and give the proper amount of pre-stress. In the anvil, spring disks are added for a more accurate applied pressure after cool down.
- Test the heater resistance a final time.

It is important that the heaters keep the same resistance and contact resistance during the measurements, so that each time the same amount of heat is transferred to the strand. Therefore, the MQE heaters need to be trained in liquid nitrogen and helium before they can be used for measurements. Both at liquid nitrogen and helium this training procedure must be performed. For each heater, send pulses until the resistance stays about the same. Each time increase the energy of the pulses and send pulses until a stable resistance is reached. Repeat this process up to a maximum pulse height of 30 V over the capacitor. The heater resistance should lower during this training and at 4.2 K, the resistance after training should be below 10 Ω. Now the heaters are ready for measurements. The sample should stay cold at 77 or 4.2 K. Warming the sample up may cause negative training or broken heaters.

A.6 Connecting the transformer to the rest of the set-up.

Adding the transformer, the press and the magnet together seems straight forward. However there are some small steps that are crucial for correct assembly of the set-up. These will lower the likelihood shorts or magnet quenches and must therefore not be forgotten. Some comments about the assembly for the MQE measurements are found at the end of this section.

- Clean and put new grease on the O-rings if necessary.
- Add the outer cylinder of the press to the sample holder, position is with the two bolts and the two fixation pins. These should fit easily.
- Add the piston with the anvil. Keep the piston in place with two bolts and some iron wire. On the short sides of the anvil a strain gauge is attached. The wires (four for each strain gauge) need to go out of the cylinder at the top. Then they can be positioned along the sample and soldered to the 24 pins connection on the side of the transformer. Keep the piston in the cylinder two two bolts and iron wire.
- Lower the transformer into the cryostat insert. Add screws on top. Take the whole insert out of the cryostat. Add bolts through the half-moon supports and tighten the screws on top.

- Add a piece of screw-thread in the piston. This piece is to keep the inner cylinder in place during the next steps. Don't let the inner cylinder drop, you might have problems getting it back in when you cannot see what you do. Second, you may break the wires of the strain gauges.
- Add the copper cylinder along the cylinder in the magnet and add the top cover of the press. Connect all bolts.
- Then add the upper press coil with on top three rods with springs and the rod with the sharp point for the extensometer. Connect it on top with a nut on each rod. Press the coil a little up such that you don't have to hold the inner cylinder any more.
- Add the bottom coil and connect its bolts. Finally add the bolt that connects the upper coil with the inner cylinder.
- Add below the copper cylinder a piece of G10 to keep the cylinder maximum up inside the bore of the magnet. Keep the G10 piece in place with two large Tie-wraps.
- Add the extensometer. There are a few rings below the extensometer. These are needed for a good basic extension. Connect the extensometer to the plug on the side of the magnet.
- Connect the current leads (NbTi cable with a lot of copper) for the press. The current leads are marked on the insert with a B(ottom) and T(op) to indicate which press coil must be connected to them. The left contacts of the coils must be connected to each other. For each connection use brass bolts and a ring between the coil and the connector. This is to avoid shorts. Add Kapton tape along any edges that might cause a short. Also make sure the whole length of the current leads is well insulated. The insulation of the current leads themselves is not good enough.
- Insert the set-up into the cryostat. Connect the bolt. Add the chimney. Check for gas-tightness and check all connections for short circuits or loose contacts. If everything is correct you can start filling the cryostat.

If the MQE set-up is used in the 11 T magnet, connect the new support structure to the flange on top of the magnet. Add also the copper ring at the bottom inside the bore of the magnet. It can be kept in place by a bolt in the support.

Appendix B

Protocol to operate the transformer

The superconducting transformer contains of a complex feed-back system and has to be operated by the protocol described below for accurate measurements. The protocol is designed to achieve maximum measuring time by changing the polarity of the primary coil. The measurements themself are controlled by a 'macro' executed from within the computer program "VI.exe".

During the measurements, keep in mind that:

- When measuring with the 11 T magnet, someone should always be near in case the magnet quenches (i.e., it takes two people to perform these experiments.
- During a measurement one should always check whether the sample quenched or not. When the power supply of the primary goes into overflow, it quickly reduces the current to zero. This ramp-down of the primary will power the secondary with negative current. The 'secondary' heater needs to be turned on as quickly as possible to prevent quenches at a negative current.
- The maximum current in the primary coil is 50 A. If you go above this, the primary coil might quench.
- The maximum force of the press is 240 kN, do not go to higher values, the system is not built for that.
- The valve to the He overpressure "chimney" should always be open during measurements. Do not remain above or near this chimney during experiments, as the He release during a sudden magnet quench may be very sudden and violent and can easily cause serious injury!
- The valve towards the helium 'return' system should be half open, which makes it easier to close if a magnet quench should occur and reduces the helium flow to the helium system during a quench if the valve could not be closed.
- Make sure there is an unobstructed emergency escape route well away from the set-up should something go seriously wrong.
- The magnet power supply may induce a lot of voltage noise in instruments standing next to it. Place this power supply as far away from the rest of the equipment.
- The measuring time is limited, therefore change the polarity of the primary current and measure the point for the resistive foot at the end of the measurement.
- Do not forget to fill the cryostat when needed.

The protocol to operate the transformer:

- Set I in the VI program at the level where you want to pick up the current.
- Check whether the press and main magnet have the correct current. The helium level has to be in the range of 75 to 85 cm.
- Control Unit at range=0, set=0 and loop=open.
- Set the current converter to position 2.
- Turn control unit on.
- Put heater H_{sec} on for 5 sec.
- Wait 30 sec and put heater sec on for another 5 sec.
- Turn offset to zero.
- Turn on the BOS/S power supply.
- Turn V_{shunt} to zero by changing the offset.
- Open a new page in VI.
- Note V_{hall}, $V_{extenso}$, V_{press} en V_{magnet} in the excel sheet.
- Take two measurement points.
- Turn on the primary power supply.
- Set range on 5 V and put set voltage between 1 and 2 V to increase the current. Quench the secondary of the transformer repeatedly to prevent negative training.
- Once the primary is charged up to the desired level (if the current is too high, you will overshoot I_{sec}), put heater sec on to remove any induced negative current, then turn heater H_{sec} off, range to zero, turn primary power supply off and change loop to closed.
- When the current in the primary is zero, change the current converter to position 1.
- When the current in the sample matches the set current, turn on the primary power supply. The current should stay constant at the set current.
- Run your script on VI.

If there is a large current in the sample and you want to remove the current from the sample, follow the next protocol in order to safely remove the current from the sample.

- Turn the primary power supply off. The current in the sample will now reduce rapidly.
- When the current is low (below $\sim$10 kA), turn on heater H_{sec} repeatedly until the primary current is zero.
- If the primary current is zero, but the current in the secondary is still too high, then just wait for the current to decay over the joint resistance until the current is low enough.

Appendix C

Calibration Extensometer

The extensometer is used to determine the distance between the two NbTi press coils, which is needed to derive the force from the coil current accurately, see Section 2.3.2. It is shown in Figure C.1. It essentially consists of a titanium alloy plate with four strain gauges bonded to it. The four gauges are connected in a Wheatstone bridge configuration, resulting in a linear relation between the distance z_2 and the measured voltage. The full Wheatstone bridge configuration has a four times higher sensitivity than a single stain gauge and a linear response to the change in resistance and is shown in Figure C.2 [40]. A current of 1 mA is used to operate the wheatstone bridge. Two of them are bonded to the top side of the Ti plate with compressive stress en two to the bottom side which is under tensile stress. The strain gauges are bonded with Micro-Measurements M-Bond 610 adhesives on both sides of the titanium where the highest stress is.

Figure C.1: The extensometer used to measure distance z_2.

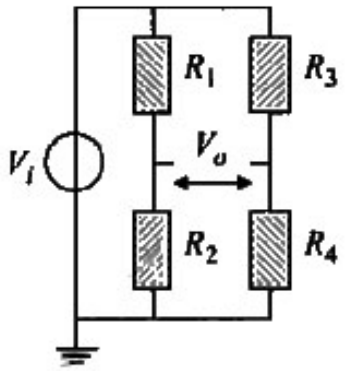

Figure C.2: A schematic of a full Wheatstone bridge.

The extensometer is calibrated both at room temperature and in liquid nitrogen. A part of the setup on which the extensometer is calibrated is shown in Figure C.3. The extensometer is mounted upside down in the calibration setup so that a point presses against the same spot as during a measurement. The sharp tip can be vertically positioned with an accuracy of 1 µm. In the design of the extensometer, a slit was added on the bottom of the plate so that the tip of the pin positions in the slit and the length of the extensometer is very well defined. However, during calibration the pin was not exactly inside the groove and during measurement the pin suddenly slipt further into the slit, resulting in a sudden voltage drop. Since this is not acceptable for a linear extensometer, it is mounted upside down so that the slit has no influence. On the press set-up, the extensometer is always mounted with a pre-stress as shown in Figure 2.14.

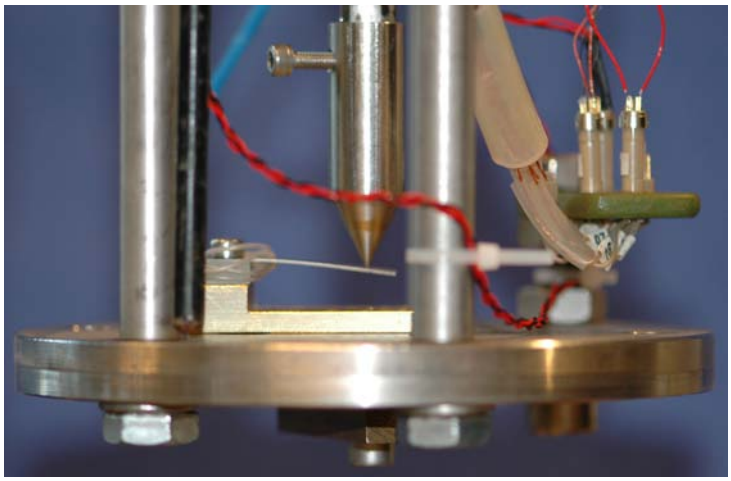

Figure C.3: The setup to calibrate the extensometer.

The strain gauges are calibrated at room temperature and in liquid nitrogen: the resulting calibration curves are shown in Figure C.4. Due to thermal shrinkage and imperfections, the calibration curves differ a little between the two temperatures. From 77 K to 4.2 K almost no change is expected since the sensor will not significantly shrink any further. Therefore the sensor is not calibrated in liquid helium and it is assumed that the extensometer behaves the same as at 77 K. The extensometer can measure at 4.2 K with an accuracy of 1 µm on a range of a few millimeters with a proportionality constant of 1.046 mV/mm. However, the read-out has some systematic errors due to positioning the extensometer. If the pin is slightly off, the slope will be different, because the arm of the extensometer changes in length. Also the whole press setup is under tensile and compressive strain (i.e. elastically deforms) which results in a small error to the distance between the press coils and also causes the most variation in distance between the two coils. The variation in distance between the two coils with varying force is mainly due to the elastic properties of the whole system and only a small part of this is due to the compression of the sample. Verweij [24] tested the distance between the press coils as function of the force with as sample a piece of aluminum. Due to the systematical errors, the distance between the two press coils can be determined within 0.1 mm. The 1 µm accuracy can be used to measure movement of the coils and creep in the sample.

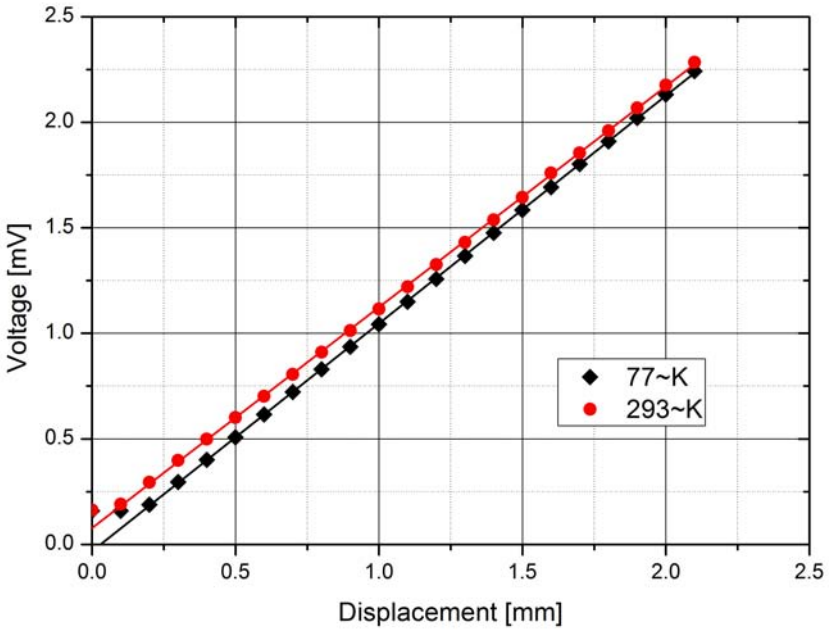

Figure C.4: Calibration of the extensometer at 77 K (black) and 293 K (red) with slopes of 1.046 and 1.080 V/m respectively.

Appendix D

Analyzing the press with the extensometer

The force applied by the superconducting press depends on the current in the press and on the distance between the press coils. The distance between the press coils is determined with an extensometer, in principle to an accuracy of 1 µm (See Appendix C).

The critical current of samples 1 and 3 are measured as a function of transverse stress. The distance z_2 between the press coils during these measurements is plotted against the applied transverse stress in Figure D.1. The third sample shows the same result before and after the thermal cycle. During the thermal cycle also the polyimide films on the anvil are replaced with new ones. The coil distance z_2 during the first sample experiments increases stronger in the first 40 MPa than that recorded with sample 3.

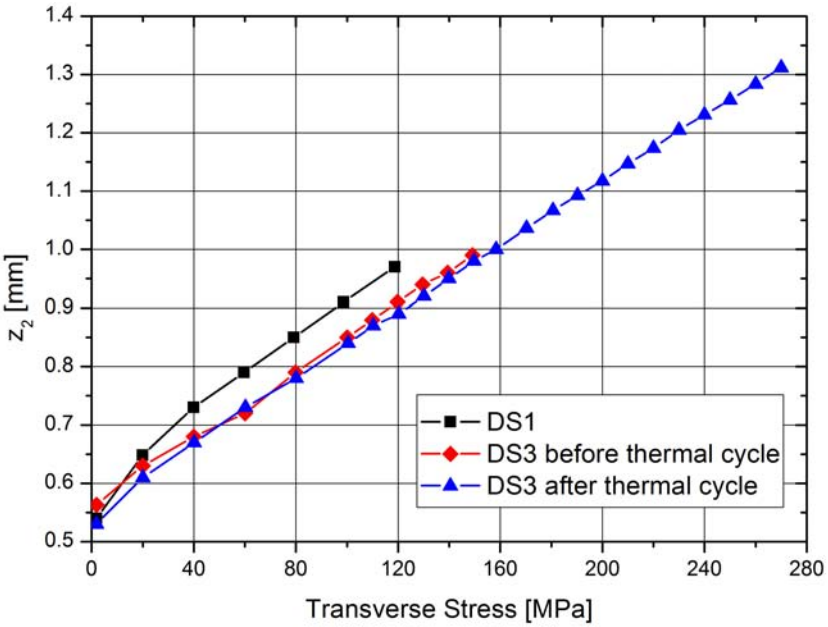

Figure D.1: The distance z_2 between the press coils as function of transverse stress on the sample.

During the measurements the polyimide film on top of the anvil will show some creep, due to its relatively the low Young's modulus and yield stress. The film is therefore in the plastic regime. The creep in the sample is determined by comparing the read-out of the extensometer at a transverse stress of 2 MPa before and after the measurements at a high transverse stress. The result is shown in Figure D.2 and it can be seen that the Kapton film on sample 3 has the same creep before and after the thermal cycle, while the creep in the film on sample 1 is much higher at lower transverse stresses.

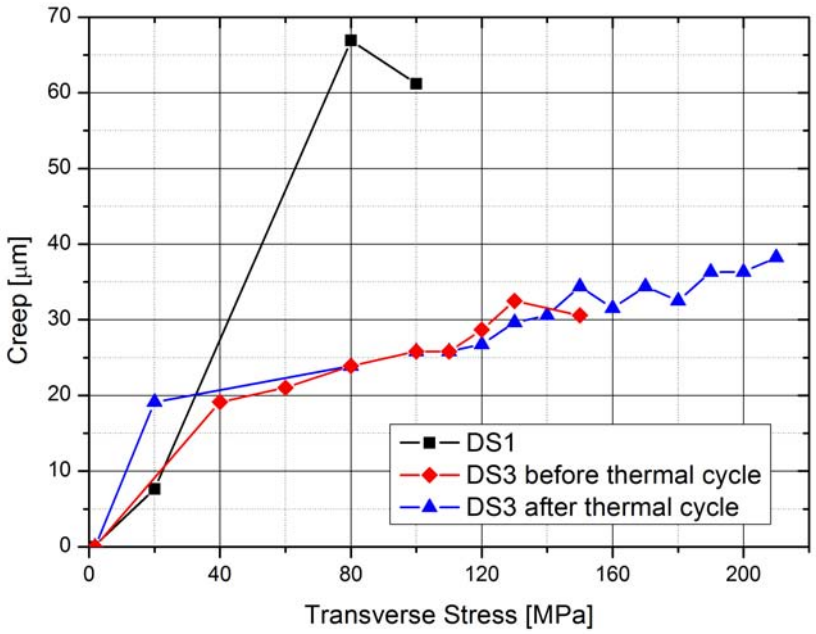

Figure D.2: The creep in the Kapton and sample as function of transverse stress on the sample.

The extensometer shows a large increase in z_2 for sample 1 in the first 20-40 MPa. However, this increase is not seen at 20 MPa. At this low transverse stress level the polyimide film is still elastic. The strong increase in the creep in sample 1 at 80 MPa explains the difference in the slopes of Figure D.1.

The third sample had to be warmed up due to a problem with the press. The question whether or not the press actually pressed with 150 MPa is the reason the strain gauges are added to the anvil. The measurements of the extensometer before and after the thermal cycle are compared and show the same result. This indicates that the transverse stress applied to the sample before the thermal cycle was indeed 150 MPa and at which level no degradation was found in the sample. Nevertheless, a short circuit between the press coil and the stainless steel case was measured after warming-up. Therefore there is an uncertainty about the precise transverse stress applied and no conclusion can be built on it.

Appendix E

Control Unit

The control unit for the transformer had to be replaced since the old one did not work any more. The new control unit was never used before and had to be tuned and calibrated before use. This control unit was made together with the one made for MIT [21]. Since the transformer setup for MIT is a little different than the one used at Twente University, the set voltage is 10 kA/V and the read-out of the secondary current from the display shows only half of the current it should. Since the current in the sample is measured directly over the shunt resistance and not using this visual display, this is not a problem. In this section of the appendix the tuning and calibration of the control unit is described.

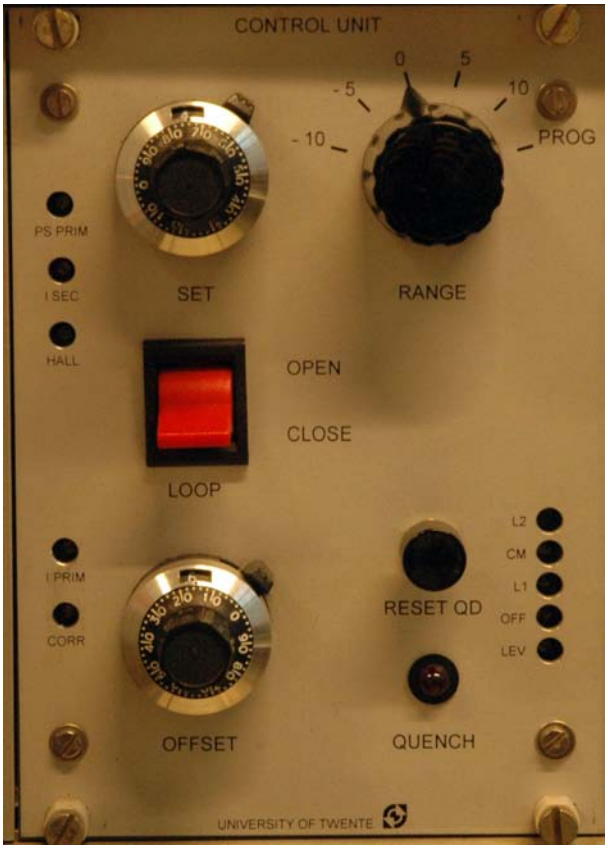

Figure E.1: Control Unit of the transformer.

The Control box consists of two plates of electronics (one for the feedback-loop and the other for the quench detector) connected to the front panel shown in Figure E.1. Connected to the left side of the front panel is the electronics of the feedback loop and on the right side the electronics for the quench detector. The quench detector is not used, since the sample is passively protected. A scheme of all instrumentation within the control unit of the transformer is shown in Figure E.3. There are five variable resistances in the control unit that can be modified with the potentiometer screws on the left side of the control unit. A more detailed scheme of the electronics can be found in the MIT report [21].

The screws I_{sec}, $HALL$ and PS_{prim} adjust the offset of the amplifiers. The input of each amplifier is shorted and the variable resistances are set such that the output is zero. I_{prim} is turned to zero, when no current is applied. A correct read-out of I_{prim} is assured by checking the voltage with a zero flux.

The correction for the undesired inductive coupling between the primary current circuit and the Rogowski sensing coil can be adjusted by turning Corr. For the measurement the primary coil is powered up to a certain value and the secondary is heated so that no current flows in the sample. The coupling induces a current in the Rogowski sensing coil and therefore a current flow through the shunt resistance. The voltage measured over the shunt resistance is the error due to this coupling. The voltage over the shunt is measured for several primary currents for maximum and no correction for the coupling. The screw is set to the no coupling location by shorting the primary power supply while the "Capteur de Courant" measured the current. Since there is no coupling at this moment, the voltage over the shunt should be put to zero for currents applied. Even with the maximum correction for the coupling between the primary current and the Rogowski, there is still an error in the secondary current as can be seen in Figure E.2. The effect of the coupling is made smaller, but the secondary current measured must be corrected for the part of the couping that remains. The correction factor is 4.728 A/A between the secondary current and the primary current. The primary current is measured accurately with a zero flux, because the read-out of the Capteur de Courant is less accurate.

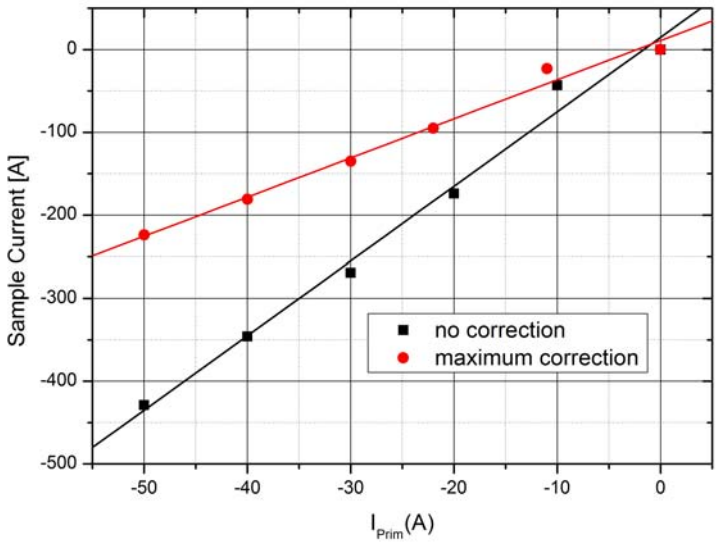

Figure E.2: Secondary current read out on the shunt resistance as function of primary current with zero current in the sample for no correction and maximum correction by the control unit.

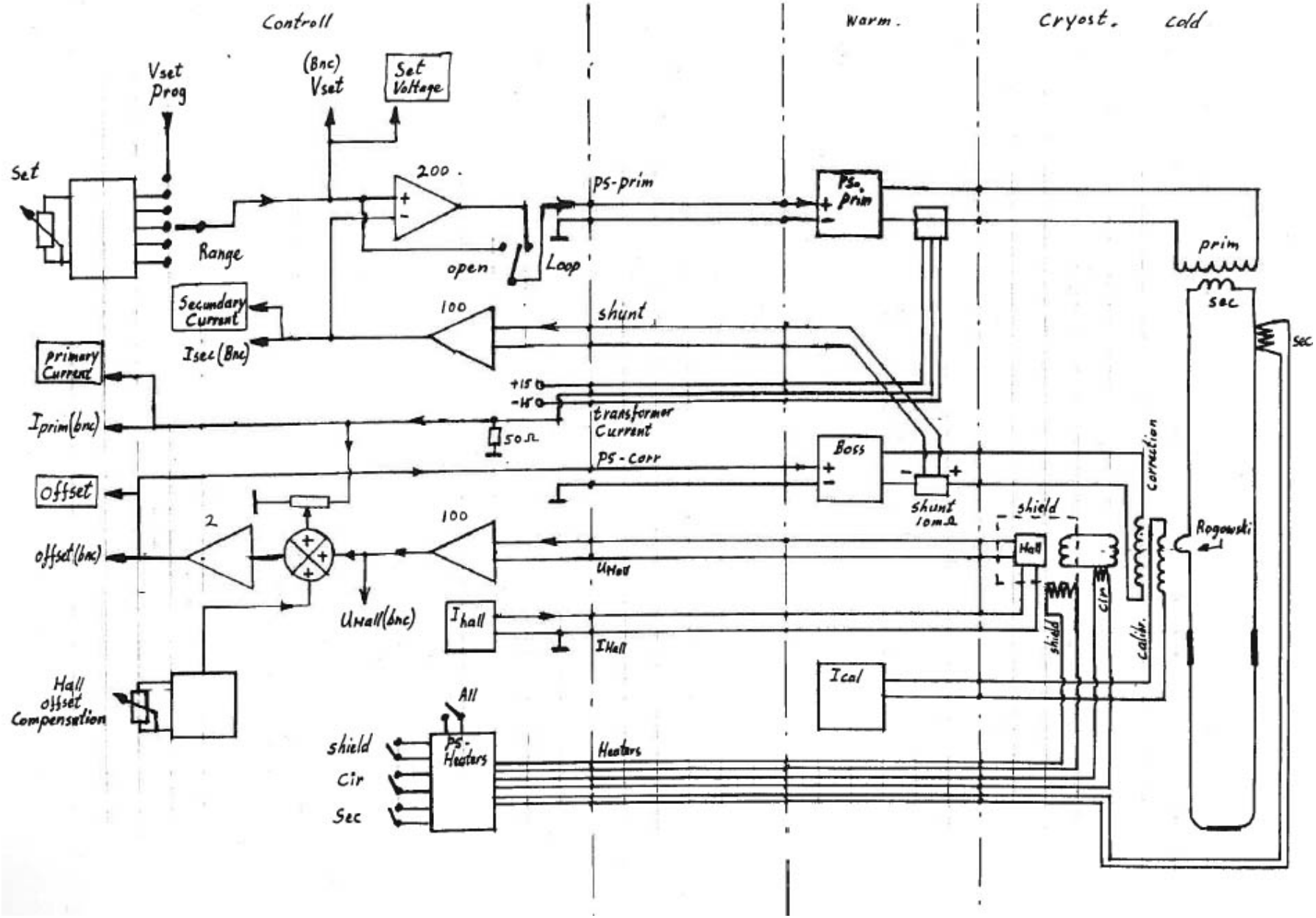

Figure E.3: Extended schematic of the transformer feedback loop with on the left all electronics inside the control unit, in the middle the external apparatus outside the cryostat and on the right side everything inside the cryostat.

Appendix F

Scheme of new support structure

For the MQE measurements a new support structure had to be designed to support the sample within the bore of the main magnet. In anticipation of critical current measurements on Rutherford cables for higher magnetic fields, the supports also must be applicable for the 15 T magnet. The new support is made from aluminium. The same sample holder as for the press measurements can be used with these new supports. The positioning pins of the press and screws are used to connect the sample holder to the support structure.

Full-size high J_c Rutherford cables measured in applied magnetic field experience a large Lorentz force. This force must be supported. With the design of the support structure, this force is supported by the flanges of the magnet and not by the magnet bore itself. (Note that the windings of the superconducting magnet lie immediately beneath the surface of the bore and may be damaged by stress concentrations.) Furthermore this support structure can also be used for larger cables as the FRESCA II cables, which needs a wider sample holder. The required thickness of the sample holder of 24 mm will fit between these supports. There is extra space in the supports for thicker epoxy clamps

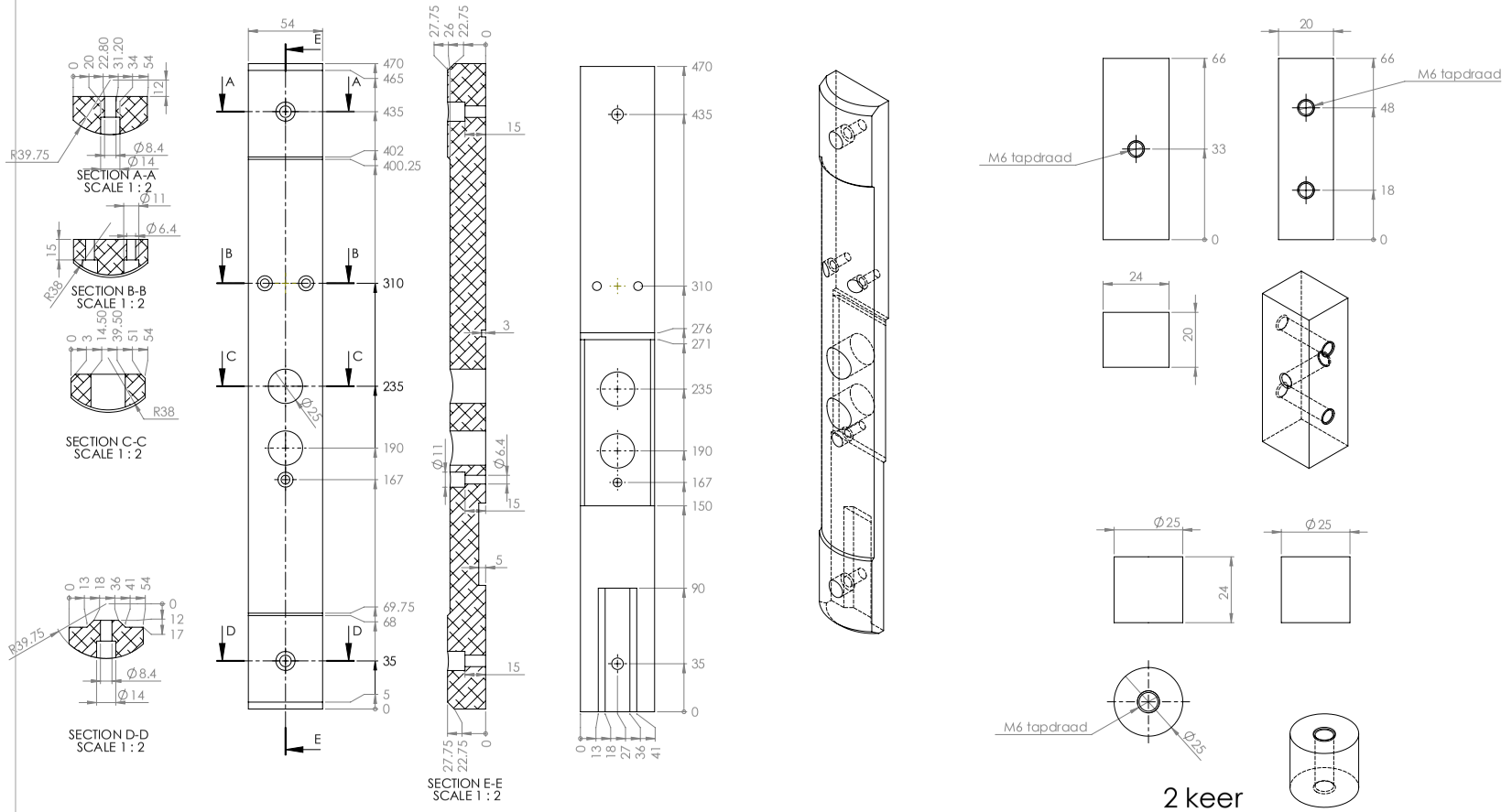

UNLESS OTHERWISE SPECIFIED: DIMENSIONS ARE IN MILLIMETERS SURFACE FINISH: TOLERANCES: LINEAR: ANGULAR	FINISH:		DEBUR AND BREAK SHARP EDGES	DO NOT SCALE DRAWING	REVISION
	NAME	SIGNATURE	DATE	TITLE:	
DRAWN					
CHK'D					
APP'VD					
MFG					
QA			MATERIAL:	DWG NO. afsteunen	A2
			WEIGHT:	SCALE:1:5	SHEET 1 OF 1